# The Characterization of and Formulation Development using a Novel Tyre Devulcanizate

**Stuart von Berg**

**Submitted in fulfilment of the requirements for the degree of *Magister Scientiae* in the Faculty of Science at the Nelson Mandela Metropolitan University, Port Elizabeth, South Africa**

**January 2016**

**Supervisor: Assoc. Prof. C.D. Woolard**

**Co-supervisor: Dr S.P. Hlangothi**

# ACKNOWLEDGEMENTS

I would like to express my gratitude to Piet Swart from New Reclamation Group who never hesitated to offer guidance and share wisdom on the research being carried out. His industrial experience was greatly appreciated and very useful. Thank you to the New Reclamation Group who funded this research and kindly supplied the novel tyre devulcanizate that was used in this research.

This research would have been made more challenging without the assistance of Gerrit Vorgers from S&N rubber who supplied the chemicals used in the rubber compounding. I am grateful to John Lithgow from Karbochem and Conway Vorster from Continental Tyre who supplied the virgin elastomers that were used for compounding and identification of basic characteristics of elastomers. Thank you to Keith Gibb and Tertius de Ridder from Bridgestone who kindly suppled the commercial tread tyre reclaim that was used to compare to the novel tyre reclaim.

It was a pleasure to work with Rekha Neglur who was always ready to assist with any problems and was a great help in keeping the research flowing smoothly, no problem was too big. Thank you to Dr James Carson and my co-supervisor Dr Percy Hlangothi who were always there to bounce ideas off of when strange results appeared. Their experience and enthusiasm was greatly appreciated and helpful during the trying times.

It was a great experience working with my supervisor Assoc. Prof. Chris Woolard who has an in depth knowledge of the rubber industry and chemistry. I am grateful that I was allowed the freedom to challenge his decisions and explore the answers to problems. His dedication to research is inspiring.

Lastly, I would like to thank my family who had unwavering faith in me. I am grateful for the support especially through the difficult times. This journey was made all the better because I could share it with all of you.

# SUMMARY

The amount of waste tyres being dumped is fast becoming a problem. These stockpiles take up valuable land and are an environmental and health problem. While incineration is the simplest way to recycle the used tyres it isn’t an efficient way to dispose of tyres.

This research looks at developing a method for characterizing the New Reclamation Group (NRG) reclaim with the main focus on Hi-Res™ thermogravimetric analysis. Good quantification was possible using this technique. A trade off was established between resolution, sensitivity and time. While increasing the resolution allowed greater separation to be achieved the time for each experiment increased rapidly. Although kinetic models do exist for quantifying rubber components in vulcanized sample, they were not suitable for this study. When devulcanization causes significant molecular changes, such as with NRG reclaim, the decomposition profiles no longer match those of virgin materials.

Formulations developed focused on mixing, rheometry, crosslink density and tensile properties. The NRG reclaim acted as a processing aid which lowered the maximum torque. This provides mixing safety as the temperature is decreased as a result of the lower torque. This effect was not seen with conventional reclaim.

Rheometry tests indicated that the addition of the devulcanizates decreased the extent of cure. It was demonstrated that this could be linked to crosslink density. Testing of the 100%, 200%, 300% moduli correlated the crosslink density to the maximum torque.

Although the addition of NRG reclaim reduced the tensile strength of the formulation, a link between crosslink density and ultimate tensile strength (UTS) couldn’t be made. The decrease in the UTS and increase in extension at break is possibly caused by an increase in low molecular weight material present in the formulations and decrease in crosslink density. This could possibly increase the mobility of polymer chains which could increases flexibility.

Keywords: NRG reclaim, Hi-Res™ TGA, compounding, crosslink density, mixing kinetics

# TABLE OF CONTENTS

# LIST OF ILLUSTRATIONS

# LIST OF TABLES

# LIST OF ABBREVIATIONS

| | |
|---|---|
| $\varepsilon_B$ | extension (strain) at break |
| AAS | atomic absorption spectroscopy |
| Acc | accelerator |
| ASTM | ASTM International, formerly American Society for Testing and Materials |
| BR | polybutadiene rubber |
| Bt | benzothiazole |
| CB | carbon black |
| CBp | pyrolytic carbon black |
| CBS | N-cyclohexyl-2-benzothiazole sulfenamide |
| CIIR | chloro isobutylene isoprene rubber/chlorobutyl rubber |
| CRI | cure rate index |
| CTP | N-cyclohexylthiophthalimide |
| CV | conventional vulcanization |
| DMA | dynamic mechanical analysis |
| DPDS | diphenyl disulfide |
| DPG | diphenyl guanidine |
| DSC | differential scanning calorimetry/calorimeter |
| DTG | derivative thermogravimetry/thermogravimetric |
| EDS | energy dispersive (X-ray) spectroscopy |
| EPDM | ethylene propylene diene monomer rubber |
| EV | efficient vulcanization |
| $F_f$ | fill factor (fraction of mixing head filled with compound) |
| FTIR | Fourier transform infrared |
| GC | gas chromatography |
| GC-MS | gas chromatography – mass spectrometry |
| GPC | gel permeation chromatography |
| GRT | ground rubber tyre |
| GTP | ground tyre powder |
| Hi-Res™ | high resolution, trademark of TA Instruments. |
| HP | high purity |
| HPLC | high performance liquid chromatography |
| ICP | inductively coupled spectrometry/spectroscopy |

| | |
|---|---|
| IIR | isobutylene isoprene rubber/butyl rubber |
| LAOS | large angle oscillatory shear |
| LNCA | liquid nitrogen cooling accessory |
| Max. | maximum |
| MBT | 2-mercaptobenzothiazole |
| MBTS | 2,2’-dithiobis(benzothiazole)/bisbenzothiazole-2,2'-disulfide |
| MBTP | bisbenzothiazole-2,2'-polysulfide |
| MDR | moving die rheometer |
| $M_w$ | molecular weight |
| NMR | nuclear magnetic resonance |
| NR | natural rubber |
| NRG | New Reclamation Group |
| OE | oil extended |
| OES | optical emission spectroscopy |
| PAH | polyaromatic hydrocarbon |
| phr | parts per hundred rubber by mass |
| PI | polyisoprene |
| PVI | pre-vulcanization inhibitor |
| PyCB | pyrolytic carbon black |
| Pyr-GC | pyrolysis-gas chromatography |
| RAE | residual aromatic extract |
| REDISA | Recycling and Economic Development Initiative of South Africa |
| RH | rubber (hydrocarbon) |
| r.m.s. | root mean square |
| RPA | rubber process analyser |
| rpm | revolutions per minute |
| RRM | renewable resource material |
| SBR | styrene butadiene rubber |
| SDT | simultaneous differential scanning calorimeter and thermogravimetric analyser |
| SEC | size exclusion chromatography |
| SEM | scanning electron microscopy |
| SMR | standard Malaysian rubber |
| sol | soluble (fraction) |
| SSBR | solution polymerized styrene butadiene rubber |

| | |
|---|---|
| SSSE | solid state shear extrusion |
| sub. | substituted |
| TDAE | treated distillate aromatic extract |
| Temp. | temperature |
| $T_g$ | glass transition temperature |
| TGA | thermogravimetric analysis/analyser |
| THF | tetrahydrofuran |
| TMTD | tetramethylthiuram disulfide |
| UHP | ultra high purity |
| UTS | ultimate tensile strength |
| XLD | crosslink density |
| XPS | X-ray photoelectron spectroscopy |
| XRD | X-ray diffraction |
| XRF | X-ray fluorescence |
| $Zn(mbt)_2$ | zinc mercaptobenzothiolate |
| ZDMC | bis(dimethyldithiocarbamate)zinc(II) |

# CHAPTER 1

# 1 INTRODUCTION

## 1.1 Motivation for this study

Approximately 1 billion used tyres exist worldwide. Currently the primary end-use solution for these tyres is to dump them in landfill sites (1). According to the Recycling and Economic Development Initiative of South Africa (REDISA), 60 million tyres are currently stockpiled around South Africa (2). These stockpiles include illegal and unsafe dumpsites within residential, industrial and rural areas. South Africa adds approximately 11 million waste tyres to existing stockpiles every year (3). The rate at which used tyres are created are three times faster than that at which they are recycled (4). Not all of the waste tyres are dumped. Some waste tyres are recycled commercially while other waste tyres are burned for the scrap metal inside them (2).

The dumping or illegal burning of rubber pose many health and safety problems. Stockpiling large amounts of waste tyres take up large amounts of space, allows the leaching of rubber additives and is a fire hazard as rubber is inflammable and the fires are very difficult to extinguish. The burning of the tyres causes air, soil and surface water pollution (1,4,5). Uncontrolled burning of tyres releases noxious gases such as carbon monoxide and dioxins as well as toxic liquids into the environment (2). Owing to the curved, hollow nature of tyres, they make good breeding grounds for mosquitoes, vermin and other animals which may promote the spread of disease (4,6,7).

There are a few alternatives to dumping in which waste tyres may be re-used, recycled or reclaimed. They can be re-used as whole tyres when re-treaded, as crash barriers or in road construction (7,8). The reclaimed rubber components, often in the form of rubber crumb, can be used for rubber mats, floorings, shoes, concrete (7) and increasingly in asphalt (7,8,9,10). Thermoplastic elastomers, with improved impact properties, are often produced by melt mixing fine rubber crumb with thermoplastics, such as polyolefins (10,11). Rubber tyres are highly inflammable and have a higher calorific value than coal; therefore waste tyres can be incinerated for energy recovery (7,8,12). The waste tyres can be broken down into simpler compounds by pyrolysis (heating in an inert atmosphere or under vacuum, with/without a catalyst); thereby producing a pyrolytic carbon black (PyCB; also abbreviated CBp), oil and gases that can be re-used as fuel or chemicals (6,7,13).

# INTRODUCTION

One of the best ways to deal with the problem of waste tyres is through recycling them so that they may be used in the manufacturing of new tyres (5,14). This involves the production of a partially de-vulcanized rubber and filler. This material is known as devulcanizate or reclaim. The aim is to create a “real recycling loop”, *i.e.* the rubber waste is re-used in new rubber products (15).

Vulcanized rubber comprises a network of sulfur crosslinks between the polymer chains which are introduced during heating (16,17). This means that vulcanized rubber is classified as a thermoset. Thermosets cannot be recycled by heating and re-moulding (1,17). Vulcanized rubber is also effectively non-biodegradable because of the sulfur crosslinks between the polymer chains (7,18,19). In order for rubber to be effectively recycled, the sulfur crosslinks need to be broken down so that the rubber may be further processed (1). This process is called de-vulcanization.

The crosslinked, vulcanized rubber prevents the softening and processing of waste tyres (1). The vulcanized structure does not bind well to virgin material; thereby negatively affecting the physical properties of the final product (20). Many methods have been developed for de-vulcanizing used tyre rubber. Some of the more successful processes include thermal, thermomechanical, mechanochemical, microwave, ultrasonic and biotechnological de-vulcanizing methods (15,21,22). These methods, however, produce de-vulcanized rubber of varying quality. Not all de-vulcanization processes produce de-vulcanized rubber suitable for re-mixing with virgin rubber for the inclusion in new tyres (14,23). Re-use is often restricted to industrial rubber products such as hoses, conveyor belting and sheeting. The highly engineered nature of tyres restricts the quantity of devulcanizate that can be used.

Some of these recycling processes have high energy requirements with respect to electricity consumption and create large environmental problems because of the use of toxic chemicals (20,24). Dealing with these problems can increase the cost of recycling rubber tyres. Another problem with the different processes is that not all are suitable for de-vulcanizing all types of rubber (16,25).

Unfortunately, most de-vulcanizing processes break not only the sulfur crosslinks but also the main carbon chains of the polymer. The quality of the final product of these processes is consequently inferior to that of virgin rubber (23,26). Furthermore the recycling processes degrade the quality of the carbon black and other fillers. It is, however, still possible to use small amounts of devulcanizate in new tyres. The devulcanizate can sometimes be added to virgin material up to a maximum of 10% without a significant drop in the physical properties of the tyre (20).

Generally blends of virgin material with devulcanizates have poorer physical properties, such as tensile strength, than 100% virgin material. This is possibly due to flaws in the structure of the blend interface between virgin and reclaimed material because co-vulcanization between the two phases is generally poor (27). The devulcanizate material (especially when only partially de-vulcanized) does not adhere well to the virgin rubber matrix and may act as a stress raiser. The devulcanizate particles do not sufficiently transfer stress between the matrix and itself. This would lead to a lower tensile strength (20,25). When reclamation is carried out in an air atmosphere, there is always the possibility of oxidative degradation when oxygen attacks the double bonds of the rubber chains. This oxidative degradation decreases the mechanical properties of the recycled rubber (20).

The breaking of the polymer backbone can lead to the formation of conjugated dienes (28). The breakdown of the polymer backbone may lead to shorter chain lengths or the backbone fragments could join together to form highly branched polymers. Both possibilities would lead to reduced final properties in the devulcanizate/virgin rubber blend (25). Some authors attribute the loss in tensile strength to the decrease in crosslink densities that are achievable (26). It is for these reasons that the reclaimed rubber is often used as an inert filler in tyres rather than a substitution for virgin polymers (20).

A novel devulcanizate has been developed by the New Reclamation Group (NRG) in South Africa using proprietary technology (3,29). This devulcanizate has different physical characteristics to other types of devulcanizate, notably a much lower viscosity. An investigation of this material and an understanding of its behaviour is necessary before it can be introduced as a commercial product into the market, in particular into road tyres. Current application has been limited to industrial rubber products and solid rubber tyres such as those for forklifts (3). The process has been described as producing “liquid rubber” through a “semi-devulcanization process” (30).

Road tyre formulations generally consist of different types of rubber, carbon black, sulfur, accelerators, activators and anti-degradants (8). Many of these chemicals are believed to be present in de-vulcanized rubber and therefore will influence any product containing the devulcanizate. It is for this reason that characterizing any devulcanizate used is important before proceeding with any blending. Furthermore the production processes, employed by

NRG, are being up-scaled and are thus still in development. Rapid methods are required to characterize the product to ensure quality control. It is for these reasons that this study was commissioned by NRG.

A primary purpose of this study is to develop an analytical procedure to assess and characterize devulcanizates so that they may be blended with virgin rubber. Important information can be gleaned from the quantity of low molecular weight materials, including oils, polymeric material, carbon black and inorganic material. Furthermore it is important to determine how much of the polymeric material is fully de-vulcanized.

The ultimate aim is to use the NRG devulcanizate in road tyres. This study therefore investigates the performance of blends of devulcanizate (from NRG and a reference material) with virgin rubber and compares the performance to standard formulation virgin rubber blends. Some properties that are known to be effected by devulcanizates are processability, curing rheology, durability and longevity of the blended product (31).

In order to monitor the changes of the physical properties of the blends, all blends are compared to 100% virgin rubber formulations. Some of the physical properties tested include ultimate tensile strength, stress at 100%, 200%, 300% strain as well as elongation at break. The study also assesses the effects that the devulcanizate has on mixing and curing properties. These include mixing torque, scorch time and cure rates.

## 1.2 Objectives

The objectives for this study are therefore to:

- determined the appropriate characterization methods for devulcanizates, particularly to quantify polymer and filler content,
- identified properties affected by devulcanizates,
- compared two reclaim products – a product from NRG and a commercial devulcanizate used by the tyre industry,
- tested the physical properties of devulcanizates and their effect on mixing properties, and

- developed improved formulations for rubber compounds[1] containing devulcanizates.

## 1.3 Scope of the study

The focus of this study was to investigate the current devulcanizate available on the market as well as a devulcanizate in development. The devulcanizates were added into a standard rubber formulation which was mixed and cured in the laboratory. The results of any tests performed were compared to virgin rubber results that were prepared using the same formulation(s). Because natural rubber (NR) and styrene butadiene rubber (SBR) are the most common elastomers, used in tyres, they were selected for the comparison virgin reference formulation. This study did not focus on the effect that other elastomers (butyl and polybutadiene rubber) present in tyres might have on final properties.

Tests carried out on the various rubber samples addressed compositional as well as physical attributes. Since the primary aim was to develop a rapid technique for bulk compositional analysis of the NRG devulcanizate, analytical work focused on thermogravimetric analysis (TGA). The primary focus was on mass loss rate controlled, also known as high resolution, TGA methods. Characterization was focussed on primary constituents which can be separated by high resolution TGA. Kinetic modelling of thermal decomposition or deconvolution techniques were deemed beyond the scope of this study.

Sophisticated laboratory techniques such as nuclear magnetic resonance (NMR) spectroscopy was excluded. Investigations into low level constituents such as accelerators and accelerator residues by gas chromatography (GC) and high performance liquid chromatography (HPLC) were excluded. Furthermore development of existing tests for the analysis of ZnO in rubber, such as atomic absorption spectroscopy (AAS) and inductively coupled plasma (ICP) spectrometry, was deemed unnecessary.

Formulation development was restricted to an adaptation of a single tyre compound formulation, containing NR & SBR. Formulation tests focused on mixing behaviour, curing characteristics (extent and kinetics) and tensile properties. Other physical properties such as abrasion resistance and fatigue resistance, as well as durability (thermal and oxidative), were deemed beyond the scope of this study.

---

[1] In the rubber industry, the word *compound* refers to an unvulcanized formulation which is a mixture of elastomers, fillers, curing agents, process aids and other additives.

# CHAPTER 2

# 2 LITERATURE REVIEW

## 2.1 Tyre composition

Road tyres consist of rubbers, fillers, steel, sulfur, zinc oxide as well as additives such as processing oil, plasticizers and vulcanizing accelerators (12). The most commonly used elastomers in road tyres are styrene-butadiene rubber (SBR) co-polymer and natural rubber (NR) (32). A major component in many road tyres is carbon black, which is used as a reinforcing filler. Carbon black increases certain properties of the rubber such as abrasion resistance, hardness, stiffness and strength (12). Other chemicals added to road tyres include plasticizers, peptizers and processing oils, which reduces the viscosity during processing as well as lowering the internal friction and improving low temperature flexibility of the vulcanized material (5). Curing agents, such as accelerators and activators, are added to speed up the curing process. Finally reinforcing fibres, such as textile or steel cords, are present in road tyres to give dimensional stability and strength to the final product. Table 2.1 presents the average composition of tyres in the market today. The large diversity of materials (polymers, ceramics, metals, and small organic and inorganic molecules) is apparent.

*Table 2.1 Average composition of production tyres (33)*

| *Material* | *Mass %* |
|---|---|
| *Rubber (RH)* | 48 |
| *Filler (carbon black & silica)* | 22 |
| *Metal reinforcement/belting* | 15 |
| *Oil, anti-degradants, wax etc.* | 8 |
| *Fabric* | 5 |
| *Zinc oxide (ZnO)* | 1 |
| *Curing agents* | 1 |
| *Total* | 100 |

The major material in a tyre is rubber which is composed of a variety of types. A complete road tyre typically contains five common different types of rubber. Besides SBR and NR, tyres also contain butyl rubber (IIR, isobutylene isoprene rubber), chlorobutyl (CIIR, chloro isobutylene isoprene rubber) and polybutadiene rubber (BR) (32). The reason for this is that each rubber is suitable for the different environments present in a road tyre. Flexibility, heat dispersion, operation in cold weather and gas permeability are some of the important properties that the various rubbers address. Figure 2.1 shows a cross section through a tyre.

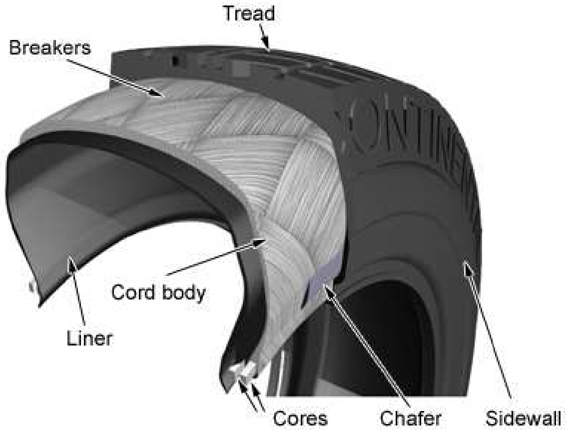

*Figure 2.1 Structural components of a cross-ply (road) tyre. (Reproduced from (34))*

The tread is the part of the tyre that comes into contact with the road. It therefore has to be resistant to oils and chemicals, resistant to abrasion and flexible. The tread typically consists of SBR, BR and NR with the former two in preponderance in modern passenger tyres and NR, dominant in truck tyre treads (32,34).

The sidewall needs to have greater flexibility than the tread so that the tyre does not burst or tear when driving over potholes or bumps in the road. It does not come into direct contact with the road so chemical resistance is not very important. The side wall is manufactured using NR and BR but may also contain SBR and speciality rubbers such as ethylene propylene diene monomer (EPDM) rubber (32,34).

The inner liner has one main role and that is to stop the air inside the tyre from escaping. The rubber used needs to be impermeable to gases. The inner liner should also have some flexibility and therefore it consists of SBR, NR, CIIR and/or IIR, the last two being the rubbers that impart impermeability to certain air gases (32,34).

Vulcanized rubber alone is not sufficient in making a good road tyre. In order to improve production time, lower production cost and still maintain a high performing product various other chemicals are needed. Table 2.2 shows a typical tyre recipe.

*Table 2.2 Typical tyre rubber compound (32)*

| *Component* | *phr* |
|---|---|
| *SBR* | 24.0 |
| *SBR OE* | 26.0 |
| *NR* | 50.0 |
| *Carbon black N-220* | 45.0 |
| *Sulfur* | 1.6 |
| *CBS* | 0.8 |
| *DPG* | 0.4 |
| *ZnO* | 3.0 |
| *Stearic acid* | 3.0 |
| *Total* | 153.8 |

phr = parts per hundred rubber by mass

Note that rubber formulations are typically reported in units of parts per hundred rubber (phr). All components are expressed as a mass (in g) required to be added to the formulation alongside 100 g of the sum of the elastomer components.

The first three components of the formulation consist of the rubbers SBR and NR with one of the rubbers containing oil (OE – oil extended). The filler used in the formulation is carbon black. Sulfur is needed to form the crosslinks between the rubber chains. N-cyclohexyl-2-benzothiazole sulfenamide (CBS) and diphenyl guanidine (DPG) act as accelerators which increase the rate of sulfur vulcanization. The stearic acid and zinc oxide (ZnO) form the activators which reduce the time taken to vulcanize the rubber. Note that the activators require the presence of accelerators. Further chemicals may also be added to commercial tyre formulations. These include processing aids and anti-degradants such as anti-oxidants and anti-ozonants which protect and extend the life of road tyres.

## 2.2 Elastomers

Elastomers contain long linear hydrocarbon chains that consist of many repeating units. They usually have a low glass transition temperature and do not crystallize although some, such as NR, do so under high degrees of strain (35,36). Vulcanized elastomers are very elastic, having the ability to be stretched and then to return to their original dimensions when the applied force is removed. This property is due to the sulfur crosslinks present after vulcanization linking the long hydrocarbon chains into a network as well as the chains being entangled. Together these resist the polymer chains being pulled apart (37). The rubber chains are still free to uncoil and elongate, but are prevented from slipping completely past each other.

### 2.2.1 Styrene butadiene rubber (SBR)

SBR is a co-polymer of two repeating units. The monomers styrene and butadiene are not present in a 1:1 ratio (typically SBR is 20-30% styrene (38,39)). The arrangement of monomers along the chains is pseudo-random.

SBR is used mainly in the tread of tyres because it provides good wet skid and traction properties while retaining good abrasion resistance and aging stability (8). The monomers and a generalized polymer formula are shown in Figure 2.2

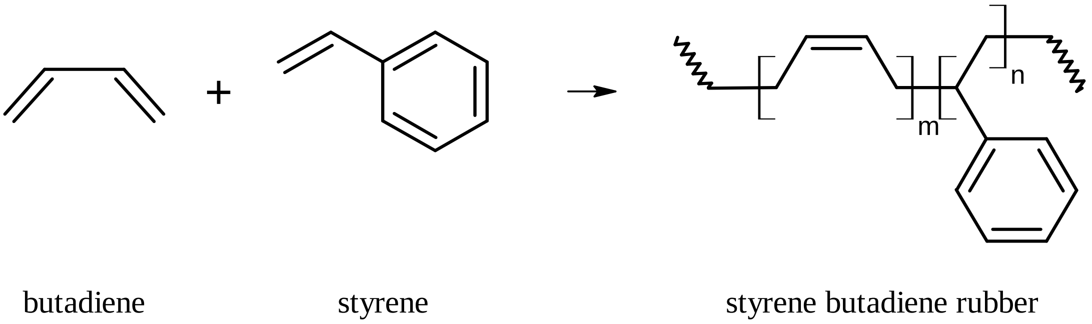

*Figure 2.2 Structure of styrene butadiene rubber and its constituent monomers, butadiene and styrene*

De-vulcanizing SBR is challenging because of the complicated structure of the rubber and the various possible molecular configurations on the monomer units along the backbone. During the reclamation or de-vulcanization process, network breakdown of the rubber occurs. At the same time, however, recombination of the network takes place (5,27).

When SBR is de-vulcanized, main chain scission occurs. This produces free radicals on the chain fragments (40). If the formation of these radicals is not controlled by a de-vulcanizing agent which is a radical scavenger, such as diphenyl disulfide (DPDS), recombination of the fragments occurs which results in a highly branched network. Such an increase in crosslink density increases the hardness of the devulcanizate (5,27).

### 2.2.2 Natural rubber (NR)

Natural rubber (NR) consists of a single monomer that is repeated several times, primarily in a *cis* configuration (>99%) (35,36). NR compounds, generally, have high ultimate tensile strength. This is partly because NR is capable of crystallizing at high strain. The crystallites so formed also increase the modulus/stiffness of the material in a manner analogous to the increase in modulus with increasing crosslink density (42). Figure 2.3 shows the monomer and rubber chain.

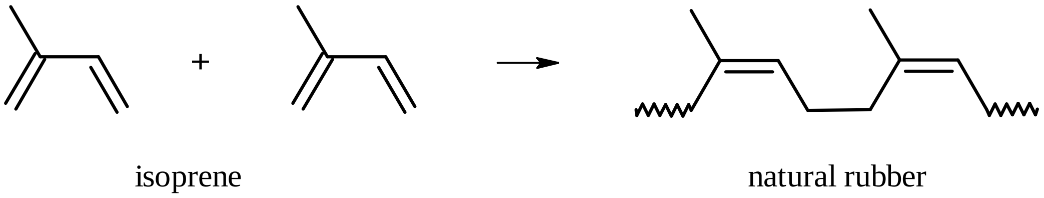

*Figure 2.3 Structure of isoprene (2-methyl-1,3-butadiene) and natural rubber (cis-1,4-polyisoprene)*

NR also contains some fatty acids, proteins, lipids, resins and natural anti-oxidants (35,36,43). During de-vulcanization of NR, the scission of the hydrocarbon molecule is the main reaction and recombination takes place to a much smaller extent than with SBR (5). NR is widely used in truck tyre treads (almost 100%) because of low heat build-up and high cut-resistance but not in the treads of passenger vehicles. In passenger vehicles, it is primarily used in the carcase and sidewall (36).

### 2.2.3 Additives

Additives are chemicals that are used in rubber to speed up vulcanization, increase scorch time (the initiation time before crosslinks form and increase the stiffness of the vulcanizate), decrease processing viscosities and hence energies, and to protect the rubber product from environmental degradation.

Initially only sulfur was used when curing rubber, originally discovered by Charles Goodyear in 1839 (44). The process was lengthy and the final mechanical properties of the rubber were relatively poor. Using accelerators allows the cure rate to be increased to provide acceptable processing times. When using diphenyl guanidine (DPG), one of the first accelerators, and sulfur the final torque was increased but the cure rate was still relatively slow.

Dithiocarbamates and thiuram disulfides with sulfur resulted in a drastic decrease in cure time and increase in final physical properties (45). Using dithiocarbamates, however, introduced a new problem. The problem with dithiocarbamates is that there is a short scorch time which can cause problems with homogeneity when curing. Premature curing during mixing is also possible. When using sulfur and 2,2'-dithiobis(benzothiazole) (MBTS), as well as other benzothiazole-based accelerators, there is an increase in the scorch time but a decrease in the cure rate relative to dithiocarbamates (45).

With the addition of zinc oxide (ZnO) the cure rate increases still further. This is because ZnO acts as an activator which speeds up the vulcanisation process. Stearic acid is also used to increase the cure rate. Just like ZnO it is classified as an activator.

There are also additives that increase the scorch time of rubber compounds, such as N-cyclohexylthiophthalimide (CTP), allowing more time for processing and stopping premature curing. These are known as pre-vulcanization inhibitors (PVI) or retarders.

Adding aromatic and other oils decreases the viscosity of the rubber compound during mixing (46). This results in lower torque during mixing which prevents heat build-up. This is important to prevent the temperature from rising too high and beginning the curing process while still in the mixing chamber. Important energy and thus cost savings are also introduced through the use of such processing aids.

## 2.3 Vulcanization

In its raw state, rubber is a viscoelastic material with fluid characteristics. Vulcanization is also called curing. Curing, however, is a more general term used to describe the crosslinking of any elastomer. Vulcanization usually refers to crosslinking where sulfur and/or a sulfur donor is used as the crosslinking agent. Most industrial curing of rubber is carried out between 150˚C and 190˚C.

Vulcanization using sulfur forms carbon-sulfur (C-S) and sulfur-sulfur (S-S) bonds which stiffens the material. The sulfur crosslinks in rubber can take the form of monosulfidic (C-S-C), disulfidic ($C-S_2-C$) and polysulfidic ($C-S_x-C$, where $x \geq 3$), depending on the curing system used (1). Vulcanization is a multi-step process which involves sulfur, activators and accelerators in order to make the process more efficient. At the start of vulcanization, more polysulfidic crosslinks are formed that contain long sulfur chains than later on in the process.

As vulcanization continues these long sulfur crosslinks are de-sulfurized into shorter polysulfidic crosslinks as well as disulfidic and monosulfidic crosslinks. The extent to which de-sulfurization takes place is partly controlled by the curing system used (1). A generalized scheme for accelerated sulfur vulcanization is provided in Figure 2.4.

During the initial stages of vulcanization, sulfur ($S_8$) is activated by the accelerator when a polysulfidic accelerator complex is formed (47,48), as shown in the top left of Figure 2.4. The polysulfidic accelerator complex (Acc-S-$S_x$-S-Acc) then reacts with the hydrocarbon rubber chain (RH) in two possible ways (major and minor pathways). The minor pathway consists of the activated sulfur being cleaved at a sulfur-sulfur bond. One half of the activated sulfur (Acc-$S_y$) bonds to the hydrocarbon chain with the removal of a hydrogen atom. The hydrogen atom bonds to the other half of the activated sulfur to form more accelerator.

The major pathway consists of the activated sulfur being cleaved at a sulfur-sulfur bond and both halves of the activated sulfur bond to the hydrocarbon chain (Acc-$S_x$-R-$S_x$-Acc). This process removes two hydrogen atoms which react with free sulfur. Accelerator pendent groups are formed on the rubber main chain. Reaction takes place at an α-methylic or α-methylenic carbon atoms (allylic to the double bond of polydiene elastomers) (49).

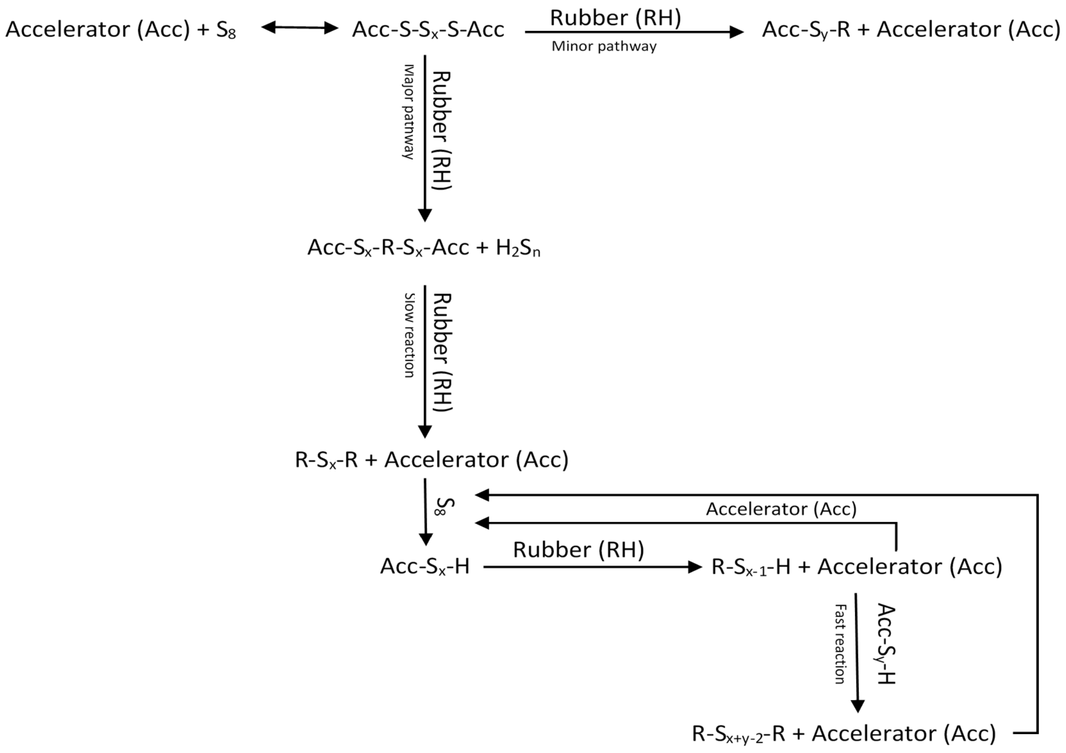

*Figure 2.4 Vulcanization pathway in the absence of an activator (adapted from (50))*

The removal of the accelerators from the hydrocarbon chain is a slow process. During this process the accelerators are removed and the sulfur pendent groups bond to another hydrocarbon chain. The interaction between the sulfur and hydrocarbon removes a hydrogen attached to an allylic carbon to form a crosslink (R-$S_x$-R). The newly created accelerator bonds to the free hydrogen to form a thiol (Acc-S-H). The accelerator, containing the thiol group, activates the free sulfur (Acc-$S_x$-H) and reacts with the hydrocarbon again. This time a thiol group (-SH) is attached to the hydrocarbon and the accelerator is regenerated. The thiol group attached to the hydrocarbon then reacts with a hydrocarbon that contains an accelerator attached to it. This is a rapid process that results in a sulfur crosslink between two hydrocarbons and the regeneration of the accelerator. The accelerators that are created in the final two steps activate the remaining sulfur and the process repeats itself until there is no free sulfur left. Figure 2.4 does not represent other reactions that take place during vulcanization. It is important to state that the sulfur can react with itself forming a pendent group on the hydrocarbon and therefore does not form a crosslink between hydrocarbons. The sulfur crosslinks and pendent groups also undergo modification where the sulfur chains can decrease in length and they can be destroyed. The reaction scheme does not consider the role of ZnO or stearic acid, which increase the reaction rate.

ZnO may be a precursor to zinc-derived accelerators in many vulcanization systems. It reacts with some accelerators, typically thiuram disulfides, to form highly active zinc salts, such as the salt ZDMC (bis(dimethyldithiocarbamate)zinc(II)) derived from tetramethylthiuram disulfide (TMTD) (51). These salts are thought to be responsible for crosslinking. Stearic acid has also been shown to complex with ZnO to form the hydrocarbon-soluble zinc stearate which may make the zinc more available to complex with accelerators (52).

With slower accelerators, such as those containing benzothiazole groups, the mechanism is more complex and the salts formed are less active and likely not responsible for the formation of most crosslinks. A mechanism for such system has been proposed by Boretti (53). Boretti used the model compound, squalene (which contains multiple isoprene units but is small enough to be studied chromatographically), to elucidate the role of ZnO in a curative system that used MBTS as the accelerator. He proposed the following scheme:

The first step in the process is the formation of MBTS polysulfides (MBTPs). ZnO promotes the inclusion of sulfur atoms into the disulfide bond of MBTS. ZnO then further catalyses the reaction between MBTPs and the allylic carbons of polydiene rubbers. In some instances, 2-

mercaptobenzothiazole (MBT) is evolved at this point and this goes on to react with ZnO to form $Zn(mbt)_2$. $Zn(mbt)_2$ and ZnO both catalyse the removal of MBT from the rubber-MBTP pendent complex and facilitate the building of a sulfur crosslink with another rubber molecule

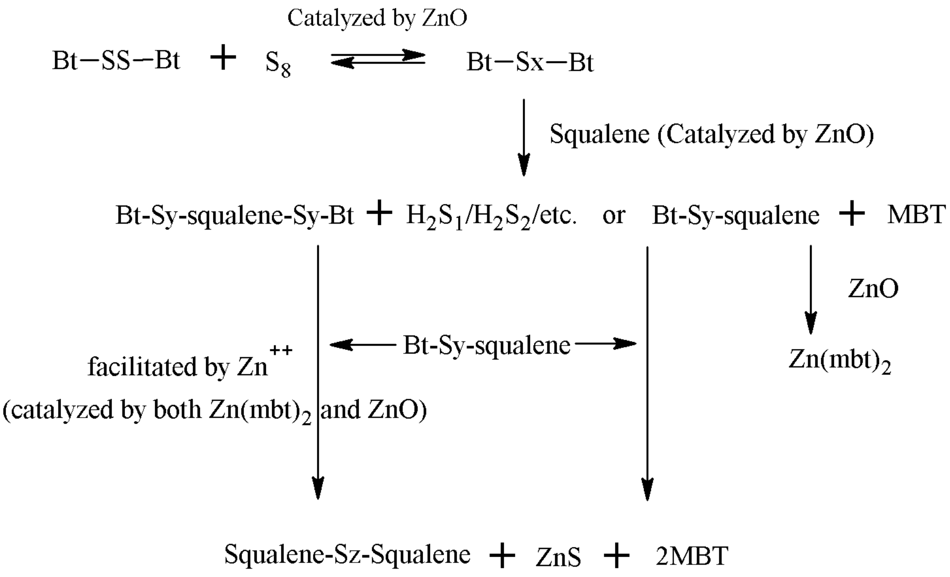

*Figure 2.5 Proposed mechanism for MBTS-accelerated ZnO-activated sulfur vulcanization. Bt = benzothiazole group, MBT = 2-mercaptobenzothiazole, $Zn(mbt)_2$ = zinc mercaptobenzothiolate (reproduced from Boretti (53))*

The MBTPs formed in the presence of ZnO have shorter sulfur chains than those formed where ZnO is absent. ZnO also improves the efficiency of the pendant groups reaction, leaving fewer unreacted. Both these processes lead to an increased amount of crosslinks formed but of a lower sulfur rank (contain fewer sulfur atoms) when ZnO is present (53).

### 2.3.1 Cure rheometry

The process of vulcanizing rubber is easily observed using a rheometer. A rheometer measures the amount of torque required to deform a rubber sample. This is usually done by placing a rubber sample on an oscillating disk (oscillating disk rheometer) or a moving die (moving die rheometer). The moving die is then rotated back and forth through a predetermined range at a certain frequency. The rheometer measures the amount of torque required to maintain this oscillation frequency through the required range while simultaneously applying heat to the sample.

Cure kinetics are easily studied using a rheometer. The torque required to maintain the strain increases with curing; thus providing a graph illustrating the cure kinetics. This graph is known as a cure curve. The resulting plot of torque versus time has three distinct phases which are illustrated in Figure 2.6.

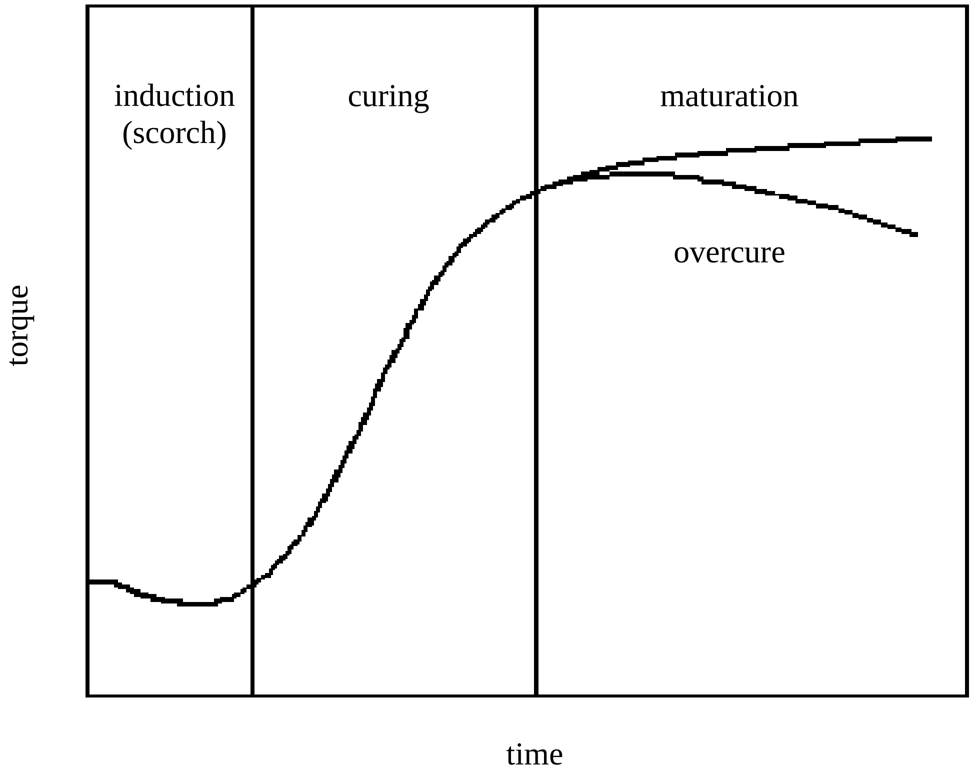

*Figure 2.6 The three phases of the vulcanization process (adapted from Coran (54))*

These phases may be characterized as follows:

***Induction/scorch*:** During this period, preliminary reactions which occur prior to actual crosslink formation take place. Often the torque decreases during this period because the rubber becomes less viscous on heating. The time of induction is also called the scorch time and is usually quantified by $\tau_5$ or $\tau_{10}$. These are the times taken for the torque to rise above the minimum torque to 5 or 10% of the difference between the maximum and minimum torque.

***Curing*:** During this period actual crosslink formation occurs. As crosslinks form, the rubber becomes stiffer because crosslinks act as constraints on mobility. Consequently the torque increases. This region may be characterised by the maximum cure rate (derivative of the torque-time curve), the average rate (the ratio of the difference between maximum torque and minimum torque to the difference between the times taken to reach maximum and minimum torque) or the cure rate index (CRI) (100/(cure time-scorch time)) (55). The end of curing is often defined by the $\tau_{90}$ or $\tau_{95}$ times which are defined analogously to the $\tau_5/\tau_{10}$ times.

***Maturation*****:** Crosslink formation reaches a maximum density for specific rubber / curative system. Crosslinks may break and reform during this period.

***Overcure*** occurs in certain curative systems. In these systems, crosslink scission/breakdown begins to dominate at longer cure times. This scission results in a reversion of the rubber's properties and the subsequent downward slope of the cure curve. This breakdown of crosslinks may also be an artefact of the mechanical stress applied by the rheometer to certain rubber formulations where the rubber becomes too brittle to withstand the applied stress. This is often seen at high crosslink densities.

### 2.3.2 Conventional (CV) vs efficient vulcanization (EV) systems

Depending on the ratio of accelerator to sulfur, a vulcanization system is classed as conventional or efficient. Conventional systems, which are historically older, have lower accelerator to sulfur ratios (0.1-0.6) than efficient systems in which the accelerator to sulfur ratio is high (1.2-2.5) (35). Systems lying in between are called semi-efficient. Efficient systems are so named because they efficiently use sulfur – more crosslinks are formed per unit mass of sulfur added (56).

Different types of crosslinks are formed by CV and EV systems, which in turn leads to differences in mechanical properties. CV leads to primarily polysulfidic crosslinks while EV produces mainly monosulfidic crosslinks (35,56). The tensile properties (tensile strength and tear strength) of these different systems are different over a wide range of crosslink densities. CV vulcanizates have higher ultimate tensile strength (UTS) than EV vulcanizates (45,57). The intrinsic stability of monosulfidic over polysulfidic crosslinks means that EV systems are more reversion resistant (56).

Lal showed that, if polysulfidic crosslinks are converted to mono- and disulfides, there is no appreciable decrease in the tensile strength or flex life of NR vulcanizates (58). This led to the conclusion that polysulfidic crosslinks, by themselves, are not responsible for good physical properties, and other factors following from the curing system, are responsible. Grobler and McGill have proposed that differences in network heterogeneity (in terms of crosslink distribution) are responsible for differences in mechanical properties (59). The degree of network heterogeneity was suggested to decrease in the following order: CV > EV. Following an idea of Hamed (60), areas of low crosslink density in a heterogeneous network are thought to be able to reduce crack growth, thereby increasing the physical properties of such a vulcanizate. Homogeneous vulcanizates do not have such crack blunting areas, resulting in poorer properties.

There is still, nonetheless, no universally accepted theory to explain the higher UTS of CV systems compared to EV systems.

## 2.4 De-vulcanization and reclamation

Before used tyres enter the reclaiming or de-vulcanizing process, they are usually reduced in size through an ambient (dry or wet) or cryogenic grinding process (9,10,17,25). Grinding at an ambient temperature produces rubber granules of uneven shapes and sizes and the surface is very rough. Cryogenic grinding produces rubber granules that have smooth surfaces (10,61). This smooth surface makes the material less suitable for use as a powder filler because adhesion to the smooth surface is poorer than adhesion to a rough surface (10).

Reclamation is the treatment of vulcanized scrap rubber with heat, mechanical energy and chemical agents (24). The end result is the regeneration of the rubber to a state that may again be vulcanized (25). This is usually accomplished through the scission of the main chain carbons as well as carbon-sulfur (C-S) and sulfur-sulfur (S-S) bonds. The reduction of the used rubber through reclamation allows it to be mixed, processed and vulcanized in new materials (5,25).

Vulcanization is the process whereby sulfur is used to create crosslinks between the polymer main chains. Therefore de-vulcanization should be the reverse of this process, namely the removal of sulfur crosslinks. De-vulcanization aims to cleave monosulfidic (C-S-C), disulfidic (C-S-S-C) and polysulfidic ($C-S_x-C$, $x \geq 3$) crosslinks (5). This can be achieved by chemical, microbial, microwave or ultrasound treatments (6,20).

De-vulcanization, however, has not yet advanced to the stage where only sulfur bonds are cleaved. Especially in the presence of oxygen, C-C scission along the polymer backbone cleaves chains and leads to de-polymerization (24). The term, de-vulcanization, is reserved for treatments that cleave primarily sulfur crosslinks while reclamation is used for more general processes which lower vulcanizates viscosity.

The process of de-vulcanization includes reactions such as main chain scission, crosslink scission, main chain modification and crosslink modifications (25). Distinguishing the difference between reclamation and de-vulcanization may not be easy because both methods break similar bonds. The main difference is the ratio with which the C-C polymer main chain bonds are broken compared to sulfur bonds broken. De-vulcanization cleaves more sulfur bonds and fewer main chain carbon bonds than reclamation processes (5). Figure 2.7 illustrates the general differences between the two processes. The de-vulcanization chemicals that are commonly used are, like many accelerators, disulfides such as diphenyl disulfide (DPDS) (62).

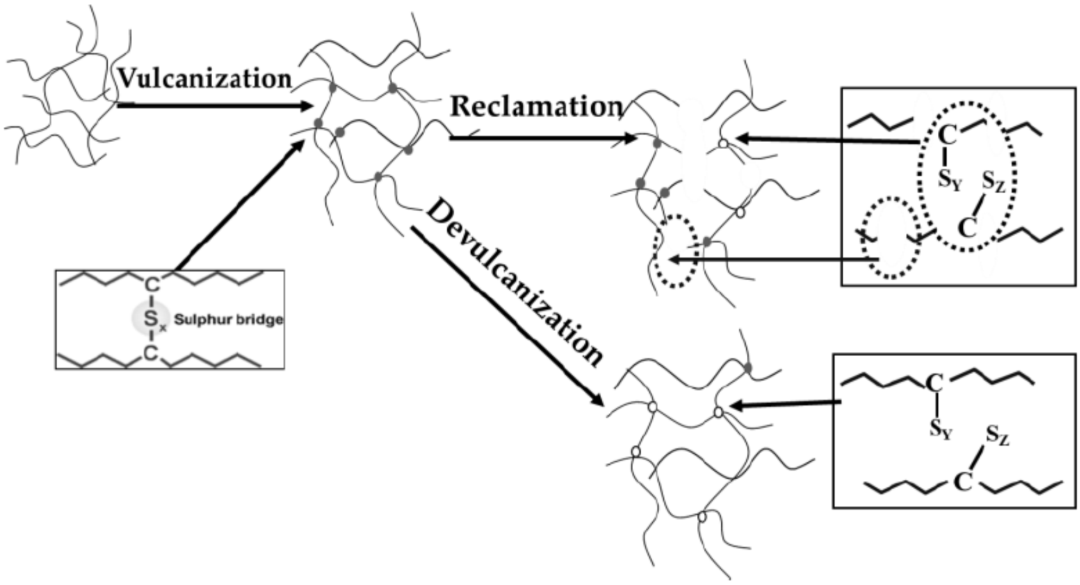

*Figure 2.7 The difference between reclamation and de-vulcanization methods (reproduced from Saiwari (5))*

The breaking of the main chain carbon-carbon bonds influences the devulcanizate physical properties and reduces the quality of the recycled rubber. Due to main chain polymer scission and the recombination of loose chains, the polymer network may become highly branched and thus differs greatly in structure from the original polymer. It is the breaking of the C-C bonds that lead to lower molecular weight polymer chains and therefore decreased physical properties (5). Increasing the de-vulcanization temperature is likely to promote random main chain scission over crosslink scission (63).

Comprehensive reviews of the field have been produced by Adhikari *et al.* (19), Myrhe and MacKillop (64), and more recently by Myrhe *et al.* (15).

## 2.5 Rubber formulation

For any devulcanizate to be successfully used, it must be incorporated into rubber formulations. This is done by comparing the devulcanizate/virgin blend properties with those of a virgin material formulation. This is performed by using a typical tyre formulation such as that shown in Table 2.2. The system in Table 2.2 is considered a semi-efficient curing system as the sulfur to accelerator ratio is approximately 1:1 (35).

Formulation development generally includes the modification of rubber formulation to increase scorch delay as well as including stiffening materials to increase the modulus. For devulcanizates this is achieved by comparing 100% virgin material with blends rather than with 100% devulcanizate material.

The first performance characteristic that is assessed during formulation development is how the formulation mixes. This involves measuring the torque required to mix the formulation in an internal mixer as well as temperature changes during and after the mixing.

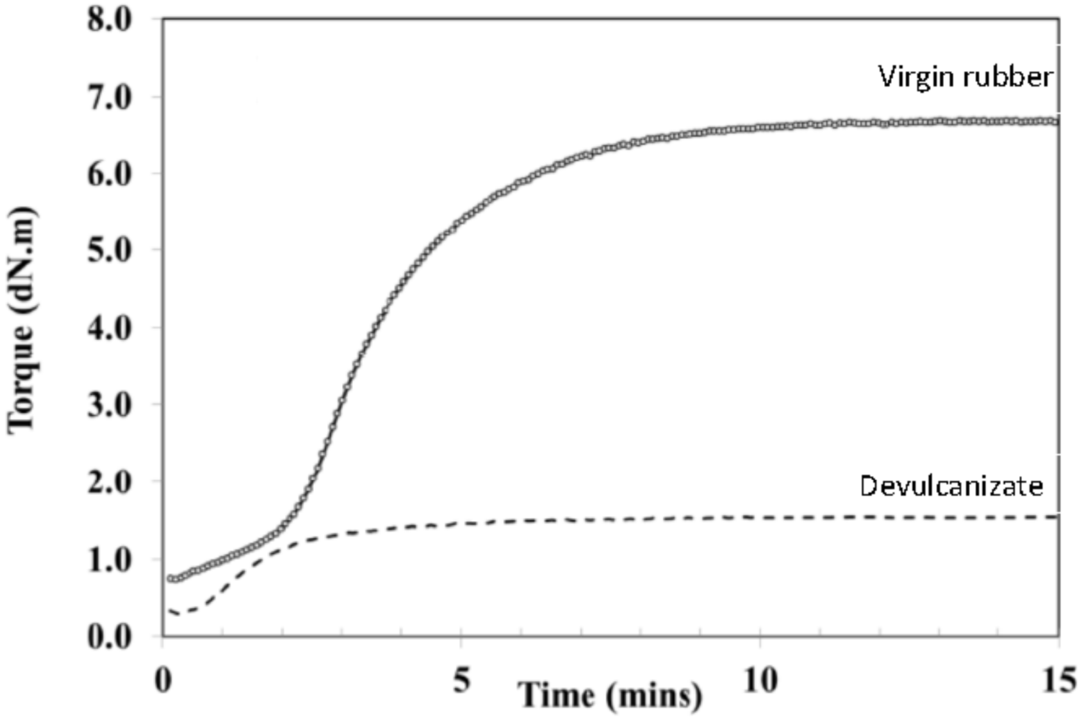

*Figure 2.8 Cure curves comparing 100% virgin material with 100% devulcanizate material (reproduced from Saiwari (5))*

A second performance characteristic studied during formulation development is how the formulation cures (cure kinetics). This involves studying how long it takes to start curing (scorch delay), how fast it cures (cure rate), how much the modulus changes (cure extent) and whether the material degrades (reversion, typically seen as a decrease in modulus at high cure times). A comparison between two cure curves is shown in Figure 2.8. The figure shows a comparison between 100% virgin material and 100% devulcanizate. What is noticeable is the large difference between the modulus of the cured virgin material and that of the devulcanizate. The scorch time of the devulcanizate is also shorter as illustrated by the earlier increase in modulus. This is a common problem experienced when formulating with devulcanizates/reclamates (24).

The last area studied for formulation development is an investigation of properties that are used to predict performance in the field. These properties are measured using a tensometer/tensile tester. Specific properties are studied which include ultimate tensile strength (UTS), extension at break ($\varepsilon_B$) and 100% modulus (the stress at a strain of 100%).

## 2.6 Compositional characterization

A number of methods exist to characterize the composite of rubber vulcanizates and devulcanizates (33). The crosslinked nature of vulcanizates makes it difficult to use solution based techniques such a nuclear magnetic resonance (NMR) spectroscopy although expensive solid state options do exist. Fourier transform infrared (FTIR) spectroscopy is often used but the technique is usually non-quantitative.

Additives are often studied by extraction and examination by gas chromatography (GC) and high performance chromatography (HPLC). These techniques are useful for identifying accelerators and accelerator residues. Unfortunately they are not suitable for identifying species that are bound to the polymer chains. Inorganic species and metals such as Zn may be analysed by ashing, digestion and quantification by atomic absorption spectroscopy (AAS).

Because devulcanizates also contain some crosslinked material, the same analytical problems, as experienced with vulcanized rubber, are also experienced. Two techniques that have been found useful for identifying and quantifying the components (particularly elastomers and fillers) are thermogravimetric analysis (TGA) and pyrolysis-gas chromatography (Pyr-GC) (65,66). A range of other thermal analytical techniques which determine the glass transition temperature ($T_g$) of the sample such as differential scanning calorimetry (DSC) and dynamic mechanical analysis (DMA) have also been used to identify elastomer constituents although their use is more qualitative than quantitative. The use of these and other thermal analytical techniques have been reviewed by Sircar *et al.* (67).

Scanning electron microscopy (SEM), coupled with energy dispersive (X-ray) spectroscopy (EDS), as well as particle sizing and surface area measurement techniques, are commonly used to characterize fillers (neat, and in vulcanizates and devulcanizates). Sample preparation may require the removal of unvulcanized material by dissolution in an appropriate solvent or by pyrolysis/combustion.

### 2.6.1 Thermogravimetric analysis

Thermogravimetric analysis (TGA) is a useful technique in identifying the composition of rubber compounds as well as devulcanizates (68). TGA provides information about highly volatile material, oil, rubber, carbon black and inorganic residues. Three of the earliest systematic applications of TGA to elastomeric systems were by Chiu (69), Maurer (70), and Sircar and Lamond (71).

During thermogravimetric analysis a small sample is heated in an inert (typically pure nitrogen, $N_2$) atmosphere. The different components of the sample decompose/evaporate at different temperature ranges (68). By measuring the mass loss across a certain temperature range under a set heating program, the amount of a specific material can be determined. A swap to an oxygen/air atmosphere will burn off any residual carbon black. This allows the carbon black content of the sample to be determined.

The Discovery series high resolution TGA has several settings to optimise separation of materials in samples being decomposed/evaporated. Two main heating programs used in this study were Hi-Res™ constant reaction rate and Hi-Res™ dynamic rate. These programs continuously modify the heating rate in response to changes in the rate of decomposition of the sample. By doing this the weight changes and the overall length of the test can be optimized. This is done by using a high baseline heating rate, when no weight change occurs, which is automatically lowered when a weight change is detected. At the end of any weight change the heating rate is returned to baseline heating rate (72). The high resolution programs vary the heating rate dynamically during the ramp in response to the derivative of weight change (%/minute). Therefore, when the %/min increases, the heating rate decreases and when the %/minute decreases the heating rate increases. The heating rate can vary between 0.001°C/min (minimum) to a maximum heating rate which can be set (normally between 10-50°C/min) (73).

The Hi-Res™ dynamic mode uses positive resolution settings. A positive resolution setting varies the heating rate between a fixed minimum and the specified heating rate. The heating rate in this mode is never reduced to zero (73). Normal heating rates for this mode are between 10-50°C/min.

The Hi-Res™ constant reaction rate uses negative resolution settings. The TGA varies the temperature of the furnace to maintain a constant preselected rate of weight change (%/minute). When the rate of weight change exceeds the threshold the heating rate is reduced, even to the point of cooling. When the rate of weight change drops below the threshold the heating rate is increased to the set heating rate (73). Heating rates for this mode are between 1-10°C/min. This is to reduce an overshoot of the decomposition range.

Both modes described above uses resolution and sensitivity settings to adjust their responses to the rate of weight change. For the TGA the resolution setting has no units and is used as a way to select the band of %/minute values that are appropriate to the sample being analysed. For Hi-Res dynamic mode the higher the resolution setting (for Hi-Res™ constant reaction rate this will be lower resolution setting) will select a lower %/min value. This will generally mean that there will be a greater separation but a longer experimental time. The resolution settings range between -8.0 to 8.0. Values from -8.0 to 0 are associated with Hi-Res™ constant reaction rate with -8.0 giving greater separation and longer experimental times than -1.0. Values from 0 to 8.0 are associated with Hi-Res™ dynamic with 8.0 giving greater separation and longer experimental times. The closer the resolution number gets to zero the larger the derivative of the rate of weight change must be before the heating rate is reduced, this is shown in table 2.3 (73). A simpler explanation of the resolution is that it controls the temperature at which the transition to a lower heating rate will occur.

Like the resolution number the sensitivity setting has no units. However, the range of sensitivity settings are from 1.0 to 8.0, where 1.0 is the lowest sensitivity setting and 8.0 is the highest. By increasing the sensitivity setting the time to complete the experiment increases. The sensitivity controls the response of the TGA to changes in the rate of reaction. Therefore by increasing the sensitivity the TGA is more reactive to small changes in the reaction rate. By using sensitivity settings in conjunction with resolution settings the rate of weight change range becomes narrower. An example of this works is shown below:

- Resolution 3 has a range of 1.0-20.0 %/minute
- Resolution 4.5 has a range of 0.1-2.0 %/minute

- Sensitivity 1 allows the full range to be used as defined by the resolution number
- Sensitivity 2 allows approximately half the range to be used as defined by the resolution number.

By reducing the range of the %/minute the TGA can bring the furnace to the transition temperature quicker. The downside of this is that the furnace will remain at the temperature for longer. Sensitivity settings are useful for the Hi-Res™ constant reaction rate mode as it helps prevent/reduce the overshoot that can occur with high heating rates (73).

*Table 2.3 The correlation between the resolution setting and the rate of weight change (adapted from (73))*

| *Resolution* | *%/min* |
|---|---|
| *-0.1* | 28.2 |
| *-1* | 10.0 |
| *-2* | 3.16 |
| *-3* | 1.00 |
| *-4* | 0.316 |
| *-5* | 0.100 |
| *-6* | 0.031 |
| *-7* | 0.1000 |
| *-8* | 0.0032 |

Using the derivative curve of the mass loss (as a function of time or temperature) can aid in the identification and quantification of the type of rubber present in a compound. This can be achieved by using a model/fingerprint mass loss curve. The early studies by Maurer (70), and Sircar and Lamond (71) were based in constant heating rate experiments and, while successful at separating oils, elastomers and fillers, were less successful at differentiating between different elastomer types

Fingerprint DTG curves for individual components are fitted to the overall sample DTG curve. Alternatively a kinetic model is developed for the decomposition (usually at constant heating rate) of the constituents (74,75,76). Approaches may use first order models or isoconversional approaches (75). These models are then calibrated by making vulcanizates from known constituents. By fitting the models for the mass loss curves of individual constituents to the mass loss curve of the total sample, it may be possible to quantify the rubber present by regressing the sum of the decomposition models for each component against the overall decomposition thermogram. Such fingerprint/model fitting approaches are often called deconvolution methods. Where only kinetic models are used they are also called kinetic simulation methods.

Figure 2.9 demonstrates how a DTG curve for the decomposition of waste tyres can be deconvoluted into 5 sections/stages – a light fraction, NR (2 decomposition events), BR and SBR. By measuring the area of each of the deconvulted peaks, the mass of each component can be determined. It can be seen that the greatest discrepancy between the cumulative modelled DTG curve and the measure DTG curve is near 400°C where BR begins to decompose. The quantification of BR in the presence of SBR still remains a challenge (76).

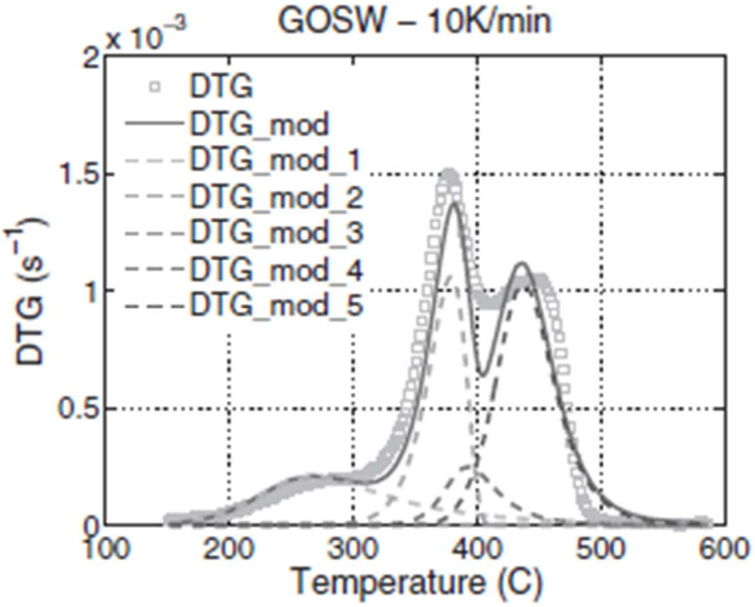

*Figure 2.9 Illustration of the application of deconvolution/curve fitting to the decomposition of a waste tyre sample (reproduced from Danon and Görgens (76))*

TGA has found wide use and success with thus and similar approaches in characterizing simple binary vulcanizates such as NR/SBR and NR/BR blends (74,77,78) as well as more complex ternary systems such as NR/BR/SBR (75) and whole tyres/tyre crumb (76,79). Both kinetic simulation and constant heating rate approaches are limited by the following:

- the individual components may be complex mixtures to which it is difficult to fit preliminary models. Examples include oil extended elastomers in which a heavy oil such as PAH TDAE is used (80). Significant overlap between the oil and elastomer may occur. Although Danon *et al.* have successfully tackled ternary NR/BR/SBR systems, they are yet to explicitly include heavy extender oils which have much more uncertain decomposition kinetics (75).

- the decomposition profile of the rubber changes when it is vulcanized. This can be compensated for by using developing models for vulcanized virgin rubbers instead of de-vulcanized reference materials.
- interactions between components may mean that their decomposition profiles are very different to the individual reference materials. Components may stabilize each other, increased stabilization of NR (increasing the decomposition temperature range) has been observed in blends with SBR as the SBR content increases (65,78). Such changes are often ignored, *e.g.* Danon *et al.* parameterized their approach using unvulcanized elastomers (75) which was then applied to waste tires (76). While NR was found to be relatively easy to quantify, the close decomposition temperatures of BR and SBR, meant that their accurate quantification remains a challenge.
- when decomposition is promoted by the presence of metallic or inorganic catalysts. This can be a problem with devulcanizates which are produced by a catalytic process.
- the vulcanizates/devulcanizates may contain components for which no model has been developed. This is especially true of the wide variety of oils, waxes, processing aids and peptizers added to rubber. It is, in some circumstances, possible to evaluate/quantify these components as OTHER by subtraction of well defined modelled compounds from the decomposition thermogram of the entire sample. If the OTHER component is relatively simple, it is possible to develop a model for its decomposition from the decomposition of a sample in which all but the OTHER component are known. Danon and Görgens have used this approach to quantify light volatiles which do not overlap with NR, BR or SBR significantly (76).
- when the decomposition produces char, the amount of char formed is heating rate dependent. Spurious quantification of carbonaceous material impacts on quantification of all other components (80).
- the devulcanizate contains an entirely unexpected constituent whose decomposition character depends on physical parameters such as molecular size, *e.g.* in some devulcanizates, there may be close overlap of the evaporation/decomposition of different fractions of the material which may complicate analysis where one

component is poorly understood. An example of this could be decomposition/evaporation of the oil fraction coinciding with a low molecular weight de-vulcanized polymer.

- peak overlap is significant such as the case with BR/SBR blends that the model fitting contains significant errors. It is possible for some SBR-OE compounds to look very similar to BR/SBR blends.

A simpler alternative to kinetic model simulations in binary NR/SBR blends that has found some success is to calibrate the ratio of the height of the two polymer decomposition peaks against the NR/SBR ratio (65,74). Because such calibration curves are often highly curved, they are associated with large uncertainties.

Another approach is to use a calibration curve obtained by correlating a temperature that corresponds to a fixed % mass loss of the original sample mass with the amount of one of the elastomers in the blend (66,81,82). This approach is much more linear and less prone to error. Unfortunately both approaches fail when one is presented with overlapping peaks of three components.

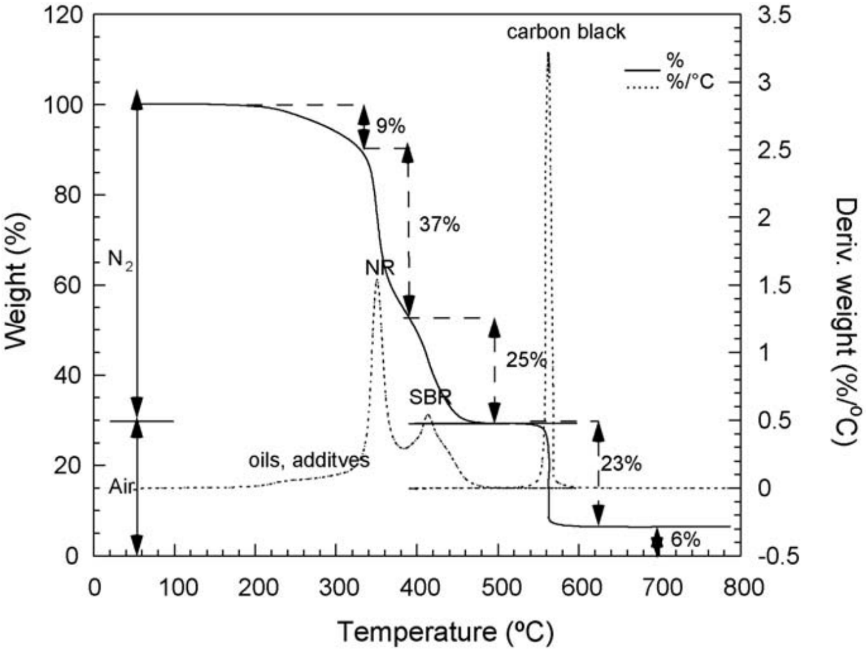

*Figure 2.10 High resolution TGA-DTG analysis of a 60/40 NR/SBR vulcanizate (reproduced from Fernandez-Berridi et al. (65)*

Figure 2.10 shows that high resolution thermogravimetry can be used to analyse a reference model vulcanizate. The decompositions of NR and SBR are sufficiently far apart to use the minimum in the DTG curve as the separation point for the quantification of these two types of rubber. It can be seen, however, that the oils do not separate completely from the NR. The presence of heavy oils is often a confounding factor which introduces uncertainty. Where the oil decomposition overlaps with polymer decomposition, the oil content is often over-estimated and the polymer content underestimated.

Because of the above difficulties, efforts have moved to use variable heating rate methods (determined by the rate of mass loss). These are known commonly as high resolution methods (80,83,84). These methods allow for greater separation to be achieved which in many cases is sufficient to allow quantification without model fitting, although more complex model fitting is also possible in a variable heating rate environment.

## 2.7 Devulcanizate fractionation

By separating the devulcanizate into smaller fractions, it is possible to identify the various components present in the sample. By separating the sol and gel fractions, a determination can be made on the quantity of polymer that is still crosslinked. This fraction will not dissolve in any solvent because it is still crosslinked. By using solvents that are polar, aromatic in nature or linear molecules with no polarity, various chemicals can be removed from the devulcanizate such as processing oils and curatives.

### 2.7.1 Solvents

Solvent extraction can be used to isolate various chemicals present in a rubber sample. Solvents are used to separate out the soluble components (curative residues, oils, uncrosslinked polymer) from the insoluble fraction (crosslinked rubber, fillers). Solvents that have been used for extraction, include toluene (26,85), acetone (86), combinations of acetone and tetrahydrofuran (THF) (27,87,88). Shi *et al.* have claimed that an extraction using acetone removes processing oils while a secondary extraction using toluene removes soluble (de-vulcanized) rubber (89). The structures of toluene, THF, acetone and *n*-hexane are presented in Figure 2.11.

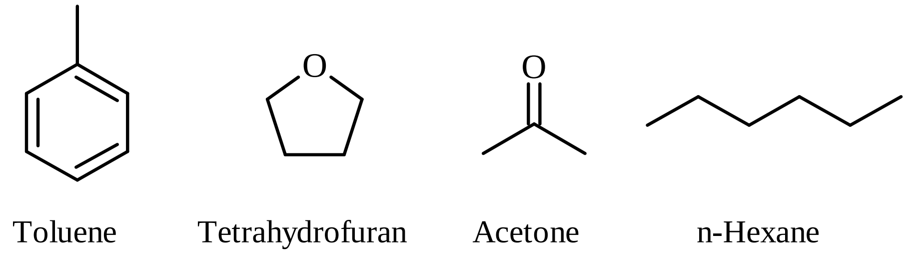

*Figure 2.11 Chemicals used in the solvent extraction of rubber devulcanizates*

### 2.7.2 Soxhlet extraction

During sulfur vulcanization of rubber material, the long hydrocarbon chains are joined together by sulfur crosslinks. This crosslinking prevents the flow of the rubber chains which results in an elastic material. Under compression and at an appropriate temperature the sulfur forms mono-, di- and polysulfidic bonds. Not all of the polymer chains react in this way and some are left free (68). Figure 2.12 illustrates this process.

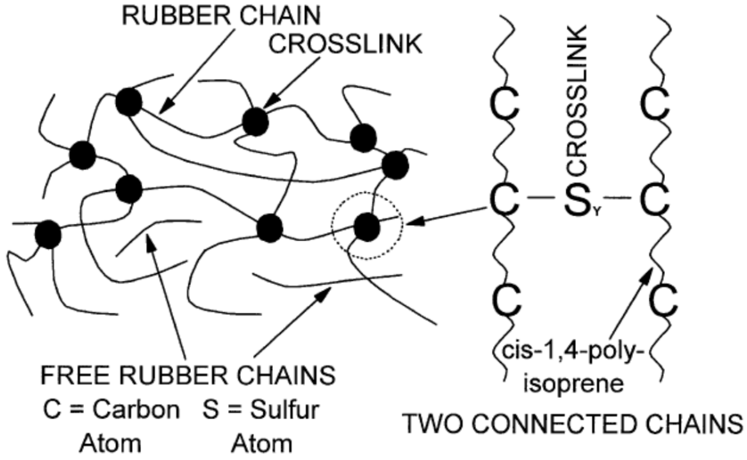

*Figure 2.12 A sulfur vulcanized polymer network (reproduced from Bilgili et al. (68))*

The linked rubber chains form part of the gel fraction and the free rubber chains form part of the sol (soluble) fraction. The gel fraction can only be swollen in a solvent whereas the sol fraction can be dissolved in a suitable solvent (68).

The breaking of C-C, C-S and S-S bonds during de-vulcanization results in the formation of soluble branched structures, known as the sol fraction, and fragmented crosslinked polymer fragments known as the gel fraction (25). Soxhlet extraction can be used to separate the soluble (sol) and insoluble (gel) fractions (68). Solvents such as acetone and THF have been used (62).

### 2.7.3 Gel content

The mechanical properties of rubber depend on the crosslink density. The properties are also influenced by the ratio of mono-, di- and polysulfidic crosslinks. The tensile strength of rubber is improved with an increase in polysulfidic crosslinks while a decrease in tensile strength is noticed with an increase in mono- and disulfidic crosslinks (25,45). An increase in the mono- and disulfidic crosslinks may cause an increase in the modulus of the rubber (25).

Because most commercial rubber recycling processes cause simultaneous main chain scission and sulfur crosslink cleavage it is important to have a method to characterize the degree of crosslinks in vulcanized rubber (1). A swelling test may be used to determine the degree of crosslinking in the gel fraction.

Figure 2.13 illustrates the dependence of some properties on crosslink density.

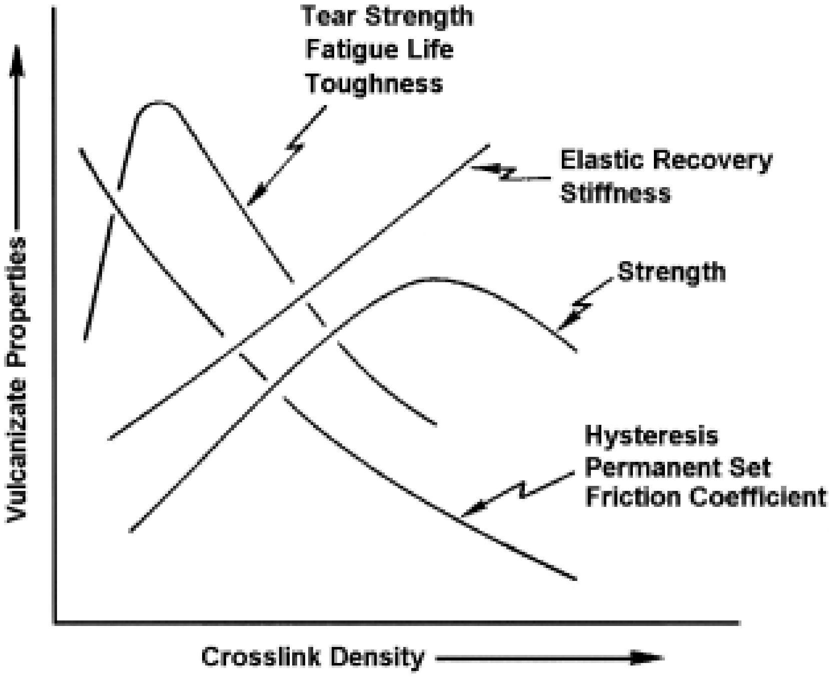

*Figure 2.13 Physical properties dependent on crosslink density (reproduced from Coran (90))*

The relationship between the physical properties and the crosslink density can be used to put the results obtained in this study in context. Two main properties that are commonly tested are ultimate tensile strength and elongation at break. A drop in the tensile strength with an increase in elongation at break would suggest that there has been a decrease in crosslink density.

# CHAPTER 3

# 3 EXPERIMENTAL PROCEDURE

## 3.1 Materials

### 3.1.1 Elastomers

Natural rubber (SMR20) was supplied by Continental Tyre (Port Elizabeth, South Africa). Oil extended styrene butadiene rubber (SBR-OE, Afsol 764) was obtained from Karbochem (Sasolburg, South Africa). This is a solution polymerised SBR, which contains 25% styrene and is extended with 37.5 phr of low polyaromatic hydrocarbon (PAH) residual aromatic extract (RAE) oil (38). Waters (Milford, MA) polyisoprene sample(s) ($M_w$ = 810, 36 200, 2 830 000 Da) was used as a reference standard.

### 3.1.2 Devulcanizates

A novel devulcanizate was supplied by New Reclamation Group (Johannesburg, South Africa). This, which had the appearance of a highly viscous oil, was produced by a proprietary high temperature process (29). A second devulcanizate sample, of a much firmer composition, used for comparison was supplied by Bridgestone (Port Elizabeth, South Africa). This sample was supplied with information that it was high in NR content (91), suggesting that its original source was a tyre tread compound, probably from truck tyres (8). This sample will henceforth be referred to as *commercial reclaim*. Note that the term, reclaim, is widely used in the tyre industry and is used interchangeably with devulcanizate throughout this dissertation.

### 3.1.3 Curatives and processing oils

The fillers, accelerators and activators were all supplied by S&N Rubber (Port Elizabeth, South Africa) and were not purified before use. Sulfur was of the rhombic form, which was confirmed by DSC analysis. The thermogram can be seen in appendix C. An α-β transition at 104°C and a melt at 119°C was observed, these two observation are consistent with rhombic sulfur (92,93).

A naphthenic processing oil was supplied by S&N Rubber while a sample of the processing oil (used by NRG, during the manufactured of their devulcanizate) were supplied by NRG.

### 3.1.4 Solvents

The solvents used were obtained from Sigma Aldrich (St Louis, MI, USA) and were used as received. All solvents were analytical grade.

### 3.1.5 Gases

All gases (nitrogen, dry air and oxygen) were obtained from Afrox (Johannesburg, South Africa). All nitrogen had a purity in excess of 99.999%.

## 3.2 Sample mixing and curing

### 3.2.1 Weighing

All curatives, rubber, fillers and reclaim were pre-weighed, before mixing, using a Mettler BB 240 top pan balance.

Measurements of masses for the determination of extractables and crosslink densities were made using a Sartorius Mettler AB204-S analytical balance.

Samples for DSC experiments were weighed using a Mettler UMT2 microbalance.

### 3.2.2 Mixing

*Table 3.1 Reference formulation used (adapted from a passenger tyre tread recipe in (94))*

| *Component* | *phr* | *% (by mass)* |
|---|---|---|
| *SBR OE* | 50* | 32.51 |
| *NR* | 50 | 32.51 |
| *Carbon black N-220* | 45 | 29.26 |
| *Sulfur* | 1.6 | 1.04 |
| *CBS* | 0.8 | 0.52 |
| *DPG* | 0.4 | 0.26 |
| *ZnO* | 3 | 1.95 |
| *Stearic acid* | 3 | 1.95 |
| *Total* | 153.8 | 100.00 |

* The SBR contained 27.3% oil which forms part of the 100 parts total rubber

This formulation is representative of older passenger tyre tread formulations as little NR is used in modern passenger tyre treads. It is, however, similar to some truck tread and many sidewall formulations (35). For this study, a conventional vulcanization system was selected. One of the characterizing features of this system is a relatively low accelerator to sulfur ratio. This is expected to result in the formation of a high degree of polysulfidic crosslinks and cyclic structures (1,56). Table 3.1 contains the formulation, produced from virgin rubber materials, that was used as a reference material for all mixing, curing and physical property testing.

When reclaim was added, it was added either as a substitute for the NR and SBR-OE equally or was added in addition to the 50 phr of these as in Table 3.1. Details of the formulations that contained reclaim may be found in Appendix A.

The amount of each component required was determined using the equation below

$$m_r = \frac{v_h F_f}{\left(\frac{1}{\rho_r} + \frac{1}{100}\sum_{n}^{i=1}\left(\frac{phr_i}{\rho_i}\right)\right)} \tag{3.1}$$

$$m_i = \frac{phr_i \times m_r}{100} \tag{3.2}$$

where $m_r$ = mass of rubber component (g)

$v_h$ = volume of mixing head (330 mℓ)

$F_f$ = fill factor (0.75)

$\rho_r$ = average density of two rubber components (g/mℓ)

$\rho_i$ = density of ingredient (g/mℓ)

$phr_i$ = parts per hundred rubber of ingredient (i)

$m_i$ = mass of ingredient (g)

Mixing of pre-weighed components was performed in a Banbury internal mixer with a fill factor of 0.75 and a chamber volume of 330 mℓ. The mixing speed used was 60 rpm for all formulations. The data collected (temperature and mixing torque) was sampled at 2 Hz. Because the torque data was extremely noisy, a 4th order Butterworth low-band pass filter was used to smooth the measured torque data (95). The settings for this filter was a sampling frequency set as 1Hz and a cut-off frequency of 0.04 Hz was used.

The mixing steps were as follows:

- The two rubber components were added and mixed for 2 min.
- The carbon black was then added and mixed for 2 min.
- The activators (zinc oxide and stearic acid) were added and mixed for 2 min.
- Lastly accelerators and sulfur were added and mixed for 2 min.

The mixing procedure was designed so that the mixing temperature did not exceed 100°C so that premature vulcanization did not occur. This is below the melting temperature of rhombic sulfur (115.2°C (92)), above which temperature accelerator polysulfides have been known to form (96).

When the NRG reclaim was added to the formulation a modification to the procedure was necessary. Three quarters of the virgin rubber was added and allowed to mix for 2 min. The reclaim was added together with the remaining rubber. The last quarter of the rubber was used as a “spatula” to add the reclaim as the reclaim was highly viscous. The mixture was mixed for 2 min and the rest of the procedure followed on as described above.

The sample was then removed and placed in a two roll Schwabenthan mill. The roller speeds were 13.1 rpm and 11.6 rpm. The mill was set to a nip size of approximately 4 mm. The sample was passed through the mill 3 times. Between each pass the sample was rotated through 90°.

### 3.2.3 Rheometer

A MonTech Moving Die Rheometer 3000 (MDR) was used to study the cure kinetics of the unvulcanized samples. Prior to use the rheometer was pre-heated to the appropriate curing temperature. The temperature used for curing in this study was 160°C. The sample was subject to an oscillatory torque with a frequency of 1.67 Hz and an arc of 0.5°. The sample size was approximately 8.5 g.

### 3.2.4 Curing

Sample pads were cured isothermally in an electrically heated vulcanization press at 160°C and a pressure of 5 MPa. Approximately 50 g of uncured rubber compound was placed between two pre-heated stainless steel platens which were immediately place in the vulcanization press. To facilitate removal of the cured rubber from the moulds, the moulds were lined with thin, disposable Mylar sheeting. One of the platens was cut to form a mould so that a pad of thickness, 1.75 mm, could be produced. Samples were cured till 90% of maximum cure was achieved, based on times obtained from rheometer experiments. On completion of curing, the cured rubber pad was remove from between the platens and quenched in cold water.

## 3.3 Thermal analysis

### 3.3.1 Thermogravimetric analysis

Initial thermal analysis was performed on a TA Instruments Q600 simultaneous differential scanning calorimeter and thermogravimetric analyser (SDT). The SDT not only measures the change in mass with respect to temperature but also the heat flow of the sample.

The SDT was calibrated for temperature using the melting temperature of pure samples of In (156.61ºC), Sn (231.88ºC), Pb (327.46ºC) and Zn (419.53ºC). Heat flow was calibrated using the enthalpy of fusion of In (28.58 J/g). Mass was calibrated using reference mass standards.

All samples were placed in open platinum pans under a nitrogen atmosphere with a gas flow rate of 30 mℓ/min. Sample size was approximately 3 mg. The heating program to which samples were exposed was as follows.

- Samples were heated from ambient temperatures at 10°C/min to a temperature of 700°C in nitrogen.
- The furnace was then cooled at 50°C/min to 350°C.
- The gas was changed to oxygen.
- The sample was heated at 50°C/min to 650°C.

A TA Instruments Discovery Series Hi-Res™ thermogravimetric analyser (TGA) was used for later analysis. The TGA was calibrated for temperature using the Curie points of samples of alumel (152ºC), Ni (354ºC), an 83% Ni/17% Co alloy (554ºC), a 63% Ni/37% Co alloy (746ºC) and a 37% Ni/63% Co alloy (931ºC). Mass was calibrated using reference mass standards.

The sample size was approximately 10 mg. This mass was chosen to reduce sampling errors, especially of the highly viscous NRG reclaim material. Samples were placed in open Pt high temperature 100 μℓ crucibles.

The Hi-Res™ TGA has the option of applying dynamic heating rates allowing for a higher resolution when analysing samples. Dynamic heating rates are heating rates that respond to the rate of mass loss. As the TGA furnace is heated, the sample decomposes/evaporates and the mass change with respect to temperature is recorded. The approach of Fernandez-Berridi *et al.* was used as a starting point for method development (65).

A number of program variables such as base heating rate, resolution and sensitivity were investigated in preliminary experiments (Section 4.1). For final characterization experiments the TGA was used in Hi-Res™ dynamic mode with a heating rate of 20°C/min, resolution of 5 and a sensitivity setting of 1. Initial decomposition was performed in 99.999% $N_2$ at a flow rate of 25 mℓ/min, the atmosphere was changed to dry air at 500°C or 600°C and the sample was then heated to 800°C. Because carbon black is sensitive to very low levels of oxygen, the ultra-high purity nitrogen gas was scrubbed of oxygen and moisture by passing the gas through Agilent $H_2O$ and $O_2$ traps.

A comparison of the usefulness of the SDT and the Hi-Res™ instruments may be found in Appendix B.

### 3.3.2 Differential scanning calorimetry

Glass transition temperatures were determined using a TA Instruments Discovery Series differential scanning calorimeter (DSC), fitted with a liquid nitrogen cooling accessory (LNCA). The DSC was calibrated for temperature using the melting temperature of pure samples of Hg (-38.83°C), In (156.61°C), Sn (231.88°C), Pb (327.46°C) and Zn (419.53°C). Heat flow was calibrated using the enthalpy of fusion of In (28.58 J/g). Heat capacity was calibrated using reference sapphire crystals.

Pre-weighed samples were sealed using Al $T_{ZERO}^{TM}$ pans and lids. An empty $T_{ZERO}^{TM}$ pan and lid was used as a reference. Samples were cooled to -140°C and then heated at 10°C/min to ambient temperature. $N_2$ was used as purge gas at a flow rate of 25 μℓ/min. Glass transition temperatures were determined at the inflection points of the heat flow signals.

## 3.4 Physical property measurement

### 3.4.1 Tensile testing

Tensile testing was done on an Instron 4411 tensile tester, fitted with a 1 kN load cell. The crosshead speed was set to 200 mm/min. All test specimens were cut using a dumbbell cutter. The dumbbells had dimensions consistent with type D in ASTM test method D412 (97). An Instron long travel extensometer with gauge length of 25 mm was employed. The stress at 100%, 200%, 300% extension, elongation at break ($\varepsilon_B$) and ultimate tensile strength (UTS) were recorded. The thickness of each sample was measured using a Wallace 2S micrometer. 5 dumbbells were cut for each test material. Data reported are the average of measurements on these 5 test pieces. Where dumbbells slipped in the grips during testing, these tests were discarded as outliers and average data were calculated using the remaining tests.

### 3.4.2 X-ray diffraction analysis

A Bruker D2 phaser X-ray diffraction (XRD) instrument was used to identify the ash content of the gel fraction after Soxhlet extraction. The instrument was set to have a tension parameter of 30kV and a current of 5mA. The X-ray source used was Cu $K_\alpha$ with an anti-scatter slit width of 1mm. Data was collected over a 2θ range of 5 to 70°. The sample stage mode was set to spinning with 20 rpm. A continuous scan mode was used. The data base used to analyse the results was Bruker EVA software.

## 3.5 Solvent exposure experiments

It is important to characterize the devulcanizate so that the materials and chemicals necessary for mixing can be adjusted. The chemical and material composition is important because they affect the mechanical and viscoelastic properties. An important parameter is the extent to which the reclaim has been de-vulcanized. This can be tested by ascertaining how much of the polymer is able to dissolve in an appropriate solvent (5).

### 3.5.1 Solvent extraction

A small sample of the reclaim (approximately 0.5 g) was weighed out in a centrifuge tube which was filled to the 10 mℓ mark with one of the solvents. The centrifuge tubes were shaken by hand for 1 minute and then centrifuged for 1 minute. The solvent was decanted leaving behind any insoluble residue. Any remaining solvent was then evaporated off in a vacuum oven (< 10 mmHg) for 3 h at 70°C. The dried sample was weighed and the percentage extracted solute was calculated. TGA was carried out on the gel (residual) and sol (soluble) fractions. Extractions on NRG reclaim were performed in duplicate; and single experiments for the commercial tyre tread reclaim.

### 3.5.2 Soluble (sol) and insoluble (gel) fractions

A sample was placed in Whatman 100 filter paper which in turn was placed into a thimble and sealed with a piece of cotton wool. The thimble was placed inside a Soxhlet apparatus. The extraction was carried out for a total of 24 h. The solvent used in the Soxhlet extraction was dichloromethane ($CH_2Cl_2$). This extraction method was extended to include a wash using acetone. When the extraction had been completed the thimble was removed and the sample in the filter paper was dried and weighed. This constitutes the gel fraction.

The solvent used in the extraction was contained in a round bottom flask beneath the Soxhlet apparatus. The solvent in the flask contained all soluble material extracted from the sample. At the end of the experiment the solvent was evaporated off and what was left behind was weighed as the sol fraction.

Dijkhuis used acetone to remove activators and accelerators and followed up the extraction with THF to remove oil and soluble material (1). Following this procedure the sol fraction was further treated with acetone to remove additives, decanted and the solvent allowed to evaporate. The sol fraction was then washed with toluene to remove the rest of the sol fraction from the round bottom flask.

### 3.5.3 Crosslink density determination

To calculate crosslink density, the samples had to be swollen in a suitable solvent. All experiments were performed in duplicate. Pre-weighed samples, weighing approximately 0.4 g were placed in 100 mℓ toluene, for 72 h at room temperature out of direct sunlight. The toluene was exchanged with fresh toluene every 24 hours. This was done to ensure that all extractable material (ie: oil) was removed and that the solvent didn’t become saturated. The solvent was clear by the end of the 72 hours.

After 72 h the samples were removed from the toluene and gently dried by dabbing the surface with tissue paper. The swollen sample was then weighed.

The samples were left to dry in a fumehood for 24 h to allow the solvent to evaporate. TGA analysis revealed no weight loss on the thermogram at low temperatures. It was determined that 24 h was sufficient to evaporate all of the solvent. The samples were then weighed again. To calculate the gel and sol fraction the following equations were used (98):

$$sol\ \ fraction\ (\%) = \frac{w_i - w_f}{w_i} \times 100\,\% \tag{3.3}$$

$$gel\ \ fraction\ \ (\%)\ = 100\,\% - sol\ \ \ fraction\ \ (\%) \tag{3.4}$$

where: $w_i$ = initial sample mass before solvent exposure

$w_f$ = final dry sample mass after solvent exposure.

The Flory-Rehner equation was used to calculate the crosslink density (99).

$$XLD = \frac{v_r + \chi v_r^{\ 2} + \ln(1 - v_r)}{V_s\left(Bv_r - A\eta(v_r)^{1/3}\right)} \tag{3.5}$$

where $v_r$ = the volume fraction of rubber in the swollen gel

$XLD$ = crosslink density per unit volume

$\chi$ = the Flory-Huggins polymer-solvent interaction parameter

$\eta$ = ratio of the r.m.s. length of the chain-end distance in the crosslinked network to free chains. For most situations this is 1.

$A,B$ = constants depending on the theoretical treatment used. For the purposes of this study, the most commonly used values of A = 1 and B = ½ were used (100,101).

$V_S$ = molar volume of the solvent, 106.2 cm$^3$/mol (102)

The volume fraction was calculated using the following equation.

$$v_r = \frac{\frac{m_r}{\rho_r}}{\frac{m_r}{\rho_r} + \frac{m_S}{\rho_S}} \tag{3.6}$$

where: $m_r$ = mass of the dried rubber after swelling,

$m_S$ = mass of the solvent in the swollen rubber (determined as the mass of the swollen sample minus the dried sample),

$\rho_r$, $\rho_S$ = density of rubber and solvent respectively.

For the rubber-toluene system, a Flory-Huggins interaction parameter with a value of 0.3795 was used (103,104).

The volume fraction of rubber in the swollen gel was determined by knowing the masses of the rubber before and after swelling as well as the density of the rubber and that of the solvent. The density of the rubber can be determined with the use of a pycnometer and the following equation.

$$Gs = \frac{m_s}{m_s + m_{b,w} - m_{b,w,s}} \times \frac{\rho_w}{\rho_{w(20)}} \tag{3.7}$$

Where: $G_s$ = Specific gravity

$m_s$ = mass of sample

$m_{b,w}$ = mass of water and pycnometer

$m_{b,w,s}$ = mass of pycnometer, water and sample

$\rho_w$ = density of water

$\rho_{w(20)}$ = density of water at 20°C

It should be noted that the samples contain a filler and so should in fact include a Kraus correction (105). However, because of uncertainties about the nature of the filler in the devulcanizates, uncertainty existed about which Kraus parameters to use. A Kraus correction was thus not performed and reported crosslink densities are effective crosslink densities rather than true chemical crosslink densities. Nonetheless their relative sizes provide meaningful information about which samples are more crosslinked than others.

# CHAPTER 4

# 4 CHARACTERIZATION

## 4.1 TGA characterization method development

Initial method development was performed using a TA Instruments Q600 simultaneous differential scanning calorimeter and thermogravimetric analyser (SDT). Problems with complete purging of the large SDT furnace to remove any residual oxygen/air meant that experiments were switched to a TA Instruments Discovery Series Hi-Res™ thermogravimetric analyser which has a smaller furnace which is more easily and thoroughly purged. Details on preliminary experiments using the SDT may be found in Appendix B.

Mass loss controlled heating rate or high resolution TGA was optimized to characterize the devulcanizates. Henceforth such techniques will be referred to using the name used by TA Instruments, *i.e.* Hi-Res™. Two potential programs were identified namely Hi-Res™ constant reaction rate and Hi-Res™ dynamic. The two programs were compared to each other before deciding to use the Hi-Res™ dynamic mode. The Hi-Res™ dynamic mode slows down the heating rate when the rate of weight change exceeds a threshold, the baseline heating rate is returned to when the rate of weight change drops below the threshold. The Hi-Res™ constant reaction rate stops the heating of the sample when a weight change is detected. When the weight change is detected the program keeps the temperature isothermal until the decomposition is complete. In order to do this the TGA will also cool down so that the temperature at which decomposition started can be maintained. Figure 4.1 shows the results of the Hi-Res™ constant reaction rate program using the standard rubber formulation.

In Figure 4.1 a) the ramp rate was set to 50°C/min with a resolution of -4 and a sensitivity of 1. The time to complete the experiment was approximately 225 minutes. In Figure 4.1 b) the ramp rate was set to 20°C/min with a resolution of -2 and a sensitivity of 1. The time to complete the run was approximately 40 minutes. In both thermograms the cooling of the furnace, to maintain a constant temperature, is noticeable as a decrease in temperature between 300 and 350$^{o}$C when a rapid mass loss occurs. With an increase in the resolution number (for Hi-Res™ constant reaction a resolution setting of -1 has a larger detection range than -4 making it less effective) the cooling is more noticeable. The cooling and isothermal temperatures make analysing the derivative curves difficult as the slopes changes sign when the furnace cools. The overshoot of the heating program can be clearly seen in Figure 4.1a at 300°C. The derivative curves have been omitted from Figure 4.1 for clarity but can be seen in the appendix D. As will be seen in section 4.1.1 the Hi-Res™ dynamic program had comparable separation to the Hi-Res™ constant reaction but with faster testing times.

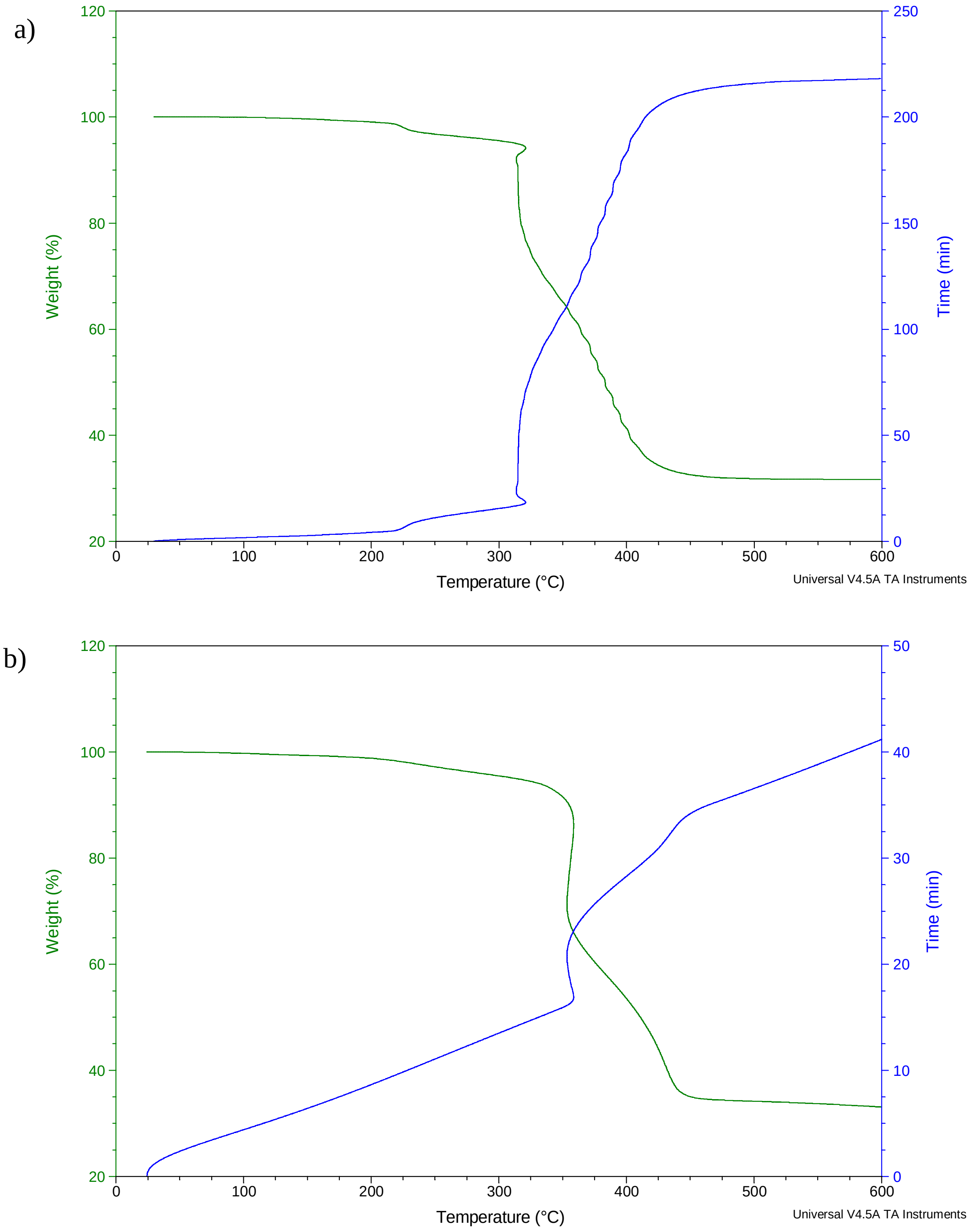

*Figure 4.1 Thermograms of standard rubber formulation using the Hi-Res™ constant reaction rate program. 4.1a) shows the heating rate of 50°C/min with a resolution of -4 and sensitivity 1. 4.1b) shows the heating rate of 20°C/min, resolution of -2 and sensitivity 1.*

### 4.1.1 Effects of resolution and sensitivity parameters

The Hi-Res™ constant reaction rate program was deemed inadequate for the type of analysis that was needed. This was decided on the basis that the experiment times were too long and the derivative curves were difficult to compare and analyse. This can be seen in appendix D. Therefore the Hi-Res™ dynamic mode was chosen. The thermograms below are of the standard rubber formulation which was analysed using the Hi-Res™ dynamic mode. Included in the development process was an assessment of the effect of changing the resolution and sensitivity settings on the Hi-Res™ dynamic mode. This was carried out on the standard rubber formulation. Once the effects of the resolution and sensitivity settings were established a standard TGA test method was developed. The standard TGA test method was then further optimized for the best separation of the materials present in the devulcanizate. The figures shown below are of the model tyre tread compound, containing NR and SBR, which was formulated and used as a test standard (see Table 3.1).

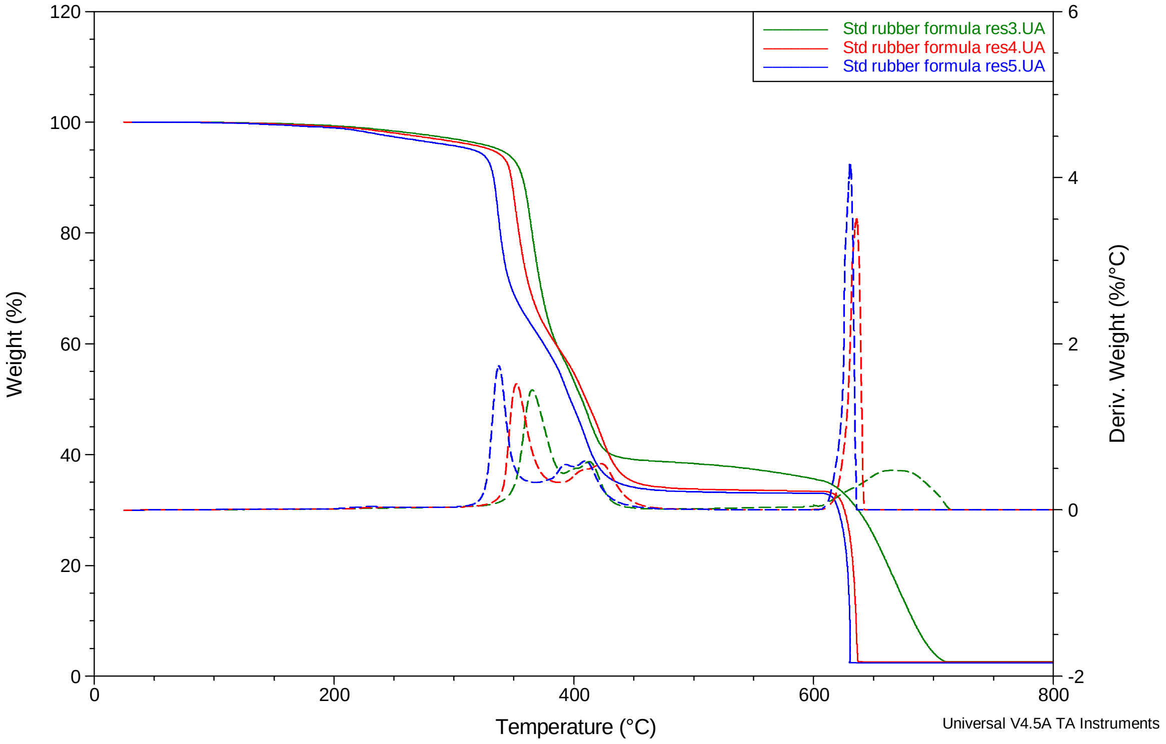

*Figure 4.2 The effect of resolution on the separation of components of a reference tread formulation. Sensitivity = 1. Resolution = 3 (green), 4 (red) and 5 (blue). Initial atmosphere = $N_2$; switch to $O_2$ at 600°C. Base heating rate = 50°C/min*

The dashed lines in the figure are the derivatives of the weight percentage curves. The colours of the derivative curves correspond to the weight percentage curves. What is evident from the graph is that as the resolution increases the response to mass loss versus temperature (the response to rate weight change, %/minute) is more pronounced. Initial decomposition occurs earlier. This early detection of changes in weight loss allows for better separation of components that are present in the sample as the decomposition steps occur over narrower temperature ranges. Inspection also reveals that the separation between the polymer degradation steps is increased. These steps can clearly be seen as peaks in the derivative (DTG) curve between 300 and 450°C. Increasing the resolution also allows for more complete decomposition of the various components which is evident by the fact that the sample is still decomposing in the temperature range 500-600°C when the resolution was 3. At 600°C, the switch to dry air initiated the burn-off of carbon black. It can be seen that this burn-off occurred over a narrower temperature range as resolution increased. Importantly at a resolution of 3 (green curves) the sample mass prior to burn-off was higher than at resolution 4 and 5. This would lead to an overestimate of the carbon black content in the first case (resolution = 3) and an underestimate of polymer content. The final residue level is the same in all cases once all organic material has been combusted, indicating the precision of the TGA instrument used.

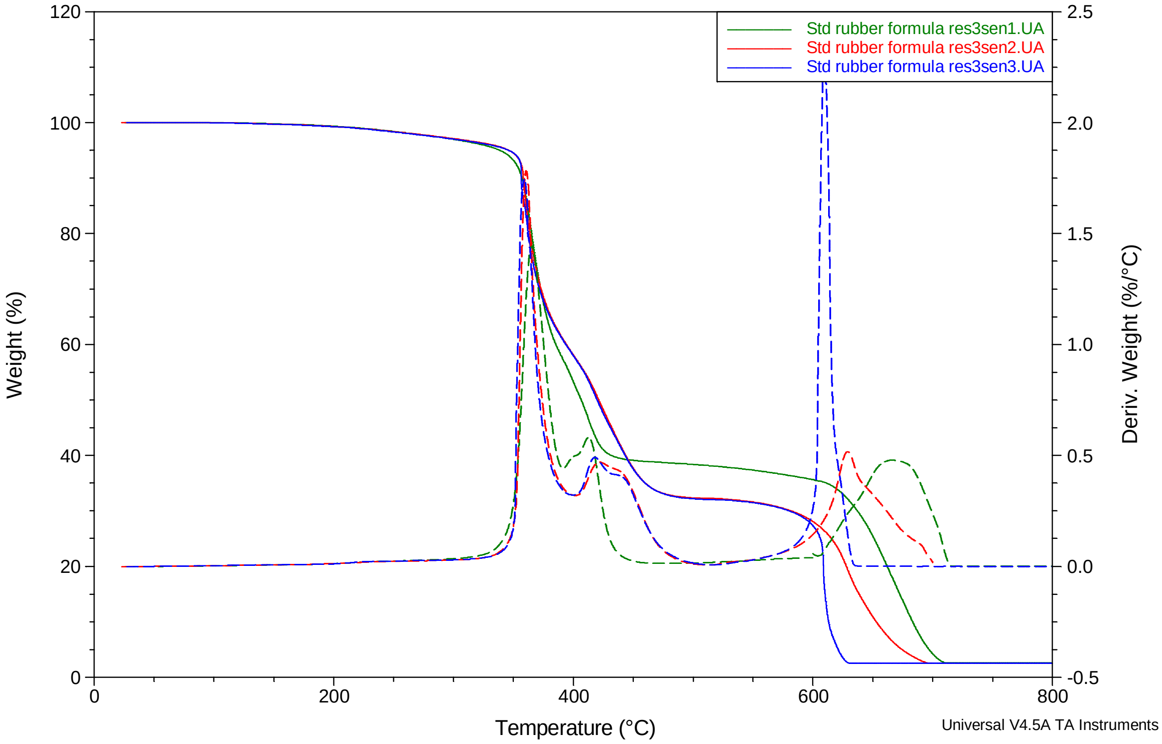

*Figure 4.3 Effect that sensitivity has on decomposition of the a reference tread formulation. Resolution = 3. Sensitivity = 1 (green), 2 (red) and 3 (blue). Initial atmosphere = $N_2$; switch to $O_2$ at 600°C. Base heating rate = 50°C/min*

A resolution of 3 was used to study the effects of sensitivity. There are two main reasons why a resolution of 3 was chosen. First, the complete analysis takes approximately 30 minutes and therefore it was important to investigate whether or not the separation could be improved while maintaining a shorter analysis time compared to the other resolution settings. Secondly, the resolution setting of 3 has a wider range for detecting the weight loss rate (described in section 2.6.1), which means that the effects of changing the sensitivity settings would have a greater effect on the analysis. This effect would be more evident using a resolution of 3 than with higher resolution settings. In Figure 4.3 the sensitivity settings of 1, 2, and 3 are shown. While the detection of the onset of weight loss is not improved, there is still an increase in separation of the various components present in the sample. This separation is improved because increasing the sensitivity allows for a more complete decomposition of the components. It is also apparent that increasing the sensitivity narrows the range over which carbon burns off, this can be seen in Table 4.1.

*Table 4.1 The peak temperatures for the first mass loss ($T_1$), second mass loss ($T_2$) and maximum temperature for carbon black oxidation ($T_{CB}$)*

| | $T_1$ (°C) | $T_2$ (°C) | $T_{CB}$ (°C) |
|---|---|---|---|
| *Resolution 3 sensitivity 1* | 365.6 | 412.5 | 668.1 |
| *Resolution 3 sensitivity 2* | 360.3 | 421.5 | 629.6 |
| *Resolution 3 sensitivity 3* | 358.8 | 438.0 | 609.1 |
| *Resolution 4* | 353.5 | 422.3 | 636.3 |
| *Resolution 5* | 338.4 | 410.2 | 630.3 |

The widening gap between the first mass loss (NR) and the second mass loss (SBR) shows that increasing the sensitivity or resolution will improve the separation of materials. This separation improves identification and quantification of samples, this is shown in Table 4.2. Furthermore a constant mass is achieved prior to carbon black combustion at higher sensitivities. As before this allows for more accurate quantification of carbon black and polymer content. In Table 4.2 the percent polymer, carbon black and inorganic material identified by the thermograms above (Figure 4.2 and Figure 4.3) are compared to the standard tread formulation used in this study (Table 3.1). Only the main components of the formulation are shown as the separation of the oil, accelerators and sulfur are more difficult to identify as they react and form part of the polymer component.

*Table 4.2 Comparison between experimental data and theoretical data shown as a percentage of polymer, carbon black and inorganic material*

| | *NR* | *SBR* | *Carbon Black* | *Residue* |
|---|---|---|---|---|
| *Standard Formulation** | 32.5 | 32.5 | 29.3 | 2.0 |
| *Resolution 3 sensitivity 1* | 39.5 | 18.6 | 36.4 | 2.6 |
| *Resolution3 sensitivity 2* | 39.2 | 25.4 | 29.8 | 2.5 |
| *Resolution 3 Sensitivity 3* | 37.9 | 26.5 | 29.5 | 2.5 |
| *Resolution 4* | 37.3 | 25.1 | 31.5 | 2.5 |
| *Resolution 5* | 32.8 | 28.7 | 30.6 | 2.4 |

* Values taken from the tyre tread standard formulation (NR&SBR) shown in Table 9.1 to compare formulation values to experimental values.

The percentages shown in Table 4.2 were obtained by decomposition steps in the thermograms. The troughs in the DTG curves were used to determine where one decomposition step ended and another began. This is explained in more detail in section 4.3. Because the SBR used in this study was oil extended the values obtained for the SBR may be lower than expected as a small portion of the polymer is oil and would decompose earlier. If any heavy oil is present in the sample the decomposition of the heavy oil could overlap with the NR. This would result in an over estimation of the NR content. The reaction of sulfur and accelerators with zinc could possibly account for some of the differences in the residue percentage. A more detailed description of these differences is discussed in section 4.3.

Increasing resolution or sensitivity results in an increase in the time for the analysis. Increasing the resolution allows for an increased response in the rate of weight change of the sample and therefore allows the TGA to decrease the heating rate sooner. This is important for detecting small weight changes which could improve quantification. Increasing the sensitivity decreases the heating rate even further when a mass loss in the sample is detected.

The data in Table 4.3 and the peak separation in Figure 4.2 and Figure 4.3 shows that a trade-off exists between component separation and overall analysis time. While there are greater resolution and sensitivity settings available, it was decided that no further benefit would be realized by using those settings. The improvement in separation between experiments with resolution 5 and a sensitivity of 1 and one with a sensitivity of 2 was barely noticeable and it was decided that using a sensitivity of 3 would serve no purpose. The times shown in Table 4.3 correspond to the time taken to reach a flat residue line at the end of the analysis rather than the time taken to reach 800°C.

*Table 4.3 Times for complete analysis of a reference tyre tread formulation at different resolution and sensitivity settings. Base heating rate = 50°C/min*

| | *Sensitivity 1* | *Sensitivity 2* | *Sensitivity 3* |
|---|---|---|---|
| *Resolution 3* | 26.5 min | 27.8 min | 27.3 min |
| *Resolution 4* | 45.6 min | 57.9 min | 65.6 min |
| *Resolution 5* | 100.6 min | 166.1 min | - |

### 4.1.2 Effect of base heating rate

The resolution settings improve the response time of the TGA to the onset of decomposition. In order to find another way to improve separation, the base heating rate was dropped to 20°C/min. The base heating rate is the maximum heating rate used by the TGA when there is no mass loss detected. A resolution of 5 and a sensitivity of 1was used to evaluate the effect of changing the heating rate.

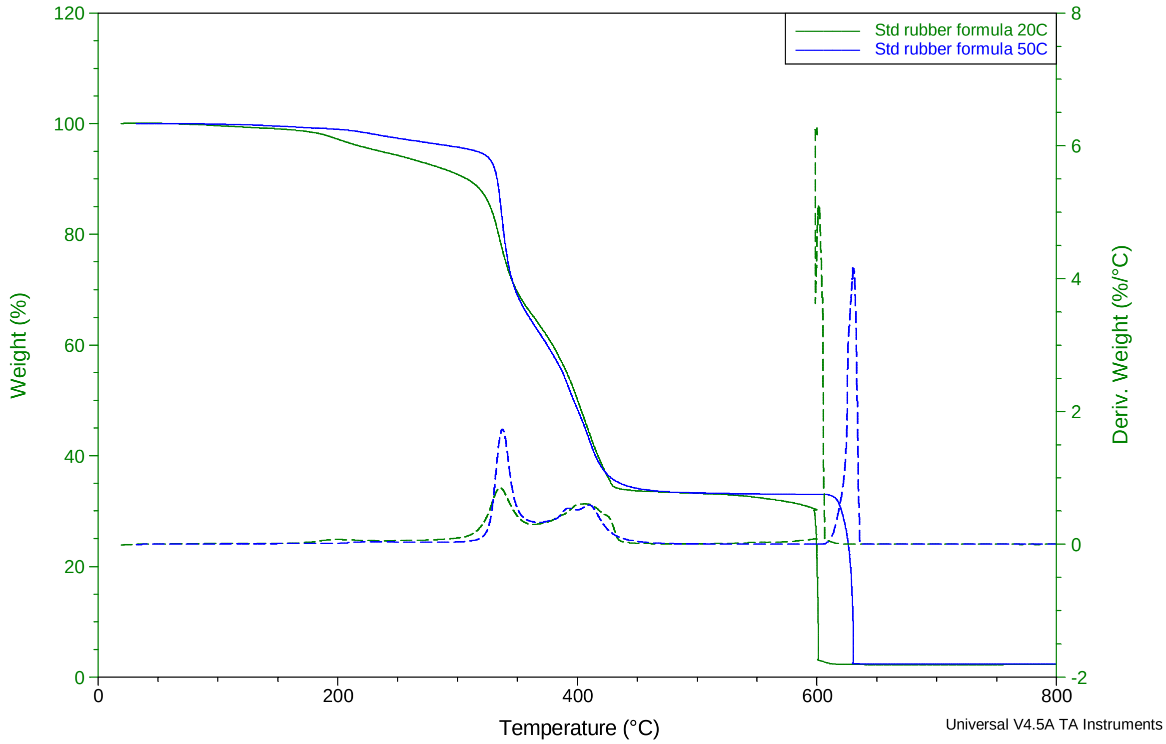

*Figure 4.4 A comparison between two different base heating rates, namely 20°C (green) and 50°C (blue), using the standard tyre tread formulation. A resolution of 5 and a sensitivity of 1 was used for both analysis*

When considering the DTG in Figure4.4 there is no real difference in the peak separation. However, using a slower base heating rate allowed for the Hi-Res™ dynamic program to react to the change in rate of weight loss quicker. This can be seen when comparing the green and blue weight % loss curve (solid line) in Figure 4.4, more specifically when comparing the decomposition between 200-300°C and the onset of carbon black combustion at 600°C. The slower base heating rate allowed the smaller weight changes to be more noticeable. However the slower base heating rate increased the time of the analysis from 100.6 minutes to 150.7 minutes. The separation effect was most noticeable for experiments when using the NRG reclaim sample. Not only was the separation of the peaks in the DTG curve improved but the decomposition of different materials became clearer. Figure 4.5 shows the comparison of the heating rates.

What can be seen in Figure 4.5 is that decreasing the heating rate further increases the separation of the materials present. The decrease in ramp rate increases the time for each experiment. The time increased from 140 minutes to 175 minutes for the heating rates 50°C/min and 20°C/min respectively. The onset of mass loss occurs at a lower temperature at the lower heating rate. One reason for this is thermal lag effects in the sample where the sample temperature lags behind that recorded by the furnace thermocouple.

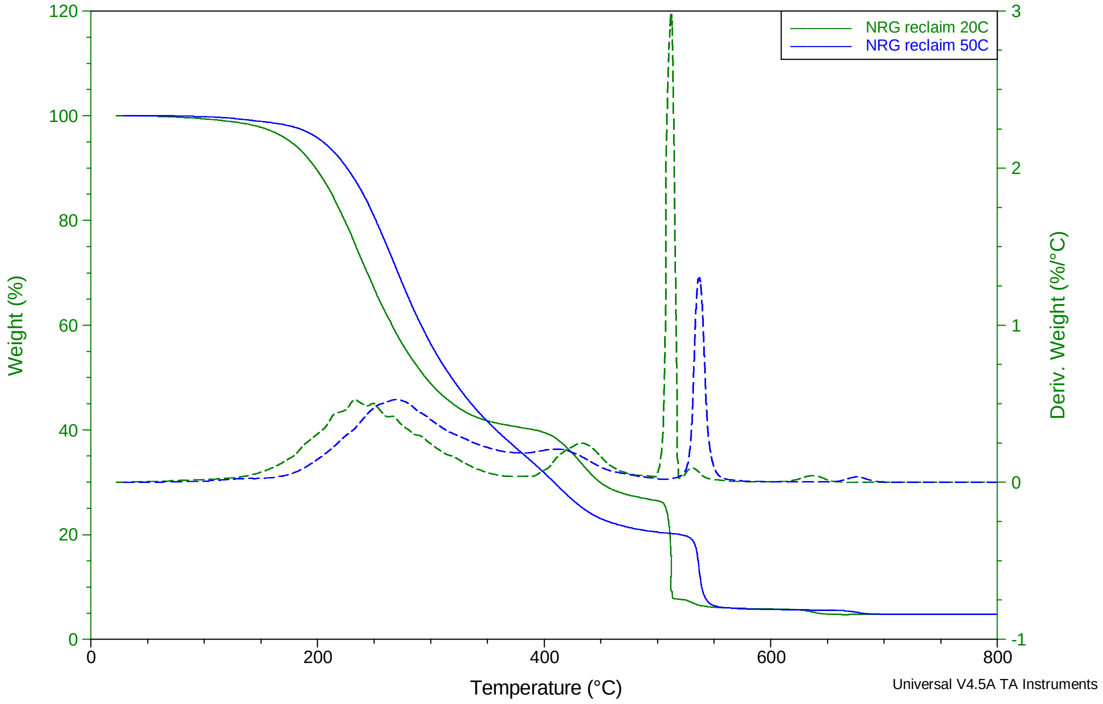

*Figure 4.5 A comparison between the effect two different heating rates using resolution 5 and sensitivity 1 on the analysis of NRG reclaim. Heating rate = 20$^{o}$C/min (green) and 50$^{o}$C/min (blue)*

Figure 4.5 illustrates further complications in the analysis of reclaim. Although the initial mass loss at 20$^{o}$C/min occurs at lower temperature, the second mass loss of polymeric material occurs at a higher temperature (433.7°C) compared to (411.7°C). This is counterintuitive and suggests that reactions are occurring that stabilize the reclaim as it is heated. These possibly arise from the formation of high molecular weight material by the reaction of low molecular weight polymer. These processes would have less time to occur at the higher base heating rate of 50$^{o}$C/min and would occur to a lesser extent. This also contributes to the total mass being greater prior to carbon burn-off which suggests that some of the carbon black measured during the analysis of NRG reclaim is not original material but pyrolytic carbon black (PyCB) that forms during the analysis experiment. This could possibly account for the second mass loss between 500-550°C seen in the NRF reclaim 20°C curve in Figure 4.5.

For characterization of samples with multiple components an emphasis was placed on separation of the components. To do this the rate of decomposition of the sample was important. A resolution of 5 with a sensitivity of 1 was therefore chosen to be the standard program used in all characterization analysis with a heating rate of 20°C/min. Multiple experiments were then carried out in order to test the reproducibility of the test. Some of these tests are shown in appendix F.

## 4.2 Characterization of a standard rubber formulation

In order to successfully characterize the devulcanizate samples chosen for this study, virgin material was first tested. This provided decomposition ranges of components present in a typical tread formulation, which could hopefully be used to identify such components in devulcanizate samples. Because there were a number of materials used in the compounding of the various samples, the overlays shown below are separated into accelerators, processing oils and elastomers. These are compared to the complete vulcanized standard rubber formulation.

It is apparent from Figure 4.6a that free accelerators decompose at low temperatures (below 350$^{o}$C) although bound residues may only be released at higher temperatures. Processing oils are also relatively volatile materials.

Figure 4.6b illustrates the evaporation/decomposition of a paraffinic (naphthenic) processing oil used to produce rubber goods and the aromatic processing oil used by NRG during their reclaim production. The mass loss that occurs above 250$^o$C in the standard tread formulation is likely the extender oil in the SBR-OE. This conclusion was reached by a process of elimination. The weight loss is most noticeable when SBR is used and, the main decompositions of the processing oils occurred at a lower temperature. The virgin elastomers all decompose at higher temperatures and the concentration of accelerators used in the formulation were not high enough.

It has been proposed that the decomposition of NR comprises 2 stages: primary depolymerization/condensation and secondary (consecutive) degradation of the condensed product. This results in 2 peaks in the DTG curve of NR between 300-500$^o$C.

a)

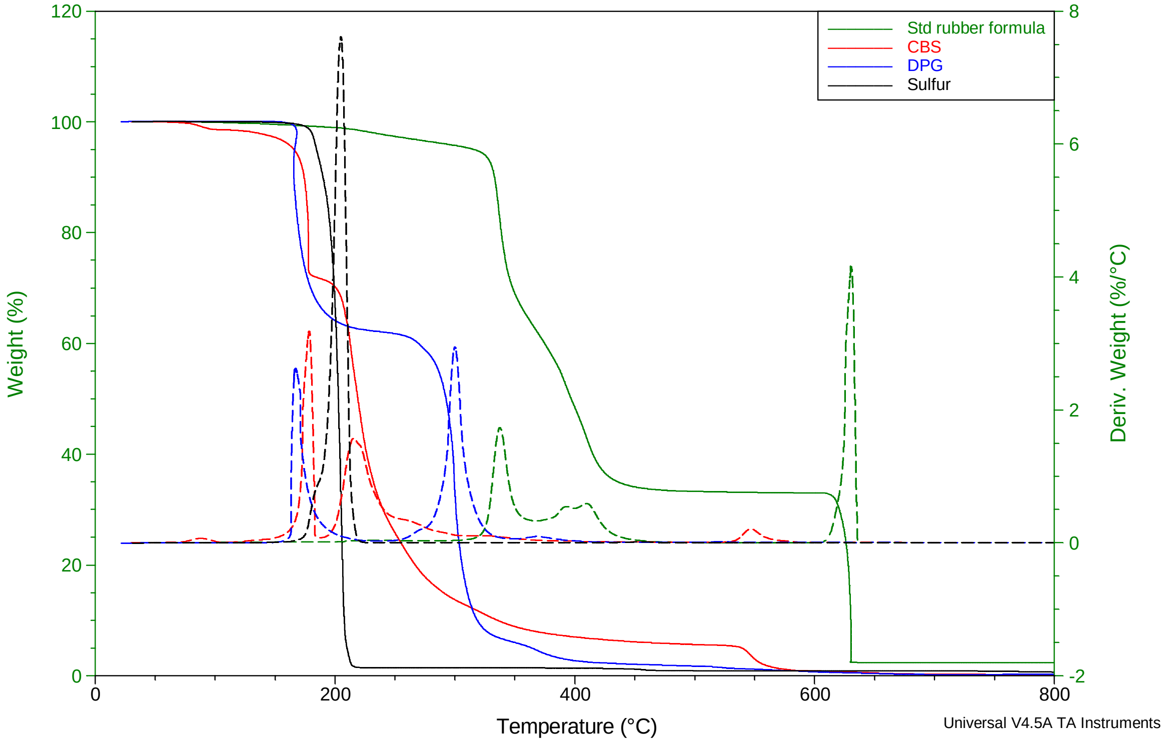

b)

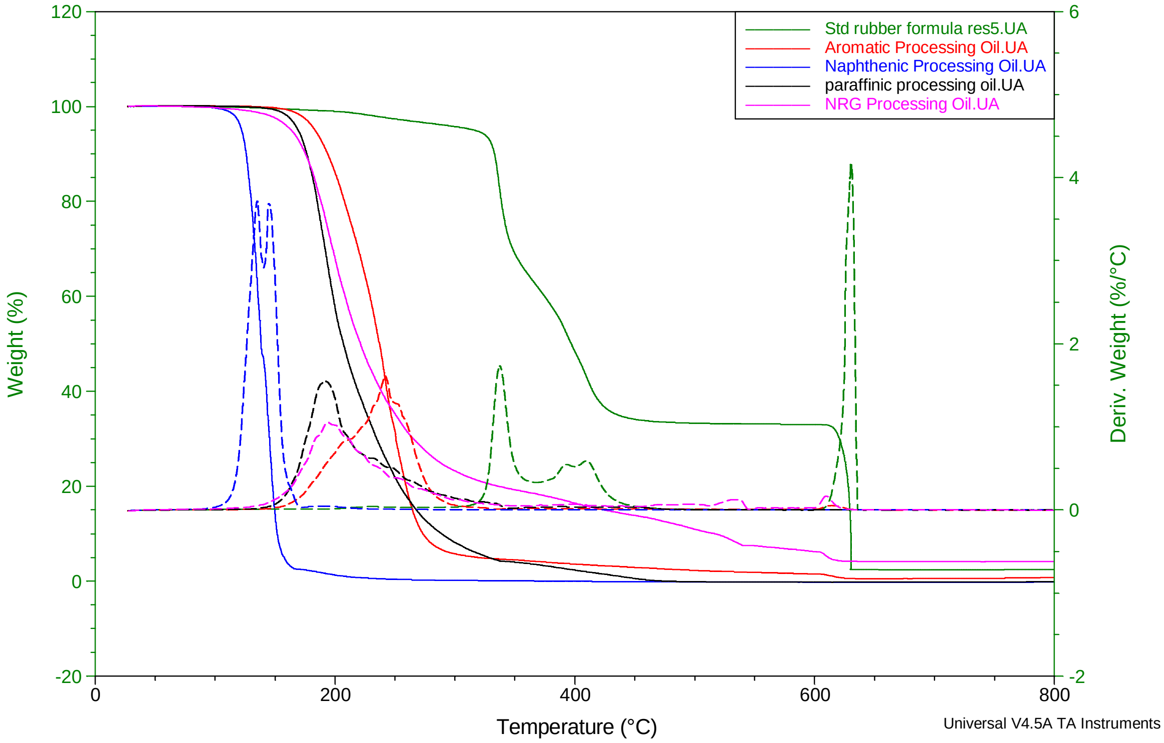

*Figure 4.6 Overlays of the decomposition of the standard rubber formulation, accelerators and sulfur (a) and processing oils (b). A resolution of 5 and a sensitivity of 1 with a base heating rate of 50°C/min was used*

a)

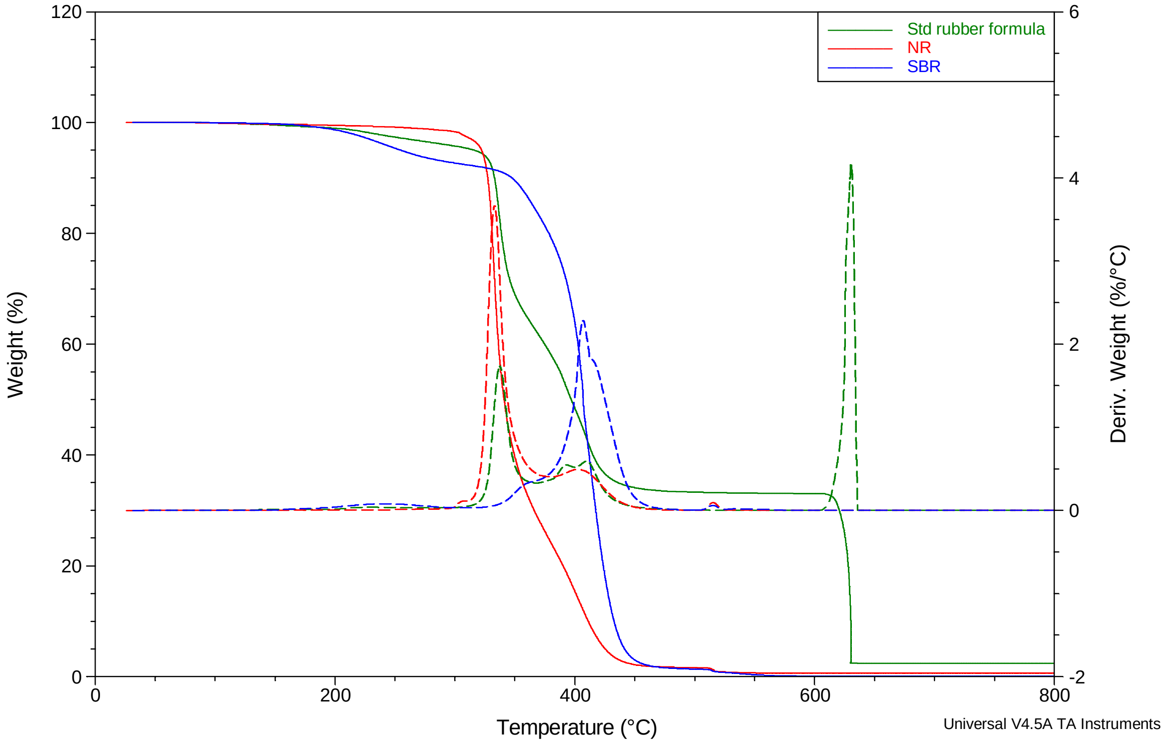

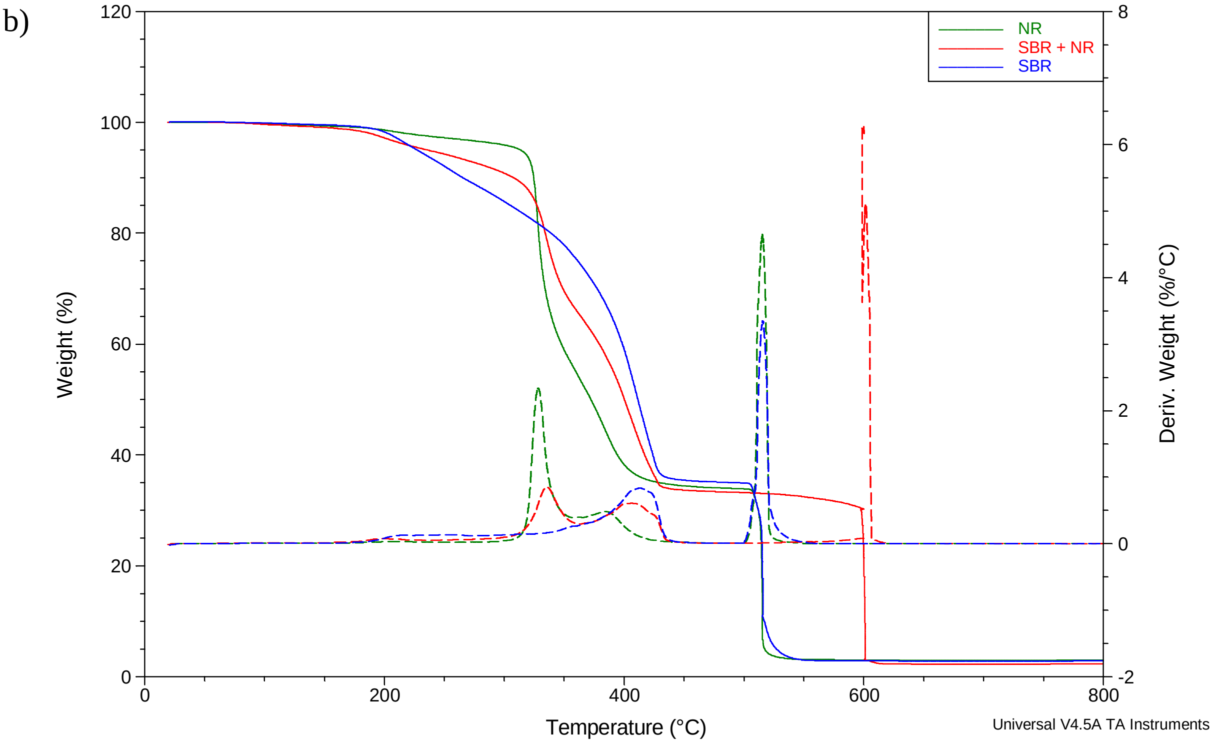

*Figure 4.7 Overlay of unvulcanized virgin elastomers (a) as well as vulcanized NR and SBR (b). A resolution of 5 and a sensitivity of 1 with a base heating rate of 50°C/min was used*

While the figures above do show some overlap between the unvulcanized virgin material (Figure 4.7a) and the standard formulation they do not match perfectly. This is expected as the interactions between chemicals and materials change their thermal stability properties. For example, it has been demonstrated by Fernandez-Berridi *et al.* that the combination of SBR and NR had a stabilizing effect on the elastomers which lead to a shift in the decomposition temperature to a higher range (65). It is for this reason that Figure 4.7b shows vulcanized NR and SBR overlaid with the standard formulation (red curve labelled as SBR + NR). Using the derivative curves it can be seen that the match up of materials is more accurate than using unvulcanized materials. The stabilizing effect can be seen in Table 4.4 where the maximum temperatures, defined as the peak of the DTG curve, of the elastomers are recorded. The materials used in vulcanizing rubber showed a stabilizing effect on SBR but a destabilizing effect on NR when vulcanized. However, when comparing the $T_{max}$ of vulcanized NR with the $T_{max}$ of the vulcanized NR&SBR the stabilizing effect that SBR has on NR can be seen. This is consistent with the findings of Fernandez-Berridi *et al*.

*Table 4.4 Stabilizing effect of vulcanization and compounding on NR and SBR*

| | $T_{max}$ NR (°C) | $T_{max}$ SBR (°C) |
|---|---|---|
| *Unvulcanized NR* | 332.4 | - |
| *Unvulcanized SBR* | - | 406.8 |
| *Unvulcanized NR+SBR* | 339.6 | 415.9 |
| *Vulcanized NR* | 327.8 | - |
| *Vulcanized SBR* | - | 415.0 |
| *Vulcanized NR+SBR* | 338.7 | 409.5 |

It can also be seen that the use of higher resolution and sensitivity settings allowed the carbon combustion step to be effected at 500ºC rather than 600ºC because of the flat baseline. This has the effect of reducing overall analysis times.

## 4.3 TGA of reclaim/devulcanizate

In order to analyse and characterize the reclaimed material and formulated samples, thermogravimetric analysis was used. A reliable test method needed to be established and tested. To do this the standard tread tyre formulation used in this study was analysed to test and confirm that the method used was appropriate. As previously indicated this formulation may be found in Table 3.1.

Because the composition is known, the decomposition steps in the thermogram can be identified. Fernandez-Berridi *et al.* used a similar technique to characterize and quantify the various components present in rubber formulations (65). The decomposition steps are also compared to the decomposition of all the virgin material used before mixing. Figure 4.8 shows the thermogram of the reference tread sample. The derivative curve has been omitted for clarity. Measurements were made using the DTG curve, all DTG curves that have been omitted can be seen in appendix D. The measuring start and end points for the analysis were taken from the troughs in the DTG curve before and after the peak. An example of this is shown in appendix D.

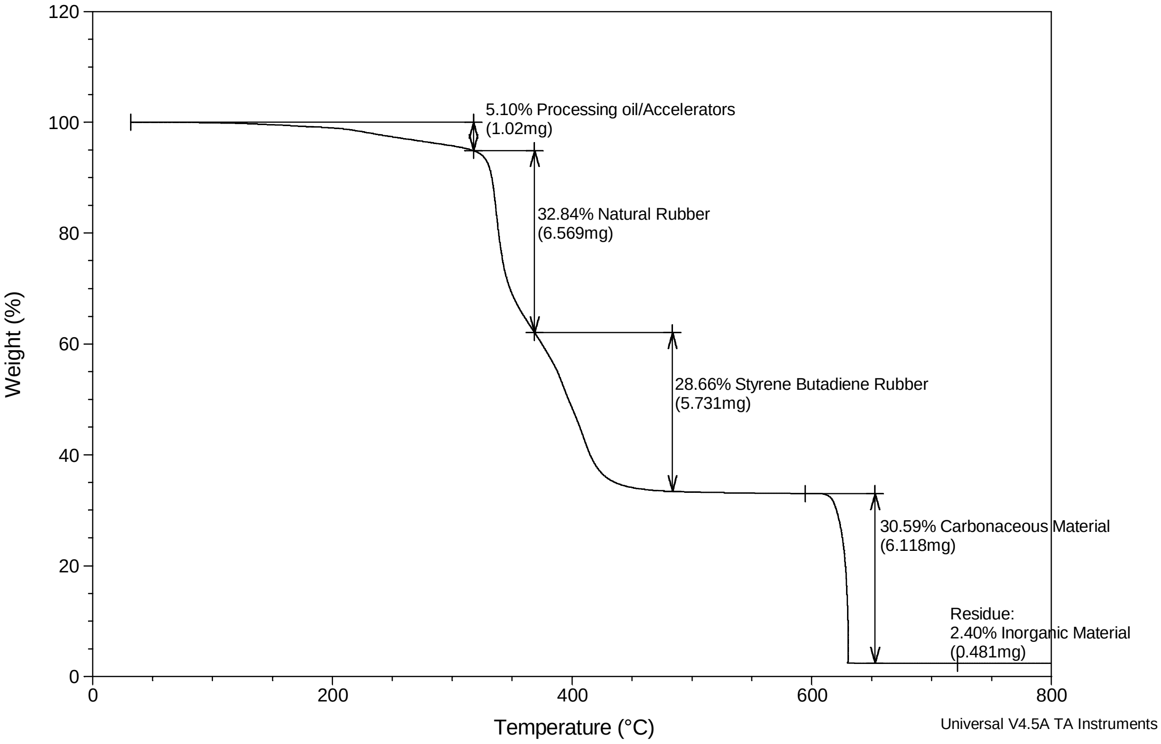

*Figure 4.8 Compositional breakdown of a reference tread sample using resolution 5 and sensitivity 1 with a base heating rate of 20°C/min*

The percentage of material indicated by the thermogram in Figure 4.8 matches closely with the percentages of the formulation in Table 3.1. With the decomposition temperatures matching those of the original materials and the percentages matching those of the standard, confidence in the technique was established.

It should be noted that the bulk of the processing oil in this formulation is the RAE extender oil in the OE-SBR. The 32.8% NR is a close match to the 32.5% that the formulation was intended to have. The carbonaceous material is 30.6% compared to 29.3% in the formulation. The slightly higher than expected value may be the result of carbonaceous residues, resulting from the decomposition of rubber bound curatives. The combined processing oil, accelerator and SBR quantity (33.8%) compares with the 34.3% in the original formulation. Note that the technique underestimates the heavy RAE extender oil slightly because the decomposition/evaporation of this oil overlaps with that of the decomposition of the polymer part of the OE-SBR (see Figure 4.7b).

The TGA method was then applied to on an unknown sample, NRG reclaim. The TGA analysis of NRG reclaim is shown below in Figure 4.9.

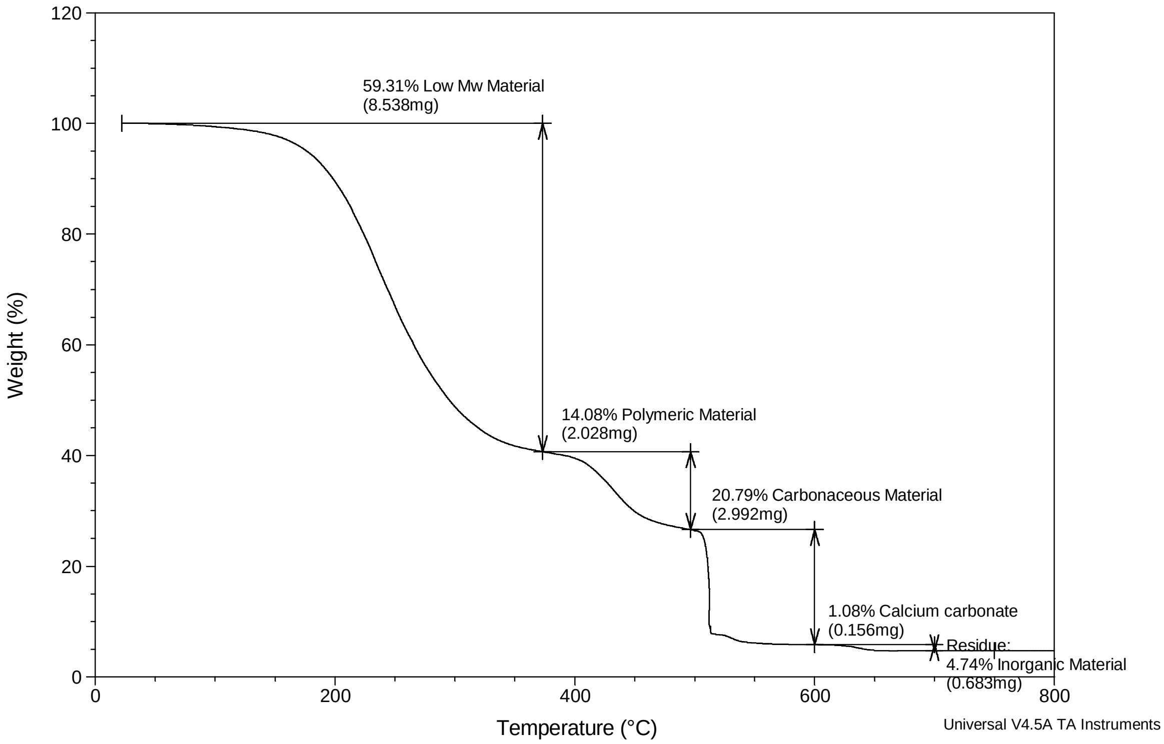

*Figure 4.9 Compositional analysis of NRG reclaim by TGA using resolution 5 and sensitivity of 1 with a base heating rate of 20°C/min*

The NRG reclaim sample is derived from recycled whole tyres (likely tyre treads) and therefore the composition is a lot more complex than the standard tread formulation. The complexity of the sample makes detailed analysis of the material more difficult and therefore multiple techniques are necessary to identify the components present in the reclaim. Using the developed TGA method, some information can be obtained.

In Figure 4.9 the material degraded first is labelled as low molecular weight ($M_w$) material. It is suggested that much of this material is processing oil. This was suggested as the temperature range that the low $M_w$ decomposes over coincides with a variety of oils. The $T_{max}$ for the low $M_w$ material, measured at the peak of the DTG curve, was 234.8°C. The $T_{max}$ for the paraffinic oil was 193.2°C, naphthenic oil 145.5°C, aromatic oil 242.3°C and the NRG processing oil was 194.7°C. The decomposition temperature coincides with that of the processing oil, presented in Figure 4.6b. Due to the highly severe nature of the reclaiming process, the presence of low molecular weight rubber (possibly polyisoprene) cannot be ruled out. While the degradation peak in the DTG curve for natural rubber is expected near 327.8°C, smaller chains produced by the reclaiming process could degrade at a lower temperature. The degradation of the low molecular weight polyisoprene would be hidden by the overlapping degradation/evaporation of the processing oil. This is illustrated in Figure 4.10.

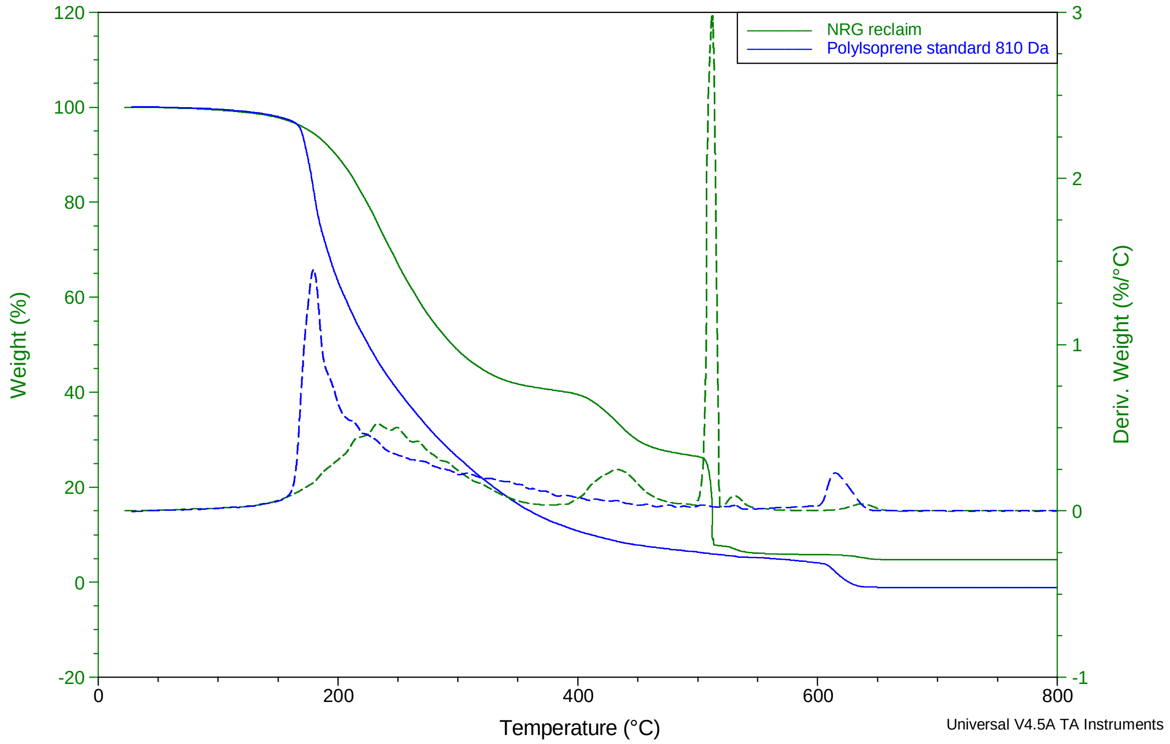

*Figure 4.10 An overlay of a low $M_w$ polyisoprene standard with the NRG reclaim. A resolution of 5 and a sensitivity of 1 was used with a base heating rate of 20°C/min*

Also noticeable in Figure 4.9 is a small mass loss in the temperature range 600-700$^{o}$C which amounts to a weight of 1.08%. Further investigation of the material responsible for this mass loss is presented later in this dissertation. This decomposition takes place over a wider temperature range than the carbon black combustion because the heating rate is reduced in Hi-Res$^{TM}$ mode in response to the rate of the percentage weight range. This rate is proportional to the quantity of material decomposing. A minor component thus decomposes over a wider temperature range. Note that the same is true of a material of variable composition, such as a processing oil which contains compounds of different molecular mass.

To corroborate the analysis done on NRG reclaim, the sample was subjected to further analysis. Thermogravimetric analysis was performed on reference materials (processing oil, polymers, accelerators, e*tc*.) and compared to the NRG reclaim thermogram. Solvent extraction was then performed on the NRG reclaim product. Different solvents were used to extract specific compounds. Soxhlet extraction was also used to separate the soluble and insoluble fraction for further characterization. Thermogravimetric analysis was performed on all the extracted material and compared to the NRG reclaim thermogram. DSC analysis was performed on the NRG reclaim to try to identify the polymers present. This data is presented later in this dissertation.

Characterization of a second reclaim product was also carried out. The sample obtained from Bridgestone was presented to be a reclaimed rubber, from a source high in natural rubber (91).

Thermogravimetric analysis was carried out on this reclaim sample and the results are shown in Figure 4.11 and Figure 4.12.

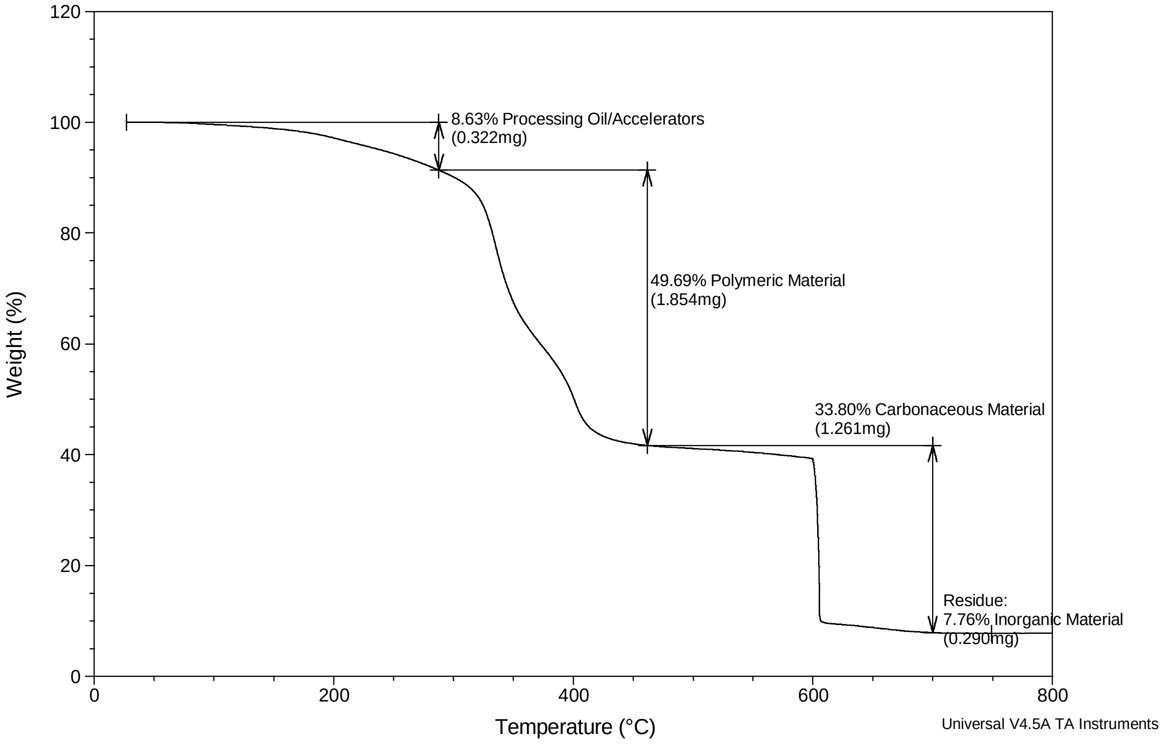

*Figure 4.11 Characterization of commercial tyre tread reclaim using resolution 5 and sensitivity of 1 with a base heating rate of 20°C/min*

When an overlay of virgin material and commercial tyre tread reclaim is analysed, shown in Figure 4.12, it appears that the Bridgestone reclaim may contain SBR. Natural rubber has two decomposition steps which are shown as a green DTG in Figure 4.12. It should be noted that the height of the second derivative peak at 401.9°C for NR is smaller than that of the first peak at 336.1°C.

The second decomposition step of natural rubber overlaps partially with the SBR decomposition. The SBR derivative curve has a characteristic shoulder (75), which possibly represents the decomposition of the two polymers that make up SBR, namely styrene and butadiene. Such a shoulder (example shown in appendix D), is difficult to discern in the DTG curve of the reclaim sample. Its absence, however, does not exclude the presence of SBR and may be the result of the relatively small quantity of SBR in the sample. Note that it is also possible that the sample contains BR which decomposes at a similar temperature (75). Developing a test method for BR was deemed beyond the scope of this study.

The ratio of the heights (and areas) of the large to small peak in the DTG curve of the reclaim sample (blue) is smaller than that observed for virgin NR (green). This suggests that the second peak cannot solely be due to the decomposition of NR. This in turn is consistent with the presence of some SBR.

The overlay for the commercial tyre tread reclaim illustrates a problem with using only TGA to characterize complex rubber samples. After analysing the commercial tyre tread reclaim it was suspected that the previous characterization of NRG reclaim might be incomplete. A comparison between the two reclaim products was analysed by an overlay of the two thermograms. Figure 4.13 shows the results.

When analysing the comparison between the two reclaim products in Figure 4.13, the derivative curves can be compared. It is clear that the apex of the second peak in the decomposition of the NRG reclaim (435.2°C) is at a higher temperature than either the two peaks in the commercial tyre tread reclaim (336.9°C and 401.9°C) or the SBR/NR reference tyre tread formulation (338.4°C and 410.2°C, Figure 4.7b).

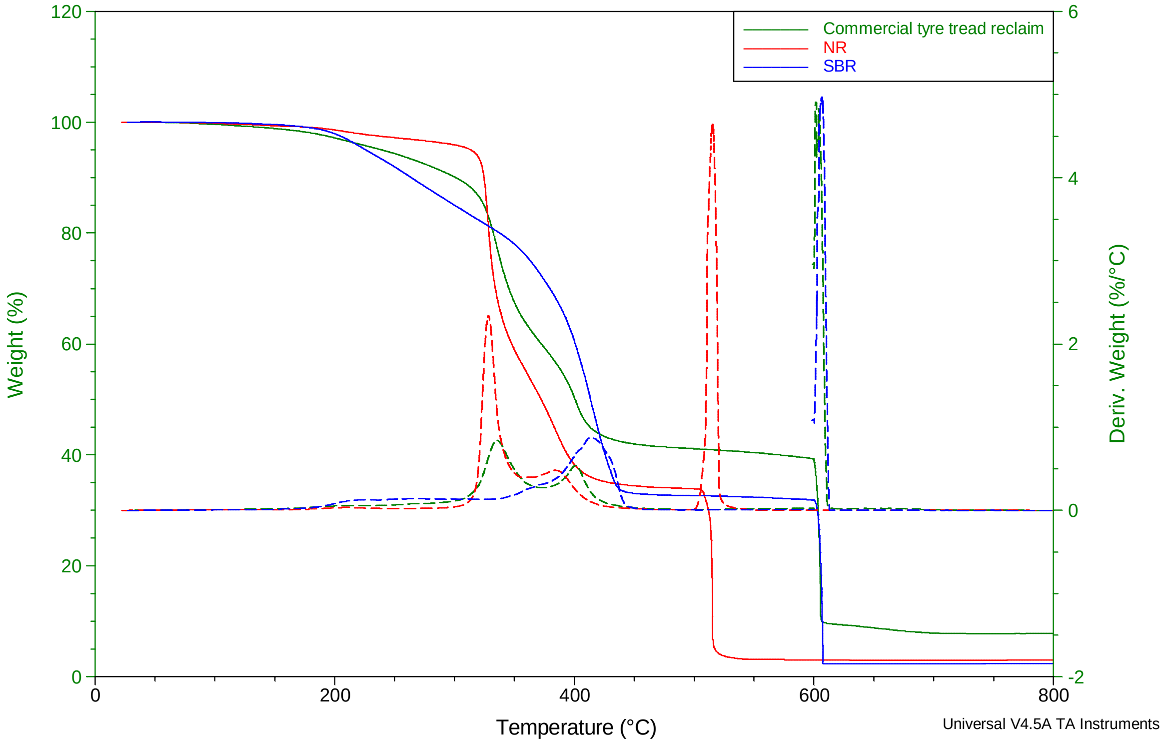

*Figure 4.12 Overlay of vulcanized virgin material (NR – red, SBR-OE – blue) and commercial tyre tread reclaim (green). A resolution of 5 and sensitivity of 1 with a base heating rate of 20°C/min was used*

Furthermore, no peak was seen at the temperature associated with the first decomposition peak of NR. This suggests that the reclamation process employed by NRG is severe enough to reduce the molecular weight of any NR component significantly. The increase in the peak temperature for the high molecular weight component in the NRG reclaim also suggests that molecular re-arrangements to form a more stable polymeric material has occurred during the NRG reclamation process. Such effects have been seen when SBR is de-vulcanized and, if uncontrollable, reacts to form a highly branched material (40), especially if air is not excluded. NR, by contrast breaks down into lower $M_W$ material. It is thus suggested that the second peak in the DTG curve for the NRG reclaim (435.2°C) might be because of the decomposition of branched SBR. The high molecular weight polymer in the NRG reclaim is thus likely SBR-derived.

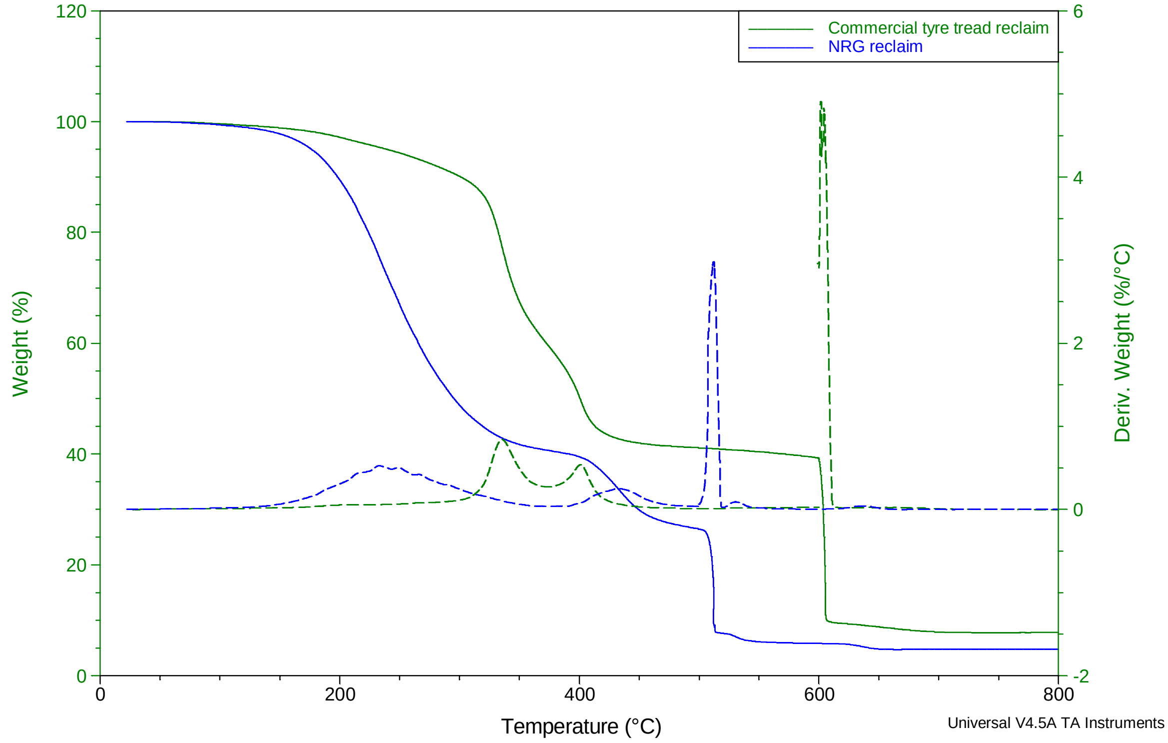

*Figure 4.13 Comparison between the two reclaim products. Commercial tyre tread reclaim (BS) (green) and NRG reclaim (blue). A resolution of 5 and sensitivity of 1 with a base heating rate of 20°C/min was used*

Thermogravimetric analysis was performed on polyisoprene (PI) standards. The standards used covered a range of low $M_w$, 810 Da (Daltons), medium $M_w$, 36 200 Da and high $M_w$, 2 830 000 Da. The low $M_w$ of the standard meant that it was a viscous oil-like material, the medium $M_w$ standard was a wax and the high $M_w$ standard was a flexible solid. Note that the $M_w$ of NR used commercially in tyres is typically in excess of $1 \times 10^6$ Da (36). The thermogram in Figure 4.14 show an overlay of the PI standards with the NRG reclaim.

It can be seen that at very low molecular weight, the decomposition temperature of polyisoprene is significantly reduced from that of NR (see Figure 4.7). This holds out the possibility that some of the low molecular weight material (decomposing below 300$^o$C) in the NRG reclaim is not just processing oil but also low molecular weight polymer. Rajan *et al.* demonstrated that during devulcanization, when the temperature was above 170$^o$C, NR chains underwent random scission to form shorter, lower molecular weight chains (63).

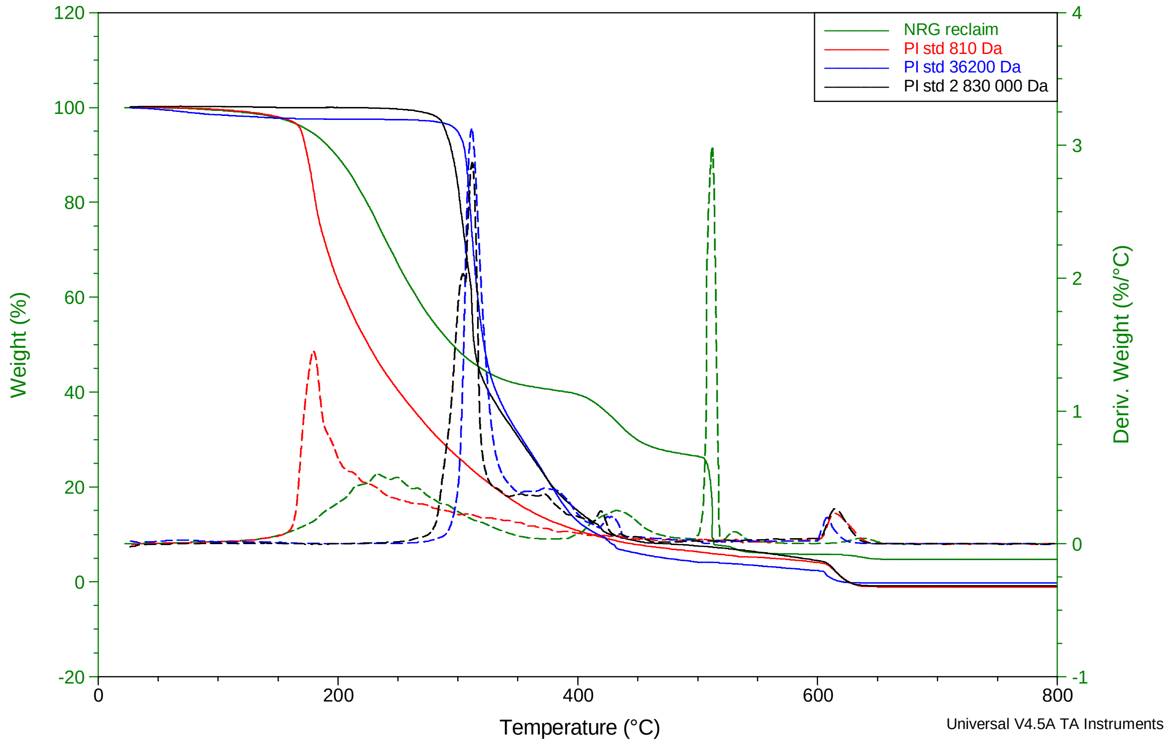

*Figure 4.14 Overlay of the thermal decomposition of NRG reclaim (green) with a low molecular weight polyisoprene standard (red), medium molecular weight standard (blue) and high molecular weight standard (black). A resolution of 5 and sensitivity of 1 with a base heating rate of 20°C/min was used*

## 4.4 DSC of reclaim/devulcanizate

Because the TGA technique employed is not able to satisfactorily separate the low $M_w$ polymer from the high $M_w$ polymer from processing oil in the NRG reclaim, the glass transition temperature ($T_g$) of the reclaim was compared to the $T_g$ of unvulcanised virgin rubbers (SBR and NR). Figure 4.15 shows DSC thermograms than can be used to identify the $T_g$ of NR and SBR.

The $T_g$ of the two elastomers were determined by taking the inflection point of the heat flow curve. On the thermograms the onset and end point temperatures of the step-change in heat flow are also shown. The same procedure was followed when determining the $T_g$ of the NRG reclaim. The two $T_g$ points identified in the thermograms correspond to reported glass transition temperatures of -67°C for NR (106), and -52°C for 23% styrene SBR (107).

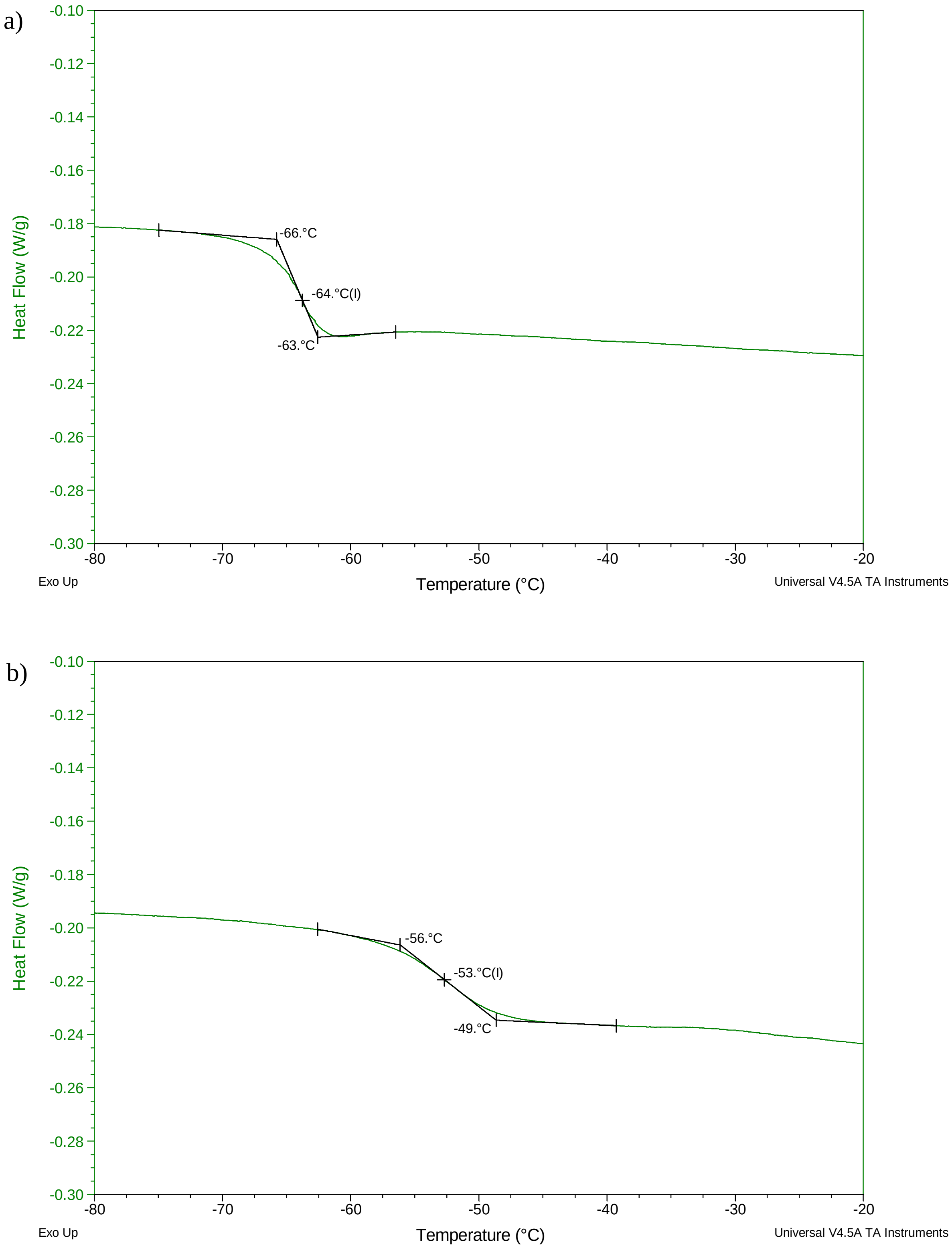

*Figure 4.15 DSC glass transition measurement for the unvulcanized virgin rubber used. a) NR with* $T_g$ *of -64°C b) SBR-OE with* $T_g$ *of -53°C*

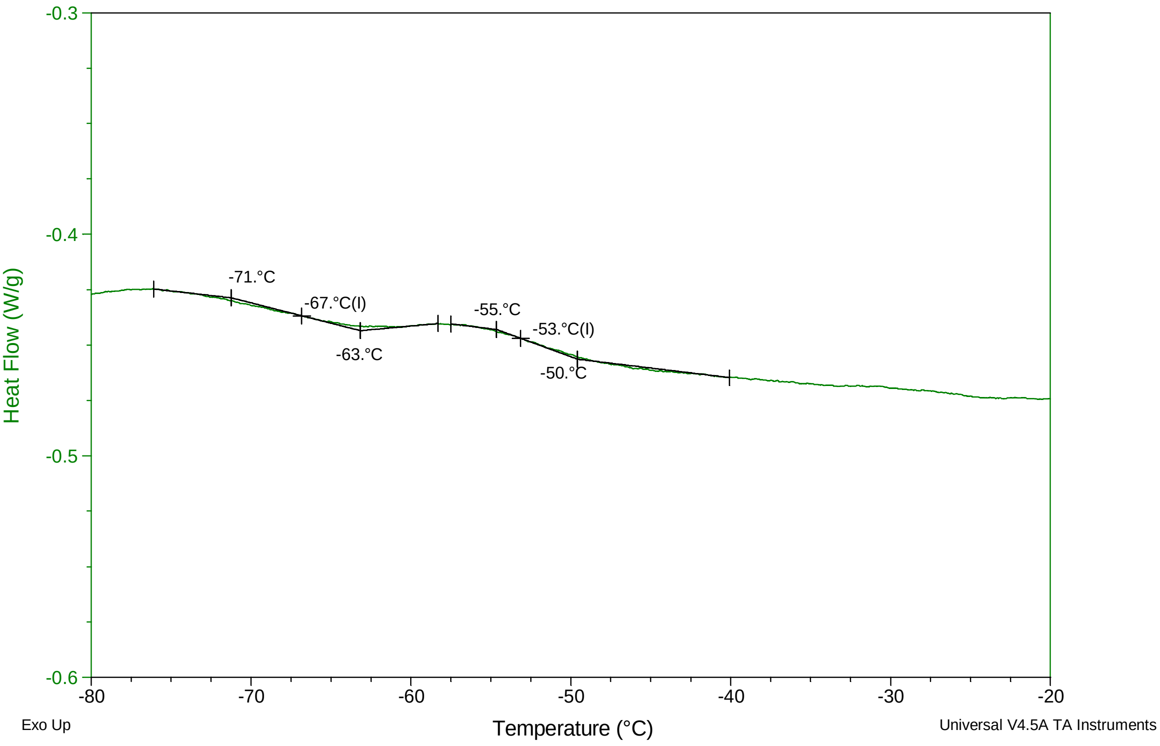

*Figure 4.16  DSC thermogram of NRG reclaim which shows two glass transition events*

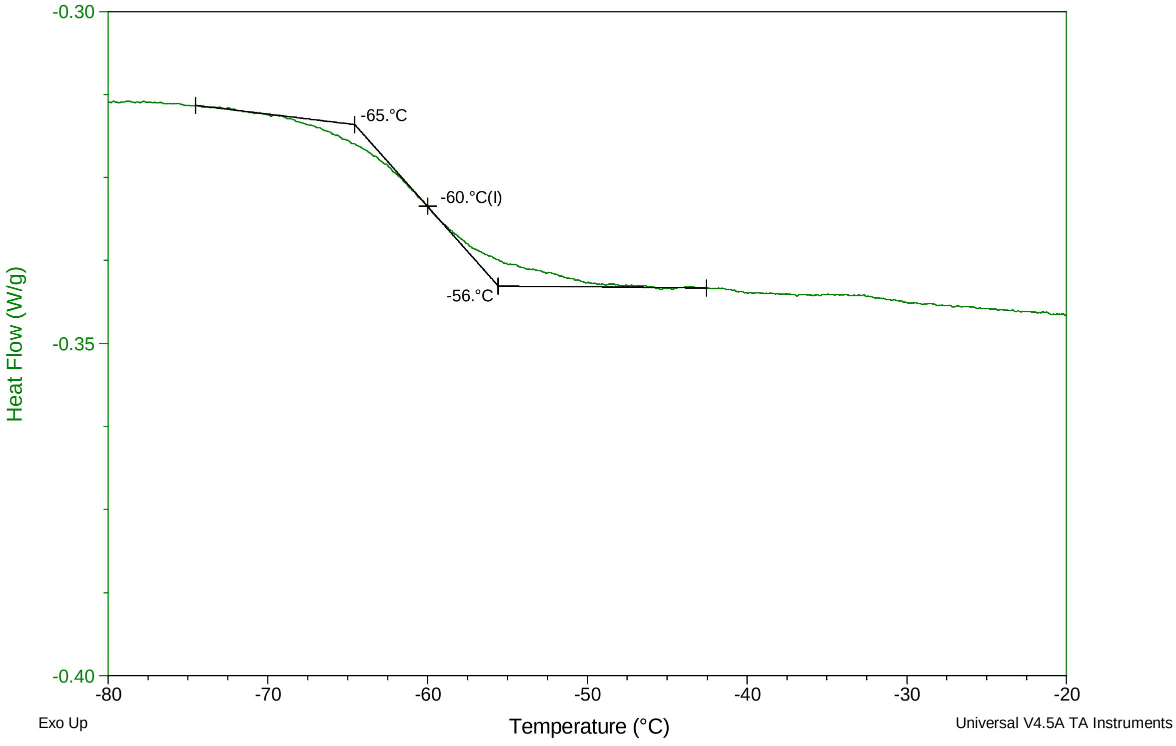

*Figure 4.17  DSC identification of the glass transition temperature of a commercial tyre tread reclaim product*

These temperatures deviate slightly from the determined glass transitions shown in Figure 4.15. It should, however, be noted that a polymer's glass transition takes place over a temperature range. Furthermore the value of the $T_g$ depends on the technique used for its determination (108).

The thermogram for the NRG reclaim (Figure 4.16) has two inflection points at -67°C and -53°C. This is consistent with the sample containing both polyisoprene and poly(styrene-co-butadiene) structures. Note that the glass transition $T_g$ is relatively independent of $M_w$ at higher $M_w$, so it is not surprising that broken down NR (with reduced $M_w$) would have a $T_g$ similar to virgin NR. This would suggest that some of the low $M_w$ material in the NRG reclaim is low $M_w$ polyisoprene. Kow *et al.* reported that the difference in glass transition temperature for *cis*-1,4-polyisoprene of molecular weight 6440 Da and one of 940 000 Da is just 2°C (109). The fact that a glass transition similar to virgin NR was observed is not inconsistent with the fact that the polyisoprene component has a low molecular mass. Note that PI of $M_w$ 6440 Da would be a viscous liquid.

The $T_g$ of the commercial tread tyre reclaim was also determined as there was some doubt as to whether or not it contained SBR. The $T_g$ of the commercial tyre tread reclaim was measured as -60°C which lies in between the values determined from Figure 4.15. Burfield and Lim (106) report that the glass transition temperature of amorphous polyisoprene (-65°C) is 2°C less than *cis*-1,4-polyisoprene. The reclaiming process experienced by the commercial tyre tread reclaim may have caused some isomerization with a resultant increase in the $T_g$. The thermogram (Figure 4.16) contains only one dominant inflection point suggesting one primary rubber type. However, it is possible that a small step might be discerned between -60 and -50°C. This is consistent with primarily NR with possibly a small quantity of SBR being present.

Unfortunately the use of DSC provides only qualitative information about the types of elastomers present and not their quantities.

## 4.5 Solvent extraction

Toluene and THF were initially used as extraction solvents because they are known to dissolve diene elastomers effectively (111). Acetone was used to extract any accelerators present in the reclaim. Acetone is known to cause diene rubbers to precipitate when added to a solution as a non-solvent (112). NR and SBR would thus not be expected to dissolve in acetone. The highly viscous nature of the NRG reclaim, as well as the large low temperature decomposition/evaporation in Figure 4.9, suggests that a significant quantity of the NRG reclaim was processing oil and or low molecular weight polymer. *n*-Hexane was tested in an attempt to try and extract the processing oil only.

It was expected that toluene and THF would dissolve all components except the crosslinked rubber. These solvents were chosen based on the different types of interactions they would have with the material present in NRG reclaim. These interaction were expected to follow the rule of like-dissolves-like. For this reason polar (of different polarities), aromatic and paraffinic solvents were selected.

Table 4.5 shows the percentage of material extracted by each solvent. Figure 4.9 suggests that between 26 and 27% of the NRG reclaim consisted of solid material (carbon black and inorganic ash). This would suggest that a maximum of 73-74% of the material could be dissolved/extracted. Since some polymer was expected to be crosslinked this value could be even less.

*Table 4.5 Percentage material extracted using different solvents*

| *Solvent* | *Initial sample mass (g)* | *Extracted mass in solvent (g)* | *Percentage extract (%)* |
|---|---|---|---|
| *Toluene* | 0.5261 | 0.4689 | 89.1 |
| *THF* | 0.5244 | 0.3581 | 68.3 |
| *Acetone* | 0.5067 | 0.0413 | 8.2 |
| *n-Hexane* | 0.5119 | 0.3483 | 68.0 |

When toluene was used as solvent, 89% of the material was extracted which is in excess of the expected maximum. This would suggest that some of the carbon black/ash residue has passed through the filter paper and been extracted (albeit not dissolved). The typical size of N200 and N300 series carbon blacks which are used in tyres are 20-25 and 26-30 nm respectively (113,114). It is suggested that this material is bound to the polymer chains which when dissolved free up the carbon black to pass through the filter. The unextracted material (11%) would be ash material, which tends to be of greater particle size, pyrolytic carbon black formed during manufacture, and crosslinked polymer. Figure 4.9 suggests that the high molecular weight material is between 14-15%. Because less than 11% of the total material was unextracted and this would have included ash residues, a significant fraction of this high molecular weight material was de-vulcanized and so could be dissolved.

Figure 4.18 presents a thermogravimetric analysis of the toluene extract once the toluene had been evaporated off (DTG curve shown in appendix D). The fact that no mass loss is observed below 100°C indicates that the solvent, toluene was effectively removed. It can be seen that carbonaceous (combustible) material was extracted. The amount of inorganic residue extracted is less than in the bulk sample (see Figure 4.9), which is consistent with the suggestion, above, that this material has a larger particle size than the carbon black. Commercial ZnO has particle diameters of between 0.3 and 1 μm, compared to commercial tyre carbon black which is typically smaller than 0.03 μm (113,114,115). The larger size inorganic materials are thus much less likely to pass through the filter paper than the carbon black, if not bound by rubber.

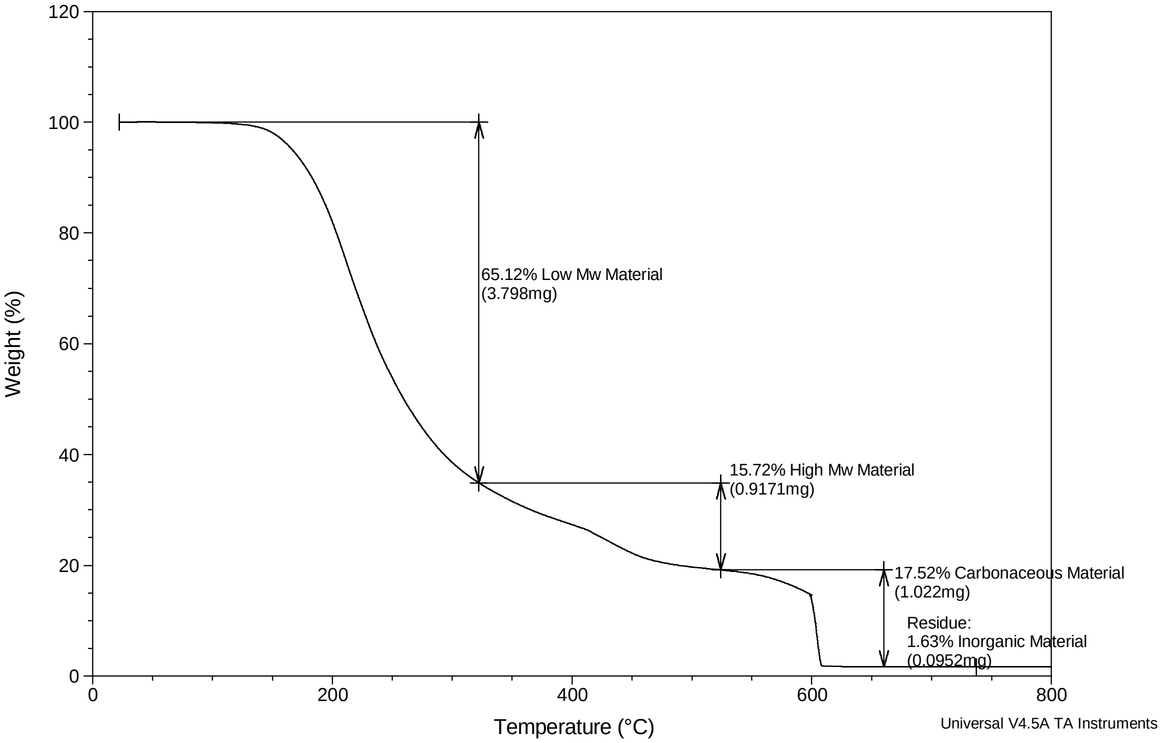

*Figure 4.18 Thermogravimetric characterization of toluene extract of NRG reclaim. A resolution of 5 and sensitivity of 1 was used with a base heating rate of 20°C/min*

19.2% of the extract constituted solid material. Given that 89.1% of the total material was extracted this suggests that 89.2 x (1-0.192) = 72.1% was soluble. It is clear that there is a significant fraction of soluble (de-vulcanized) high molecular weight material present (15.7% of the extract; 12.7% of the total). When this is compared with the high molecular weight material in Figure 4.9; the amounts are similar suggesting that almost all the rubber in the tyres, used in the NRG process, has been de-vulcanized or broken down into independent smaller chains. This is consistent with the severity and higher temperatures of the NRG process.

THF and *n*-hexane contained a similar quantity of extract. This would suggest a similar extract which is possibly processing oil. It is suggested that both solvents are extracting processing oils and low molecular weight polymer. The low quantity of material extracted in acetone would suggest that it only extracted accelerators and additives. Acetone is highly polar which is consistent with the polar nature of most curing agents and anti-degradants. It can be seen in Figure 4.19 that the acetone extract contains very little high molecular weight material (material that decomposes above 300$^{o}$C). The amount of carbon black is also low. This is not surprising because the carbon black is likely bound together by polymer in the NRG reclaim (116). In order for this material to be extracted (pass through the filter) this material would need to first be removed by dissolution which acetone is unable to do.

The thermograms of the extracts in Figure 4.19 show that the different chemical natures of the solvents did have an effect on what was extracted.

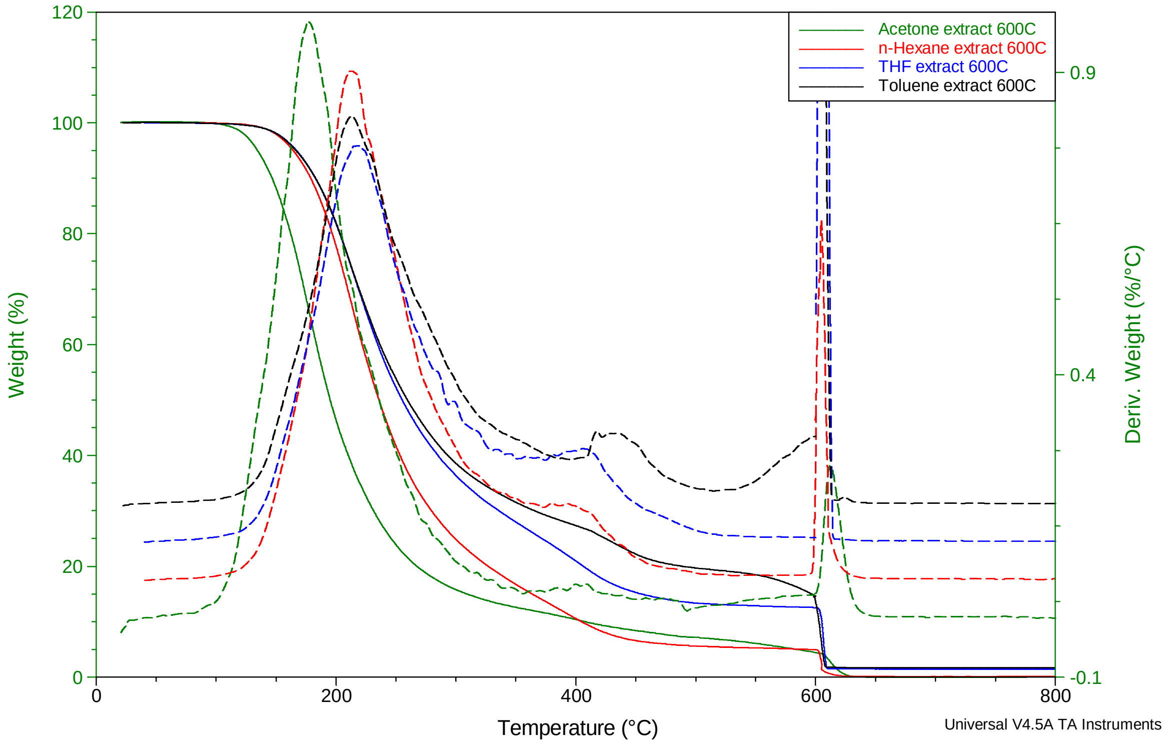

*Figure 4.19 Thermogravimetric comparison of the thermograms of the different solvent extracts from the NRG reclaim. Acetone extract (green), n-hexane extract (red), THF extract (blue) and toluene extract (black). The derivative curves were offset to make analysis easier. A resolution of 5 and sensitivity of 1 was used with a base heating rate of 20°C/min*

What is noticeable is that although the total weight percentage extracted material using THF and *n*-hexane (Table 4.5) were similar, from Figure 4.19, it can be seen that the two solvents extracted different concentrations of material. Toluene and THF were expected to extract similar materials because each solvent is known for their ability to dissolve elastomers (111). Figure 4.20 shows the thermograms of the two extracts by these solvents.

In Figure 4.20 it can be seen that the initial decomposition around 200°C is similar for the two solvents, suggesting similar material is being extracted. The difference starts to occur in the temperature range between 300-600°C. In this range the decomposition of polymeric material such as NR and SBR is expected (see Figure 4.7). It is apparent that the material that is extracted by toluene contains a fraction that has a higher thermal stability. This material is not extracted by THF. This would also explain why less material was extracted by THF in total (Table 4.5).

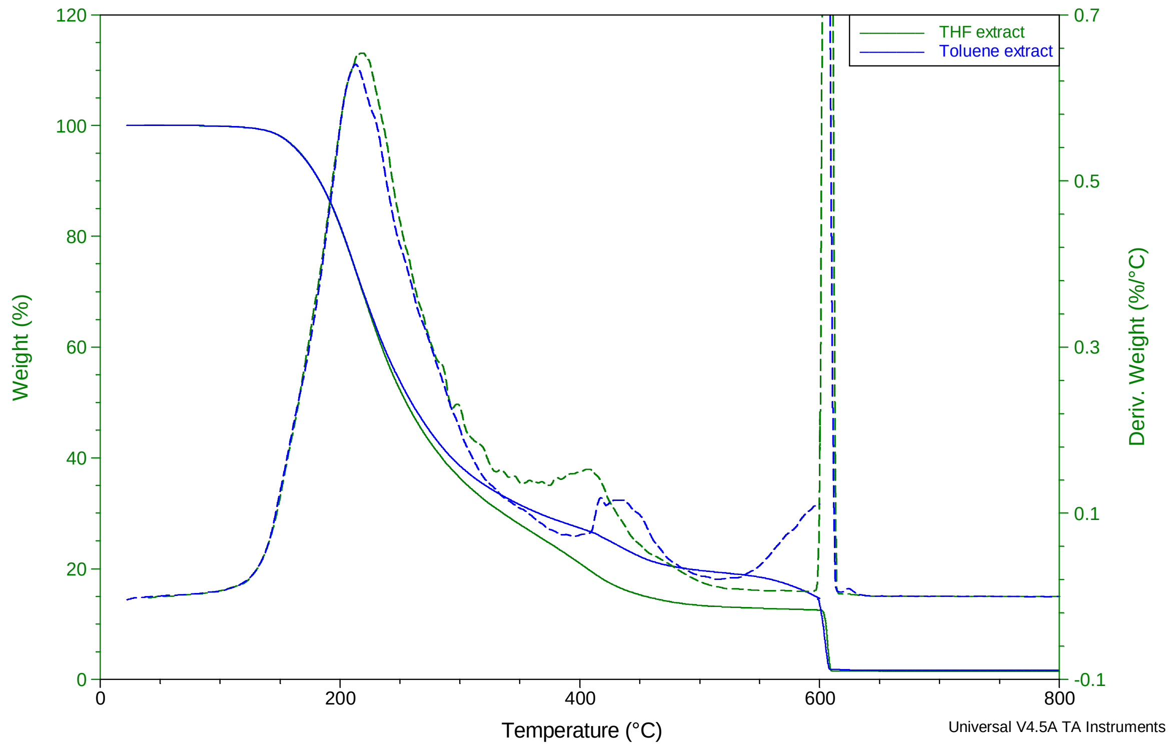

*Figure 4.20 Thermogravimetric comparison of the toluene (blue) and THF (green) extracts. A resolution of 5 and sensitivity of 1 was used with a base heating rate of 20°C/min*

A possible reason for this could be that the THF extracted mostly natural rubber and polyisoprene material whereas the toluene extracted greater quantities of SBR-derived material. Possible evidence for this is the shift in the decomposition range between the two solvents as well as the shape of the derivative curves. While the THF extract (green dotted line) shows a single peak around 400°C, which could be the tail end of a natural rubber decomposition peak, the toluene extract (blue dotted line) shows a slight shoulder at a higher temperature. The higher concentration of carbon black extracted with toluene would also support the idea that more polymeric material was extracted as carbon black is bound into the NRG reclaim matrix by polymer. Both solvents extracted similar low quantities of inorganic material of approximately 1.7%.

The comparison shown in Figure 4.21 is of the extracts of THF and *n*-hexane. What can be seen is that the thermograms are very similar in terms of the thermal decomposition events which would indicate that *n*-hexane extracted not only processing oil but some polymer as well.

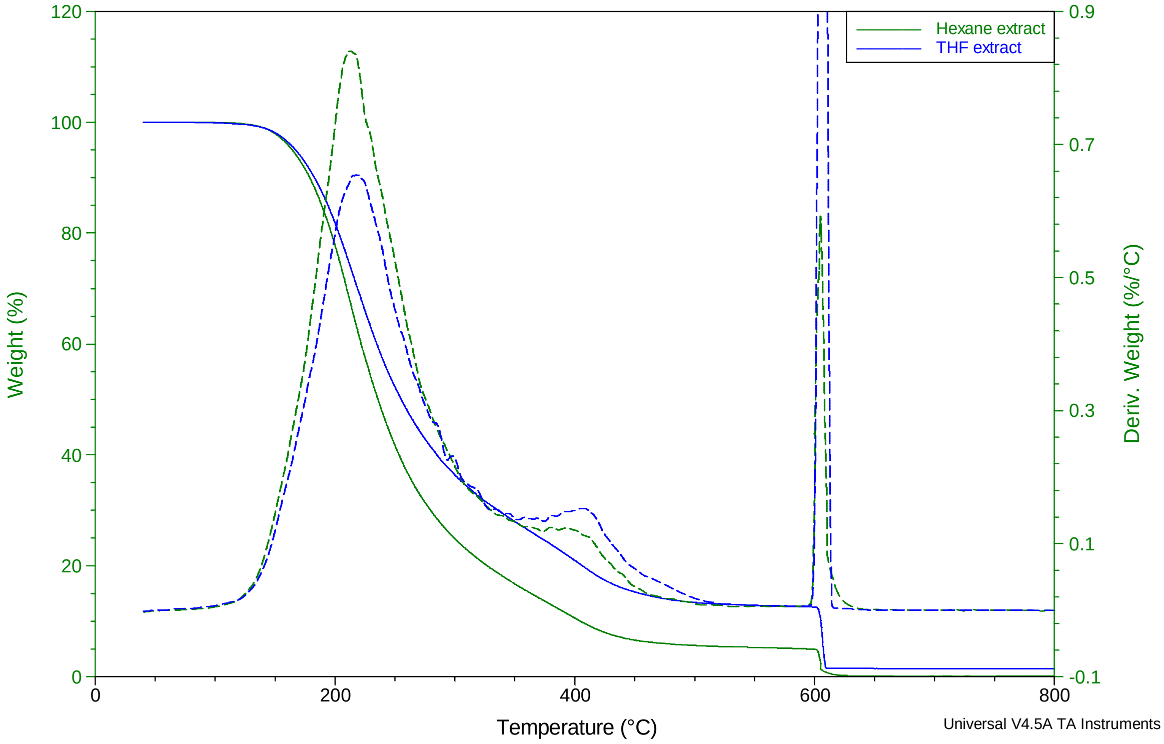

*Figure 4.21 Thermogram comparing the materials extracted from NRG reclaim using THF (blue) and n-hexane (green). A resolution of 5 and sensitivity of 1 was used with a base heating rate of 20°C/min*

When analysing the derivative curves of the two extracts the height of the peaks is taken into consideration. The height of the derivative peaks can be linked to the quantity of material present. *n*-Hexane extracted more processing oil and less polymer that THF. Further support for this idea can be seen in the low concentration of carbon black present in the *n*-hexane extract since polymer (not extracted by *n*-hexane) would retain this material in the NRG gel matrix.

## 4.6 Soxhlet extraction

### 4.6.1 NRG reclaim

The NRG reclaim product was separated into its gel and sol fractions in order to isolate any high molecular weight polymer that might have been present. Thermal analysis on both fractions was carried out and compared. Figure 4.22 shows a thermogram of the thermal decomposition of the gel fraction.

It was expected that a mass loss would be observed at a high temperature (> 400$^o$C) congruent with high molecular weight polymer decomposition and then another mass loss when burnt in oxygen/air due to carbonaceous material combustion. The residue after combustion would be inorganic material that is not combustible.

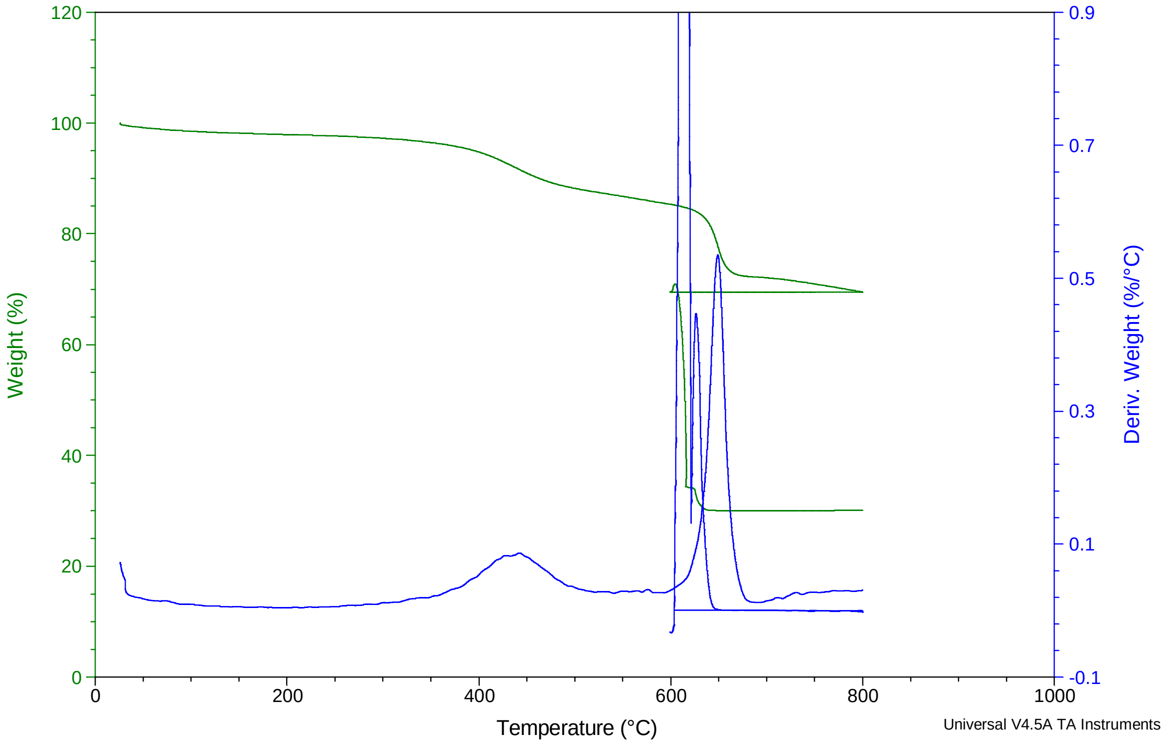

*Figure 4.22 Thermogram of NRG reclaim gel fraction*

Initial experiments revealed an unexpected decomposition step between 600 and 650°C. As a consequence the thermal program was adapted for the analysis of the gel fraction. The program was as follows:

1) Hi-Res$^{TM}$ dynamic, base ramp rate of 20°C/min, resolution 5, sensitivity 1;
2) heat to 800°C in nitrogen;
3) cool at 50°C/min to 600°C;
4) switch purge gas to dry air;
5) Hi-Res$^{TM}$ dynamic, base ramp 20°C/min, resolution 5, sensitivity 1;
6) heat to 800°C in dry air.

This adaption was to allow a decomposition event to occur in nitrogen at 647.9°C which otherwise would have been obscured by the carbon black combustion.

As was expected the thermogram in Figure 4.22 shows that a high percentage of the gel fraction was solid material (in excess of 80%). Carbonaceous material constituted approximate 42% and inorganic material (30%) with only 14% polymer (high $M_w$ material). A further mass loss of 14% is associated with a decomposition between 600 and 640°C. If one looks at the region 700-800°C in $N_2$ one can see that the residual carbon is still losing mass. Ultra high purity nitrogen with an oxygen trap was used, so this mass loss cannot be ascribed to carbon black combustion. It is suggested, however, that this mass loss is the result of the carbonization of PyCB, formed during the NRG reclamation process, rather than commercial carbon black. PyCB contains more oxygen-containing groups on its surface than commercial carbon black as revealed by X-ray photoelectron spectroscopy (XPS) (117). As the PyCB carbonizes, more graphitic structures of formed with a loss of mass due to the loss of these oxygen-containing groups and the removal of asphaltene molecules (13).

The sharp decomposition in the range of 600-650°C was not expected as the gel fraction was being heated in a nitrogen atmosphere. In order to investigate this decomposition step, the ultimate powder residue was subjected to analysis by X-ray diffraction so that inorganic constituents in the ash could be identified.

Figure 4.23 is a powder X-ray diffractogram of this ash. It is apparent that the residue contains both crystalline material (sharp peaks) and amorphous material (seen by the large bump in the baseline in the $2\theta$ range (10-35°). ZnO, the activator, is expected in the ash as well as $SiO_2$ which is an alternative reinforcing filler used in tyres. The powder X-ray diffractogram was compared against the predicted diffractograms of inorganic compounds using Bruker Eva software.

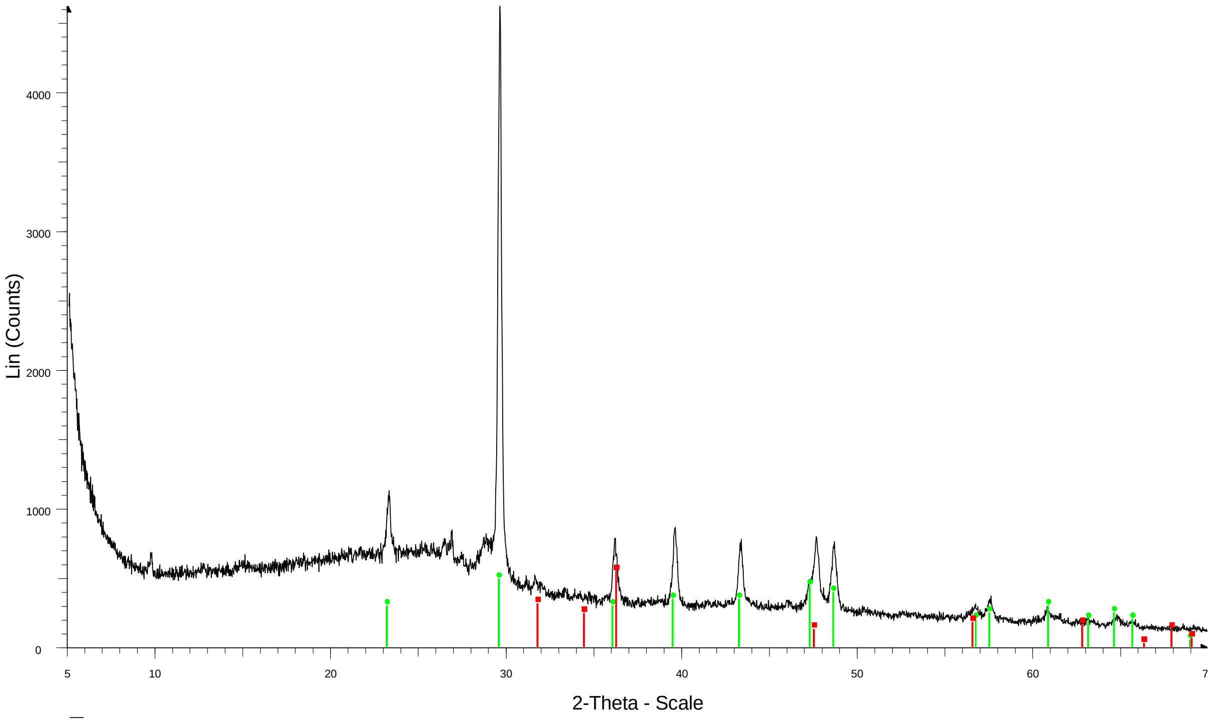

*Figure 4.23 X-ray analysis of the ash. The green bars indicate CaO and the red bars ZnO*

Small quantities of ZnO were identified although no peaks for $SiO_2$ (quartz or cristabolite) could be observed. The latter is not surprising since the silica used in tyres is usually amorphous and thus would not cause sharp X-ray reflections (8). This material would be responsible for the large bump in the baseline (118).

After the ZnO peaks had been removed, large peaks remained. Matching these with the database revealed this material to be CaO. This material is likely derived from calcium carbonate ($CaCO_3$). $CaCO_3$ is known to decompose in the region 600-650$^{o}$C (630$^{o}$C reported by Slough (119) for calcite, heating rate unknown).

$$CaCO_3(s) \rightarrow CaO(s) + CO_2(g)$$

The 14% mass loss before 650$^{o}$C is thus associated with $CO_2$ evolution. Using the molar masses of $CaCO_3$ and CaO, one can calculate that the gel contained approximately (14 x 100.1/44.0) = 31.8%. The CaO would contribute (31.8-14) = 17.8% of the total mass. Thus much of the final residue (17.8/30)x100% = 60% is due to CaO, with the rest being ZnO and probably silica.

Although $CaCO_3$ is used as a filler in industrial rubber compounds, it is not reinforcing and is thus not used in tyres (8,120). It is suggested that the source of the $CaCO_3$ is the reclamation process used by NRG where it may be added to facilitate de-vulcanization. The decomposition of the $CaCO_3$ residue can be seen above 600°C in the thermograms for the complete NRG reclaim sample (Figure 4.9 and Figure 4.13). Figure 4.24 shows a close-up of the region where the $CaCO_3$ was identified.

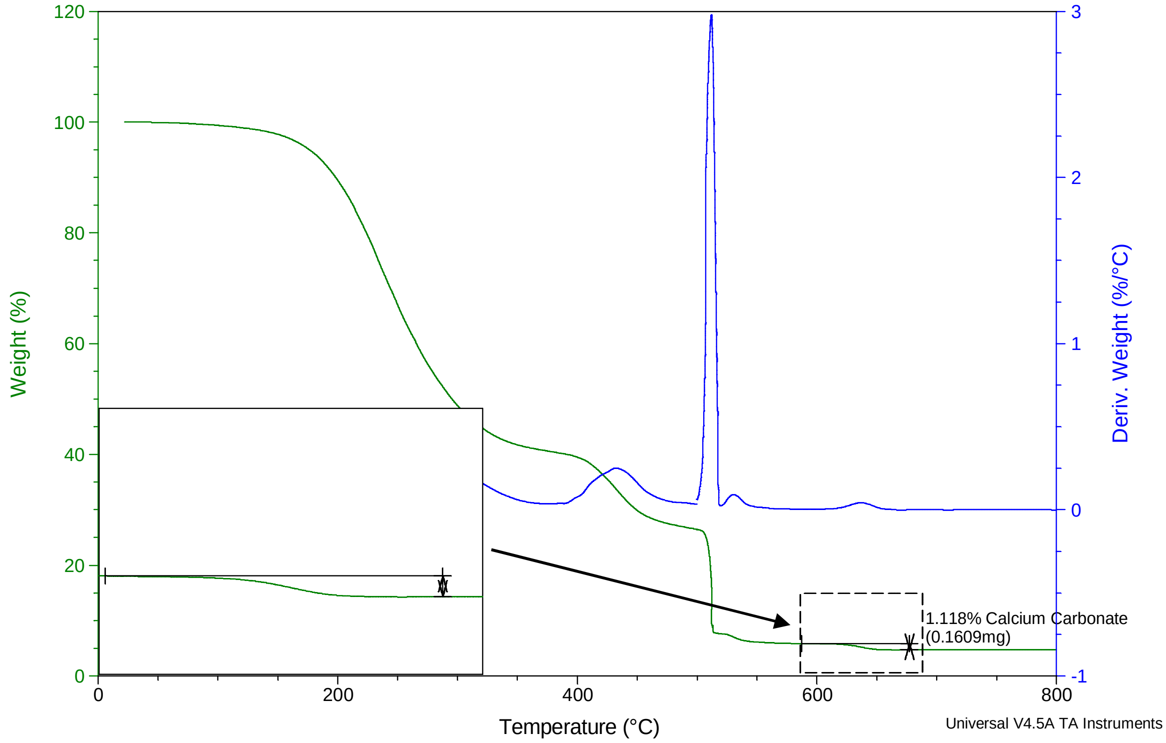

*Figure 4.24 $CaCO_3$ weight loss on the original NRG reclaim*

Figure 4.25 is a thermogram of the sol fraction. The sol fraction is expected to contain processing oil, accelerators, additives and some polymeric material. The same heating program that was used for the gel fraction was applied to the sol fraction.

The thermogram in Figure 4.25 shows that a high percentage of the sol fraction probably consists of processing oil or low molecular weight polymer.

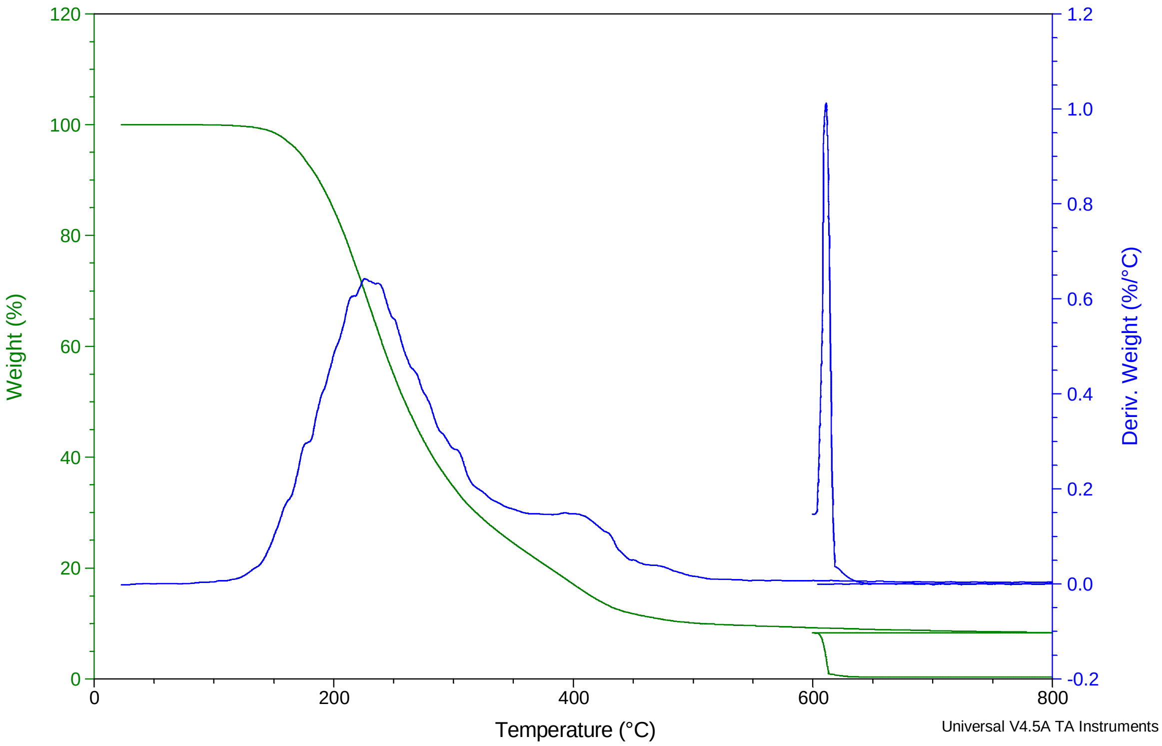

*Figure 4.25 Thermogram of the sol fraction of NRG reclaim.*

70% of the sample has decomposed/evaporated by 300°C. At 400°C the thermogram shows weight loss that is associated with higher molecular weight polymeric material. It is also apparent from the thermogram that filler material such as carbon black is present in much smaller quantities than in the gel fraction. This is not unexpected. This material would be carbon black, released upon the dissolution of polymer binding it in the NRG matrix. Noticeable the inorganic residue is minimal, suggesting this material is of larger particle size; nor is the decomposition in $N_2$ in the temperature range 600-650°C observable. This indicates that the $CaCO_3$ is completely associated with the gel fraction.

Figure 4.26 shows a comparison between an acetone and toluene wash of the sol fraction. After the soxhlet extraction the solvent used in the extraction was allowed to evaporate. Acetone was then added to the dry sol fraction to remove any accelerators present. This constituted the acetone wash. This wash should not dissolve any polymeric material. The acetone was then decanted and allowed to dry. The sol fraction left behind was dried before the toluene wash. Toluene was added to the sol fraction to dissolve any processing oil and polymeric material remaining. This constituted the toluene wash. The toluene was then decanted and allowed to dry. This was done partly to make sure that no significant quantity of insoluble material had passed through the filter paper and thimble. This process also served the purpose of verifying some results obtained with the previous solvent extractions, ie: does acetone only extract accelerators.

The aim of washing the sol fraction with acetone and toluene was for characterization purposes. The overlay in Figure 4.26 suggests that acetone removed any accelerators present. However, it also appears to have removed processing oil. The toluene wash shows that there was some polymer extracted into the sol fraction. Very little polymer was extracted by the acetone wash. The two solvent washes corroborate the analysis of the sol fraction done in Figure 4.25. It is noticeable that the carbon black remains in the toluene fraction because the polymer that is not removed by the acetone keeps it bound.

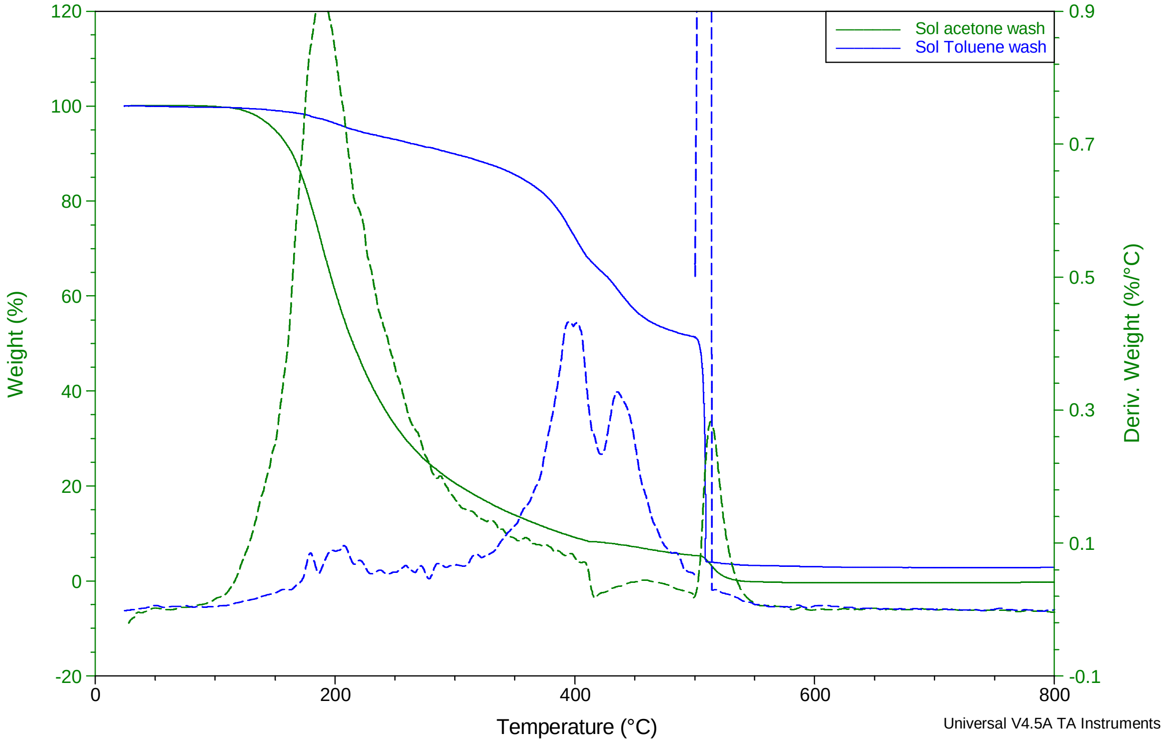

*Figure 4.26 Comparison of the thermograms of an acetone and a toluene wash of the sol fraction. A resolution of 5 and sensitivity of 1 was used with a base heating rate of 20°C/min*

### 4.6.2 Commercial tyre tread reclaim

As the commercial tyre tread reclaim was solid it was decided that doing multiple solvent extractions would not result in any useful results. It was expected that, given the physical nature of the sample, the reclaim would contain small amounts of oil, soluble polymer and carbon black. Soxhlet extraction was carried out on the commercial tyre tread reclaim (*ex* Bridgestone) under the same conditions as the NRG reclaim. Thermal analysis was carried out on the gel and sol fractions. It was not necessary to alter the basic heating program since this reclaim contained no $CaCO_3$ material. The procedure that was followed is outlined in section 3.3.1.

As expected the gel fraction contained polymer, carbon black and inorganic material. The gel fraction, Figure 4.27, showed multiple decomposition steps. The two peaks in the derivative curve between 300-400°C is most likely NR although the decomposition peaks in the DTG curve are similar in height suggestion other rubbers such as SBR may be present. The fact that polymer is present in the gel fraction is indicative of the fact that not all of the rubber has been completely de-vulcanized. If all crosslinks had been broken, the material would have been soluble. It can be seen that unlike the thermogram of the gel of the NRG reclaim (Figure 4.22) there is very little mass loss between 500-600°C.

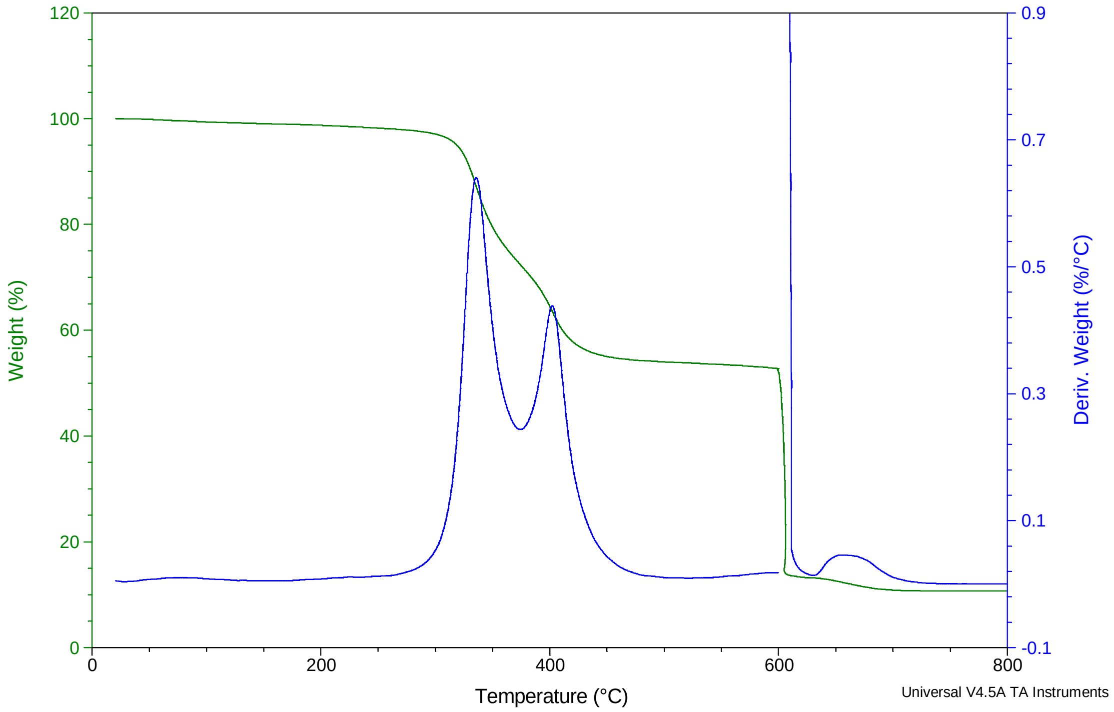

*Figure 4.27 Thermogram of a commercial tyre reclaim gel fraction. A resolution of 5 and sensitivity of 1 was used with a base heating rate of 20°C/min*

This indicates that the carbon black is fully carbonized and very little PyCB forms during the production of this reclamate. Figure 4.28 contains the thermogram of the sol fraction. It can be seen that this fraction contains both low molecular weight material (decomposing below 300°C) and higher molecular weight material. This latter forms approximately 60% of the sol fraction. Comparing the relative heights of the 2 decomposition peaks in the DTG curve (above 300°C) it can be seen that the first peak is much larger than the second. This is unlike the gel fraction (Figure 4.27).

This is consistent with the polymeric material present in the sol fraction being derived from NR (compare Figure 4.28 and Figure 4.7). This is not surprising since it is known that it is easier to de-vulcanize NR than SBR (5). Very little carbon black was present in the sol fraction. This is probably because the presence of partially vulcanized rubber in the gel fraction binds the fillers, unlike the NRG reclaim.

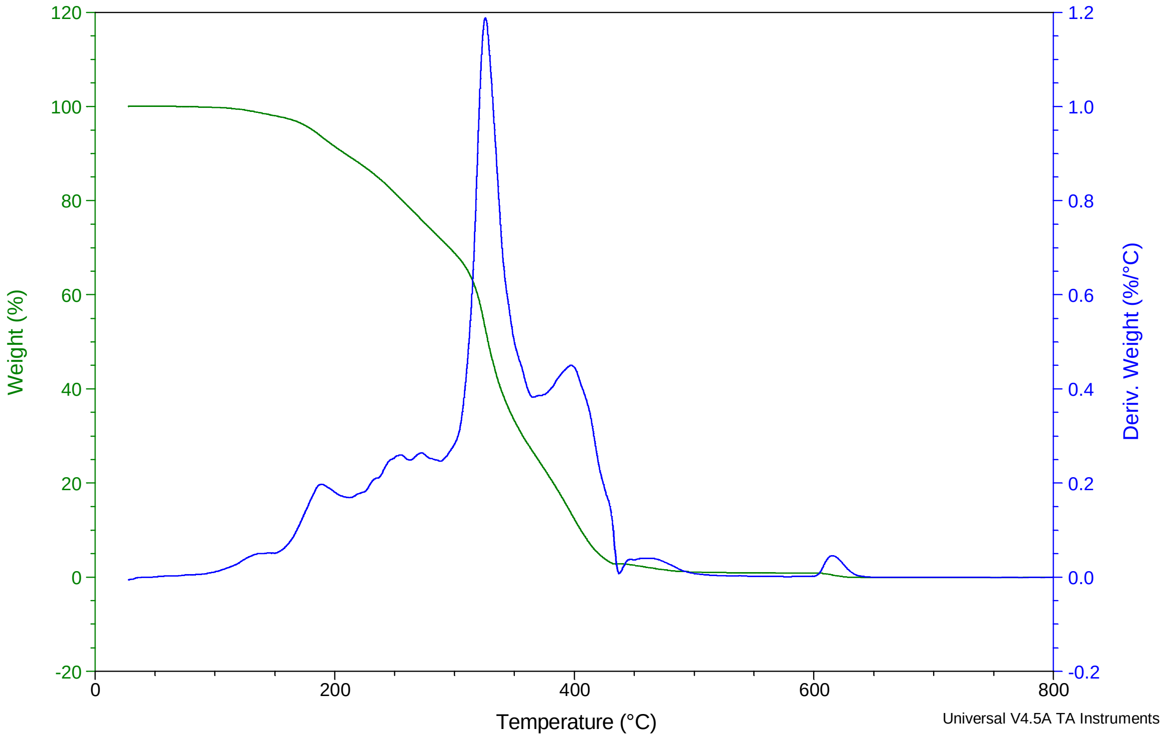

*Figure 4.28 Thermogram of the sol fraction of a commercial tyre reclaim. A resolution of 5 and sensitivity of 1 was used with a base heating rate of 20°C/min*

The large number of peaks in the DTG curve below 300°C suggest that sol fraction comprises a complex mixture of processing oils and curatives as well as possible low molecular weight polymer. Figure 4.29 provides a comparison between the sol fraction thermogram and the low molecular weight polyisoprene standard. This, however, is not conclusive of the presence of low molecular weight polymer in the sol fraction.

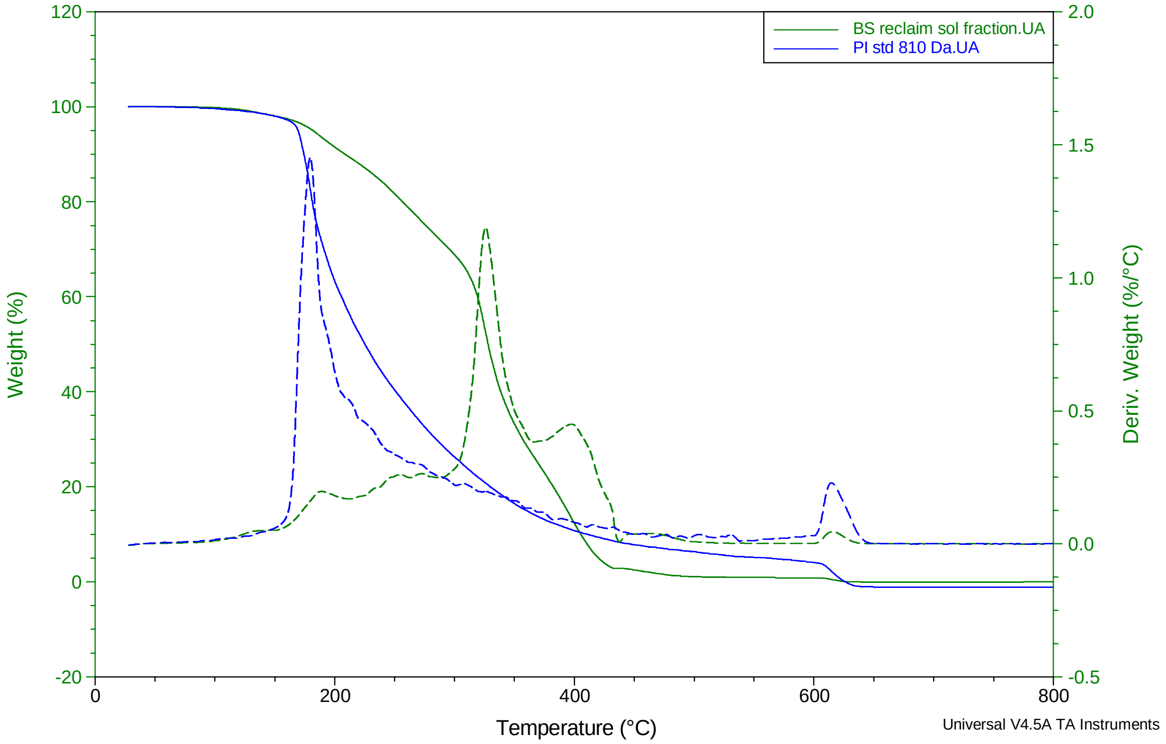

*Figure 4.29 Comparison of the thermograms of a polyisoprene standard (blue) with a commercial tyre tread reclaim (green). A resolution of 5 and sensitivity of 1 was used with a base heating rate of 20°C/min*

# CHAPTER 5

# 5 FORMULATION DEVELOPMENT

## 5.1 Processability

The first challenge when developing new rubber formulations is the ease of mixing/processability of the compound. This is concerned with the maximum temperature reached during mixing as well as the overall torque of the mixture. Ideally both these parameters should be as low as possible to reduce the chance of premature curing and to lower the overall energy and hence cost required for manufacturing. The figures in this section show the mixing temperature and torque during the mixing of a variety of rubber compounds. The procedure for mixing was outlined in section 3.2.1. The formulations that are reported in this section may be found in Appendix A.

NRG reclaim was substituted for both NR & SBR equally and for just the SBR component. The NRG reclaim substituted formulation was a direct substitution based on the Hi-Res™ TGA analysis of its composition. According to the analysis the NRG reclaim consisted of approximately 14% high molecular weight material (decomposition temperature consistent with SBR), 22% carbon black and 5% inorganic material. These values were subtracted from the virgin material and replaced with the NRG reclaim. For the NR & SBR the 14% polymer was subtracted from the 100 phr and then divided by 2, thus the loss of virgin material was equally distributed between both polymers. The total substituted virgin material was 15%.

For comparative purposes a non-substituted NRG reclaim formulation was created. For this formulation the virgin material was not substituted and the NRG reclaim was added as any other material in the formulation. The same process was followed when using the commercial tyre tread reclaim.

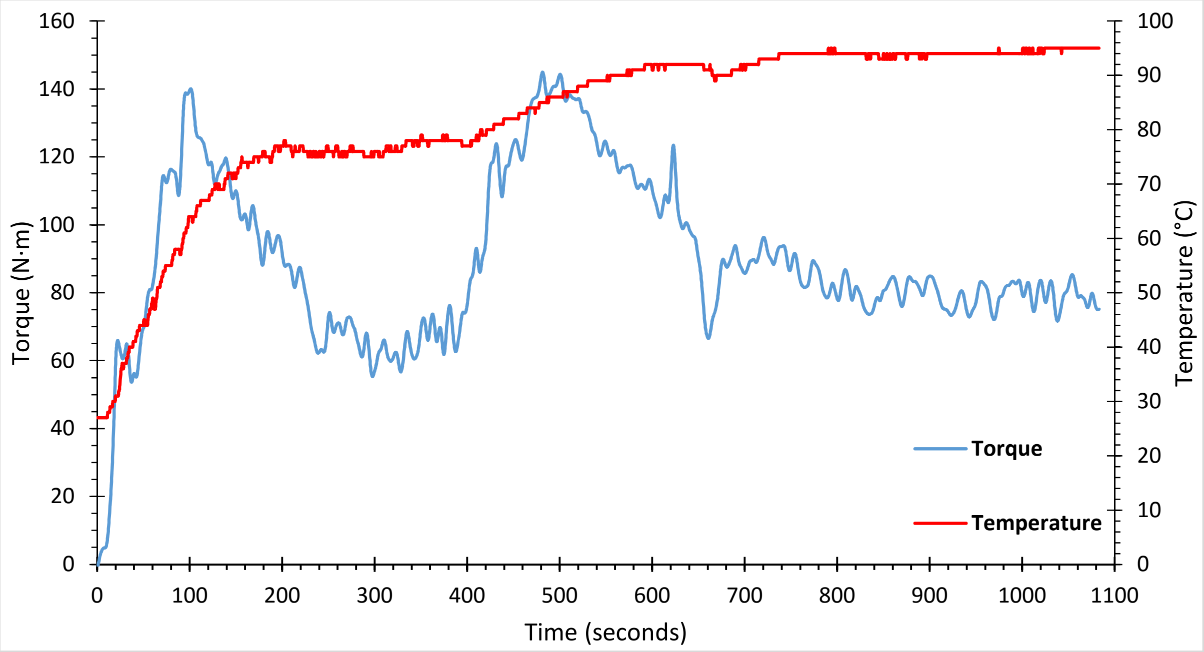

*Figure 5.1 The effect of mixing on torque and temperature during the mixing of natural rubber (NR)*

Figure 5.1 shows how the mixing torque and the temperature vary during the mixing of a NR formulation. The initial increase in temperature and torque is due to the addition and subsequent mastication of the rubber (121). The sharp drops in the torque that can be seen, *e.g.* near 650 s, are when the ram, which closes the internal mixer, was lifted to add the next chemical. This relieves the internal pressure and thus the torque required to move the rubber in the mixing chamber. The increase in torque, starting at 400 s, is due to the addition of carbon black. During this period, agglomerates in the carbon black are broken down. A corresponding increase in temperature can be seen as a result of this. Large increases in torque, require significant energy which is absorbed by the material. The total mixing time was 1090 s, although a level torque had been reached after 850s. The final torque was about 79 N·m and the final temperature was 95°C (reached after 740s).

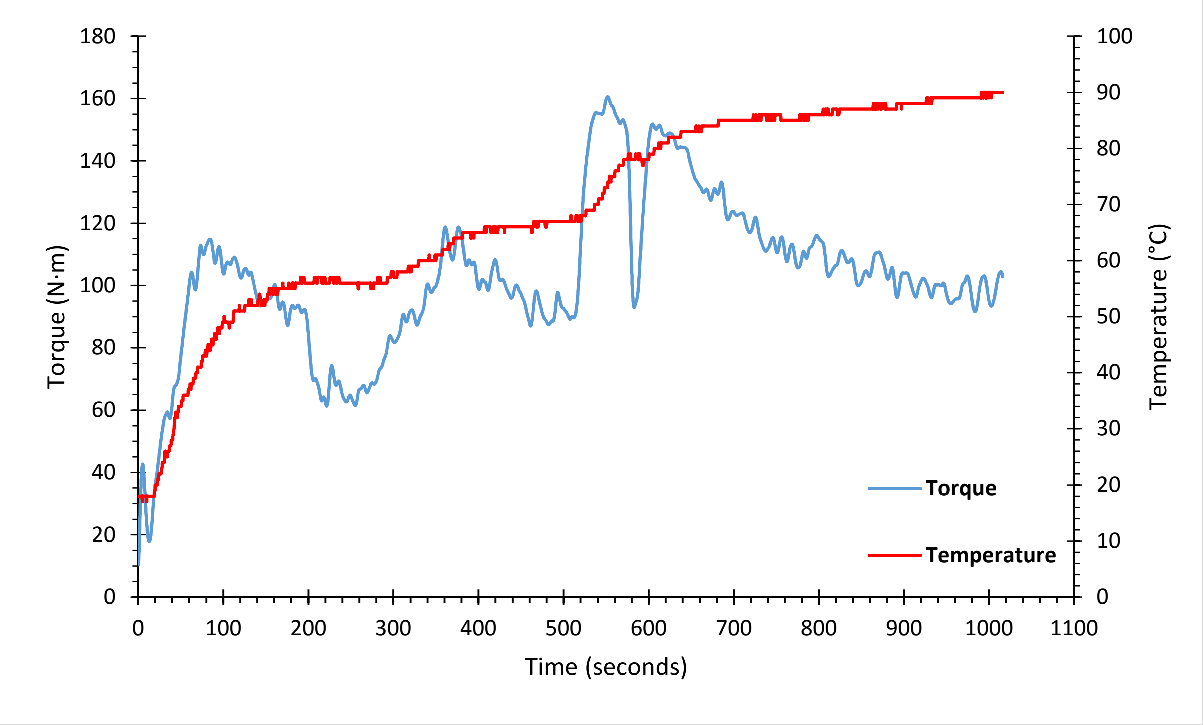

*Figure 5.2 The effect of mixing on torque and temperature during the mixing of oil extended styrene butadiene rubber (SBR-OE)*

Figure 5.2 displays the increase in torque and temperature for the mixing of a SBR formulation. The maximum torque reached after the addition of the rubber (115 N·m) is less than that required for NR (140 N·m), it is possible that SBR had a lower viscosity due to oil that makes up part of the OE-SBR. The temperature rise during this first step (reaching 58$^{o}$C vs 76$^{o}$C) is consequently lower. However, the torque after adding carbon black was higher for SBR than NR.

The increase in temperature and torque around 300 s is again due to the loading of carbon black. The increase around 500 seconds corresponds to the addition of ZnO and stearic acid. The final mixing started at 895 s, the total time was 1015 s (constant torque achieved after 900s). The final torque was 98 N·m and the final temperature was 90°C. It should be noted that the SBR used was a solution SBR which typically has higher Mooney viscosities than emulsion SBR (39).

NR and SBR were combined to make a standard tyre formulation (Table 3.1). The mixing behaviour of this formulation is illustrated in Figure 5.3.

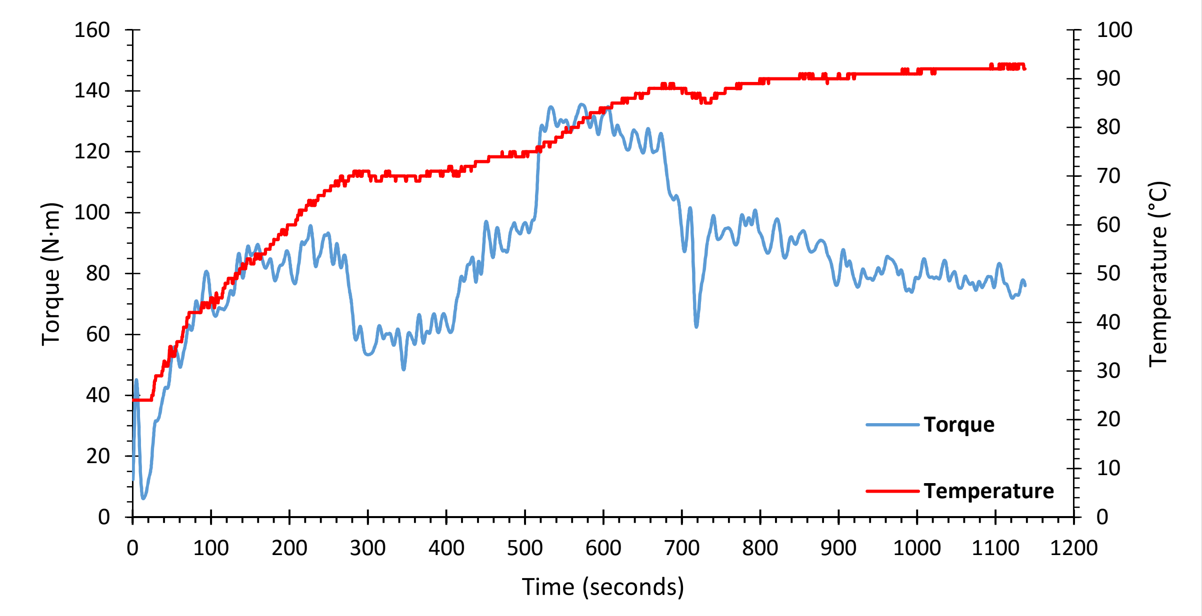

*Figure 5.3 The effect of mixing on torque and temperature during the mixing of a standard (NR & SBR) tyre tread formulation*

The mixing behaviour of the combined (NR & SBR) formulation is similar to that when NR was mixed. The initial torque rise, during the addition of the rubber, however was lower (98 vs 140 N·m). This may be the result of the lower viscosity of the SBR-OE component. This initial torque spike lasted for longer than with the rubbers alone, presumably because not only do the rubber blocks need to be heated and mixed but one of the rubbers will become a dispersed phase in the other. In a 50:50 blend of NR/SBR, NR constitutes the continuous phase (122).

The total mixing time was 1140 s (level torque achieved after approximately 980s). The final torque was 77 N·m and the final temperature was 92℃. These values are similar to those observed when preparing the NR formulation.

Figure 5.4 shows the mixing behaviour of a formulation in which some of the rubber (NR & SBR) has been substituted by non-filler components of NRG reclaim. This formulation reduced the amount of virgin material used so as to offset the material present in the reclaim rubber. The total reclaim added amounted to 15%. Because the NRG-reclaim contains filler, the virgin carbon black added was also reduced. See Table 9.1.

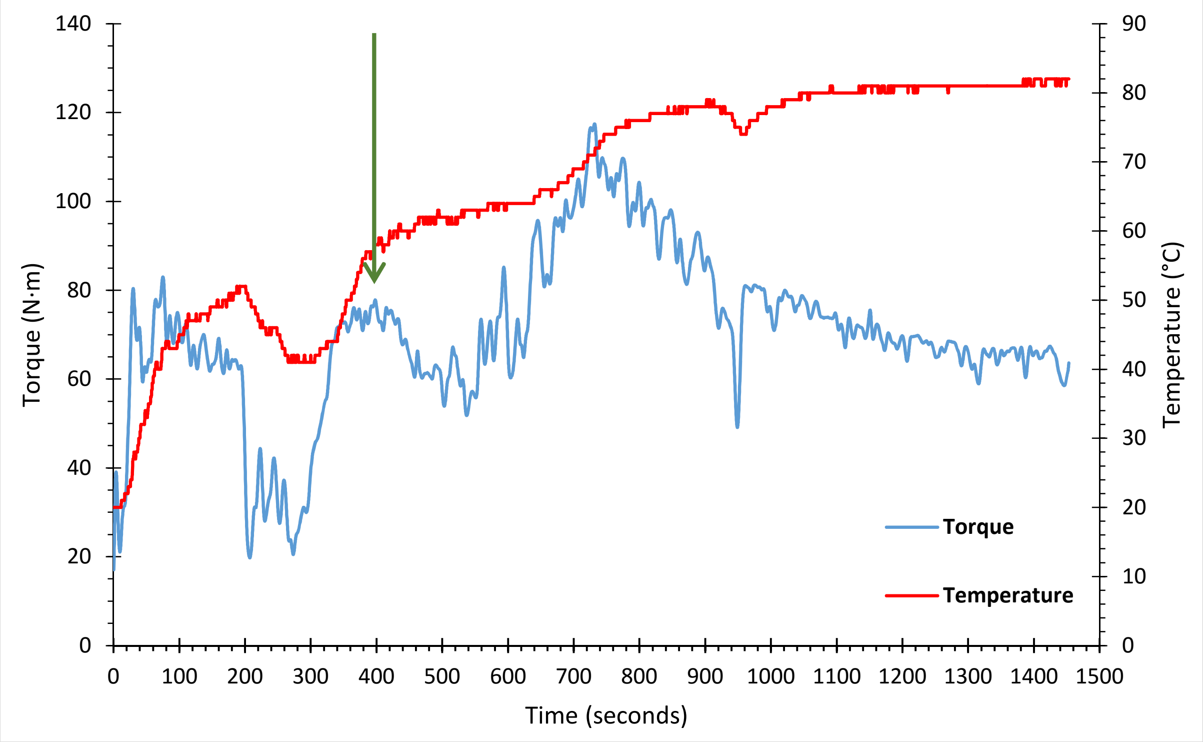

*Figure 5.4 The effect of mixing on torque and temperature during the mixing of a NRG 15% substituted reclaim rubber formulation*

The addition of the rubber was split into two parts in order to use the rubber to assist with the addition of the NRG reclaim product. Three quarters of the rubber was added in the first step and allowed to mix before the addition of the last quarter with the NRG reclaim. The drop at 200s in the torque indicates when the reclaim was added. Maximum torque, after all rubber including reclaim, was added but prior to carbon black addition was 80 N.m. This point is marked by a green arrow in Figure 5.5. This value is significantly lower than measured in the NR, SBR and (NR & SBR) formulations. It is possibly the result of the large quantities of processing oil in the NRG reclaim which acts as a process aid.

The temperature increase is also much lower such that the maximum temperature after the addition of carbon black is lower than the previous 3 formulations. Note that the temperature reached (50$^{o}$C) after the addition of ¾ of the rubber is lower than the NR & SBR formulation because the mixing chamber is not full and less friction is experienced.

The large increase in torque around 600 s is due to the addition of the carbon black but what should be noticed here is that the maximum torque reached is lower than the other formulations (Figure 5.1, Figure 5.2 and Figure 5.3). The total mixing time was 1365 s which is longer than before because an extra step is needed to add the reclaim. Constant torque was achieved after 1300s. The final torque was 65 N·m and the final temperature was 81°C. The former is the result of the processing oils in the reclaim acting as plasticizers. Maximum torque (116 N·m) is also lower, indicating that the addition of NRG reclaim would lead to energy savings.

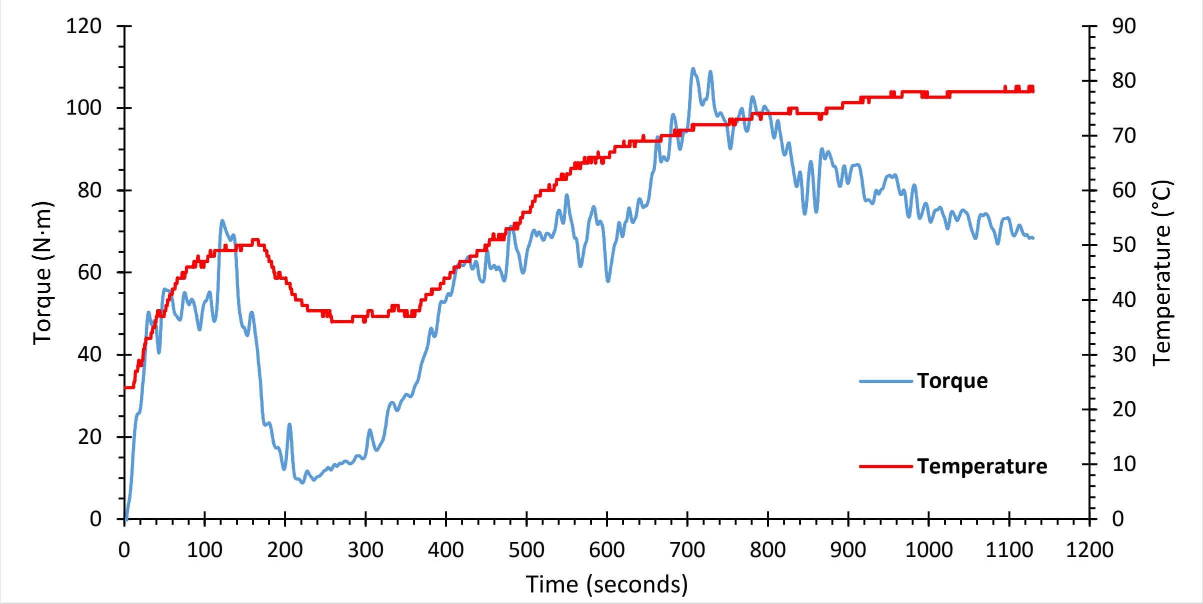

*Figure 5.5 The effect of mixing on torque and temperature during the mixing of a NRG 15% non-substituted reclaim rubber formulation*

Figure 5.5 shows the mixing behaviour where NRG rubber reclaim was added in addition to the 100 phr of existing rubber. For this formulation there was no substitution of the virgin material, instead the NRG reclaim was added as a processing aid (Table 9.1). Because the NRG reclaim contains carbon black and inorganic residue, the amount of filler is higher than for the formulation whose behaviour is presented in Figure 5.4.

The rubber was added in two stages to facilitate the addition of the NRG reclaim product. After each mix using NRG reclaim the beaker used to add the reclaim was weighed again. The average weight of reclaim left behind was 2.3 g. This could not be avoided because of the highly viscous nature of the NRG reclaim.

When the carbon black was added, around 400 s, the increase in temperature is almost immediate. The increase in torque, however, lagged behind and only showed a noticeable increase once the ram was closed. This suggests that frictional heating was occurring in the region of the thermocouple, immediately on CB addition. The total mixing time was 1120 s. The final torque was 71 N·m and the temperature was 79°C.

The sharp drops in the torque were observed when the ram was lifted in order to add in the next material/chemical. When adding the NRG reclaim the viscous reclaim would initially coat the mixing pins with a thin layer of oil and this would cause the rubber to push out of the mixing chamber. This would show up as large drops in torque for extended periods of time while the Reclaim acted as a lubricant on the surface of the mixing rotors. This also explains why the mixing times for the samples containing NRG reclaim were longer than the other mixes.

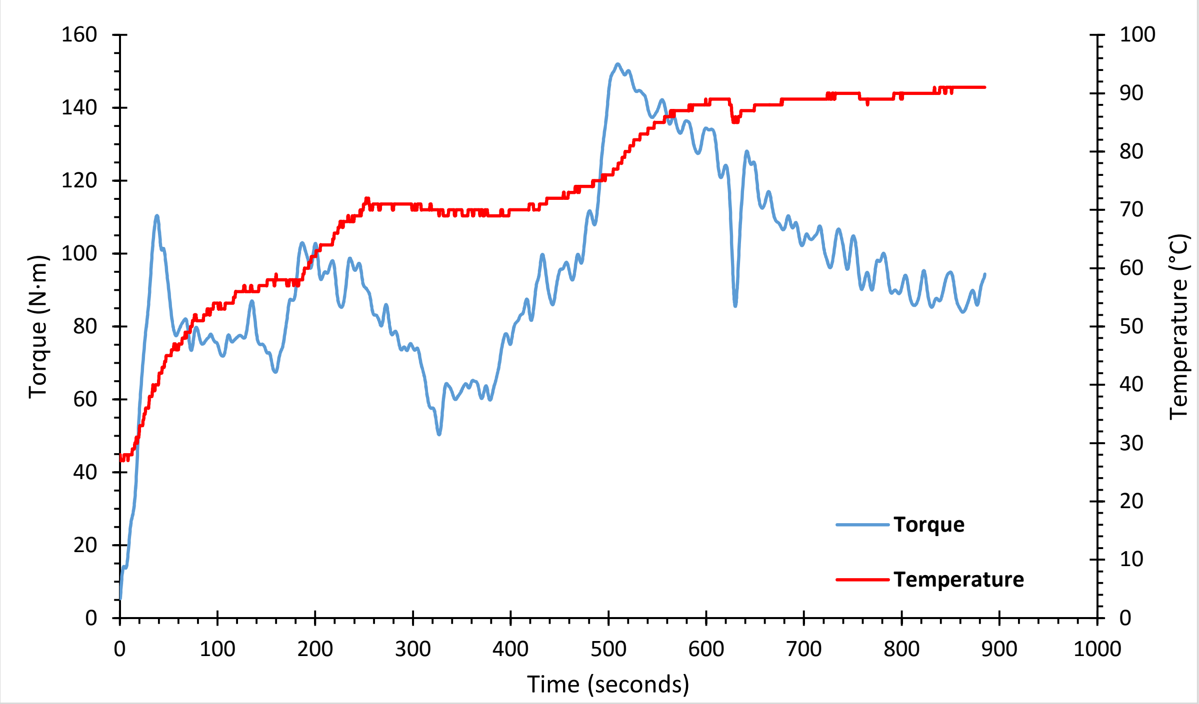

*Figure 5.6 The effect of mixing on torque and temperature during the mixing of commercial tyre tread reclaim 15% substituted formulation*

Figure 5.6 shows the mixing behaviour for the commercial tyre tread reclaim rubber (*ex* Bridgestone) in which 15% of the virgin rubber had been substituted. The virgin NR, carbon black and ZnO were reduced in accordance to the quantities of these materials found by thermogravimetric analysis. Although the reclaim is a solid, it was added in a separate, later step to the virgin material. This allows the effects, which the two types of reclaim have on processing, to be clear and compared.

Around 200s there is an increase in torque and temperature. This is in response to the commercial tyre tread reclaim being added. When the torque before the addition of carbon black is compared to the torque of (NR & SBR), an increase can be seen. At this point in the mixing, however, the temperature closely matched that of the (NR & SBR) formulation that was used as a standard. At 500 s the spike in torque and temperature is as a result of the addition of carbon black. When compared to the other formulations this increase in torque is higher than any other formulation other than the 100 phr SBR formulation. The final mixing time was 900 s with a torque of 94 N·m and temperature of 91°C.

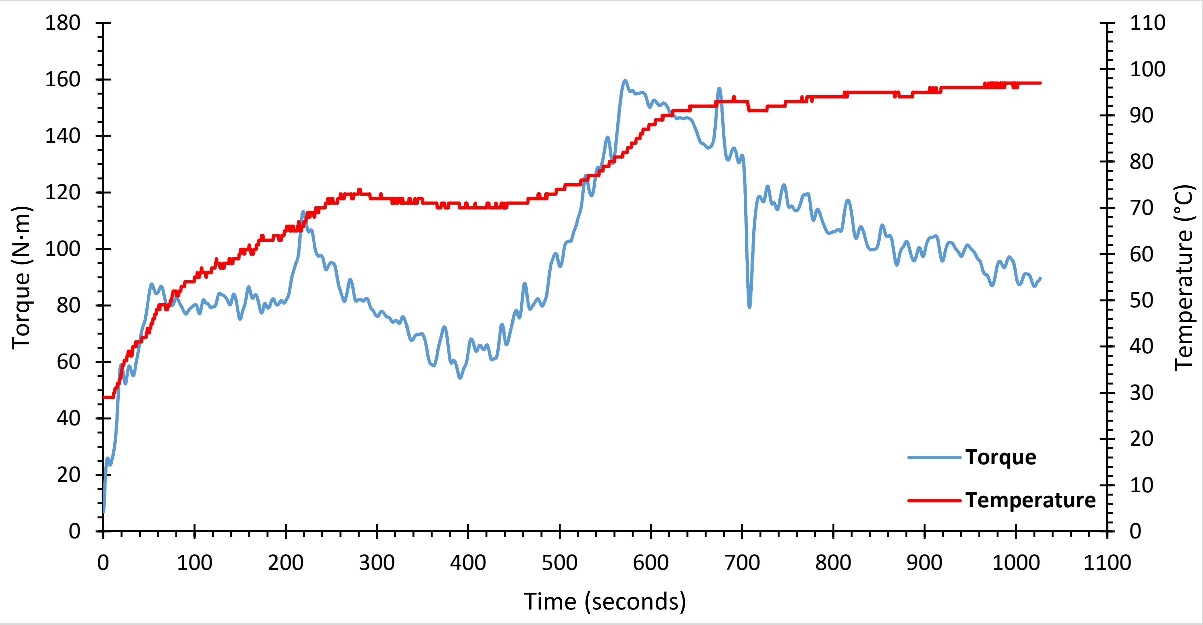

*Figure 5.7 The effect of mixing on torque and temperature during the mixing for commercial tyre tread reclaim 15% non-substituted formulation*

Figure 5.7 shows the mixing behaviour of the commercial tyre tread reclaim 15% non-substituted formulation in which the reclaim was added in addition to the 100 phr (NR & SBR). At 200 s the effects of the commercial tyre tread reclaim can be seen by the increase in torque and temperature. The addition of the carbon black explains the increase in torque and temperature after 500s. The trend of the Bridgestone reclaim 15% non-substituted formulation is similar to that of the substituted formulation. The final mixing time was 995s with a torque of 94 N·m and a temperature of 97°C.

*Table 5.1 Maximum mixing torque, final torque, final temperature and mixing times for conventional vulcanization (CV) rubber formulations*

| *Formulation* | *Maximum torque (N·m)* | *Final torque (N·m)* | *Final Temp. (°C)* | *Total mixing time (s)* | *Time to reach constant torque (s)* |
|---|---|---|---|---|---|
| *Natural rubber* | 144 | 79 | 95 | 1090 | 850 |
| *Styrene butadiene rubber* | 161 | 98 | 90 | 1015 | 900 |
| *NR & SBR* | 137 | 77 | 92 | 1140 | 980 |
| *NRG reclaim 5% non-sub.* | 140 | 78 | 95 | 1408 | 1100 |
| *NRG reclaim 15% sub.* | 116 | 65 | 81 | 1320 | 1360 |
| *NRG reclaim 15% non-sub.* | 110 | 71 | 79 | 1120 | > 1100 |
| *NRG reclaim 15% SBR sub.* | 110 | 71 | 76 | 1116 | >900 |
| *Commercial tyre tread reclaim 15% sub.* | 160 | 94 | 91 | 900 | > 900 |
| *Commercial tyre tread reclaim 15% non-sub.* | 159 | 94 | 97 | 995 | > 900 |

Table 5.1 presents the final torque, temperature and mixing time of each of the rubber formulations. It should be noted that although the mixing chamber is cooled by ambient cooling water, this is uneven across the chamber. The side of the mixing chamber that received the cooling water was noticeably cooler than the opposite side. The thermocouple was placed on the warmer side of the mixing chamber. The mixing pins were not water cooled and therefore heat dissipation relied on the water being pumped through the walls of the mixing chamber. Therefore, when analysing the differences in temperature, only large differences should be viewed as significant.

It was noticed that the final torque for SBR was considerably higher than that of the NR and (NR & SBR) compounds. This is opposite to what was noticed for the initial mixing of the elastomers. This would suggest that the addition of the filler and other materials played a large role in the final torque value. It could be possible that the disaggregation of the carbon black in SBR requires a higher energy input than in NR. This could explain the higher maximum torque and final torque of SBR when compared to NR. While a high torque normally means a high temperature when mixing, it was concluded that because the SBR used was oil extended this would aid in processing and reduce the temperature. This can be seen in the case of NR, which was not oil extended. Despite the maximum and final torque being significantly lower than observed with the SBR formulation, final mixing temperatures were similar.

The samples containing NRG reclaim have a longer mixing time as the addition of the reclaim caused the mixing pins to slip. This resulted in the rubber being pushed out of the mixing chamber. The addition of carbon black to samples containing NRG reclaim also took longer as the carbon black was not as easily mixed into the rubber as with the other samples. This might be because the reclaim is coating the rubber, inhibiting the thorough mixing of carbon black. It should be noted that common industrial practice is to masterbatch the carbon black into rubber prior to adding process aids/oils (114). This is the opposite of what was done here. The complete incorporation of the NRG reclaim therefore took longer than other samples. When analysing the NRG reclaim formulations, it is clear from the drop in maximum mixing torque that the reclaim was acting as a processing aid. The lower final temperatures also adds an element of mixing safety by mitigating against premature cure. The lower mixing torques mean lower mixing energies but this is somewhat offset by the longer total mixing times that are required.

When the commercial tyre tread reclaim was mixed with virgin material the result was higher torque and temperature values when compared with 100% virgin material formulations. This could be due to the reclaim being a flexible solid, unlike the highly fluid NRG reclaim. This reclaim contained low levels of oil, and was primarily polymer (NR mainly) and carbon black (see Figure 4.11). Therefore when compounding, the virgin NR and carbon black was decreased and substituted with 15% of this reclaim. What may have occurred is that the reclaimed NR acted more as a filler than a polymer. If the reclaim was acting as a filler this could mean that the NR content could be less than the 100% virgin formulation. This could possibly leave SBR as the dominant polymer. From the 100% virgin SBR formulation it would seem that SBR increases the temperature and torque values. It is thought that these two reasons, Bridgestone reclaim acting as a filler and SBR having an inherently high torque and temperature, could explain the higher than normal torque and temperature values.

### 5.1.1 Effects of TMTD and CTP

The previous mixing study was done using a conventional vulcanization (CV) system where the ratio of accelerator to sulfur was approximately 1:1. Note that some authors call this a semi-efficient system (35). Because reclaim may have effects on cure kinetics, studies were also performed using an efficient vulcanization system (EV). Data on mixing was also compared for these two systems.

The EV curing system studied the effects of a semi-ultra accelerator tetramethylthiuram disulfide (TMTD) which is also a sulfur donor (8). In the presence of ZnO, the ultra accelerator ZDMC is formed (8,51). The CV system contained the slower accelerator, CBS. The EV curing system used has the ratio of accelerator to sulfur is approximately 1:0.25. These formulations may be found in Appendix A in Table 9.2 and the mixing kinetics are shown in appendix G. It’s called efficient because of the lower use of sulfur (56).

When mixing temperatures rise, it is possible that preliminary reactions of the vulcanization sequence may be initiated and premature vulcanization is possible. In order to increase the scorch safety (increase the induction time) of the formulations, the effects, which N-(cyclohexylthio)phthalimide (CTP) would have on the kinetics of vulcanization of the formulations, were investigated. CTP is a pre-vulcanization inhibitor (PVI) which reacts with key intermediates to delay the onset of crosslink formation (53,123). CTP has been shown to be highly effect for the inhibition of vulcanization using benzothiazole-type accelerators, such as CBS and DPG (53,123).

Investigations into EV systems was restricted to formulations based on a 50:50 blend of NR and SBR. The two types of reclamate were then added to the base formulation and compared against the (NR & SBR) formulation. Where CTP was added, it was added with the ZnO and stearic acid and allowed to mix for 2 min before the accelerators and sulfur were added. CTP was added to the conventional curing system containing DPG and CBS. Table 5.2 is a summary of the mixing behaviour of these formulations.

*Table 5.2 Mixing behaviour of the formulations, containing TMTD and CTP*

| *Formulation* | *Maximum torque (N·m)* | *Final torque (N·m)* | *Temp. (°C)* | *Total mixing time (s)* | *Time to reach constant torque (s)* |
|---|---|---|---|---|---|
| *NR & SBR TMTD** | 156 | 89 | 97 | 920 | 800 |
| *NRG reclaim 15% sub. TMTD* | 122 | 72 | 85 | 1220 | 1100 |
| *Commercial tyre tread reclaim 15% sub. TMTD* | 163 | 94 | 92 | 970 | 900 |
| *(NR & SBR) CTP* † | 160 | 93 | 92 | 840 | >900 |
| *NRG reclaim 15% sub. CTP* | 122 | 71 | 84 | 1250 | >1200 |
| *Commercial tyre tread reclaim 15% sub. CTP* | 156 | 90 | 95 | 970 | 900 |

* TMTD indicates that an EV system was used
† CTP indicates the addition of CTP to a CBS/DPG curing system

The addition of the TMTD and CTP was not expected to affect the mixing behaviour because the quantities of curatives added are small. Furthermore no reactions are expected to occur at the temperatures, experienced during mixing. Table 5.2 reveals very similar behaviour to that seen for the equivalent systems in Table 5.1. NRG-reclaim acts as a processing aid, lowering torque and temperature, while the commercial tyre tread reclaim had no such effect.

## 5.2 Curing characteristics

When curing the different formulations, attention was paid to the scorch safety (as measured by $\tau_{10}$), cure rate (as measured by the maximum rate of torque increase) and the extent of cure (as measured by the maximum torque achieved). The aim of cure kinetics investigations was to test:

i. the ability of the material in the reclaim to be taken up into a crosslinked matrix and its role as a plasticizer – indicated by maximum torque
ii. the effect of curative residues, present in the reclaim, on scorch and cure rate.

Cavalieri *et al.* have noted that a faster cure could be due to unreacted accelerator present in the devulcanizate/crumb rubber powder (20). Curative residues may also influence cure kinetics. As an example, in benzothiazole accelerator systems, 2-mercaptobenzothiazole (MBT) is formed during vulcanization (50). MBT is known to play a key role in benzothiazole accelerator vulcanization. The onset of crosslink formation is determined by MBT formation (50). Furthermore, MBT is an accelerator in its own right (124).

Figure 5.8 illustrates the cure characteristics of the standard rubber formulations (see Table 9.1) and those in which reclaim had been substituted for virgin rubber.

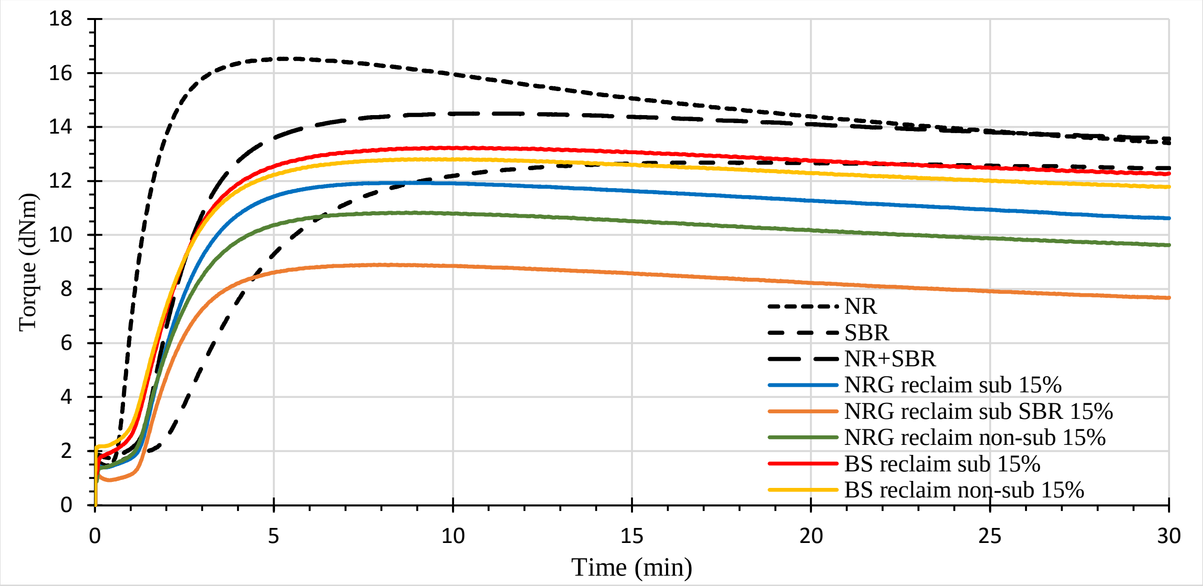

*Figure 5.8 Rheometry cure curves of the standard and reclaim formulations at 160°C. BS = commercial tyre tread reclaim*

With respect to kinetics, the NR and SBR formulations formed an upper and lower limit. NR cured the fastest while SBR cured the slowest as is typically observed for most commercial curing systems (8,39). This is likely due to a lower number of reactive allylic sites in the SBR compound. The final torque achieved with SBR was also lower, possibly for similar reasons, although it should be borne in mind that the SBR was oil-extended which would reduce the stiffness of the material at elevated temperatures. It can be seen that the (NR & SBR formulation) lies between the NR and SBR extremes. NR displays a very short scorch time as well as a fast cure rate. SBR had the longest scorch time and a relatively slow cure rate. Table 5.3 contains a summary of the relevant cure data. Because NR is the continuous phase in a 50:50 SBR blend, it has the greatest influence on determining modulus (122). The cure kinetics are thus observed to have shape more in common with NR curing than SBR curing. Figure 5.9 shows the derivative curves of the cure curve in Figure 5.8.

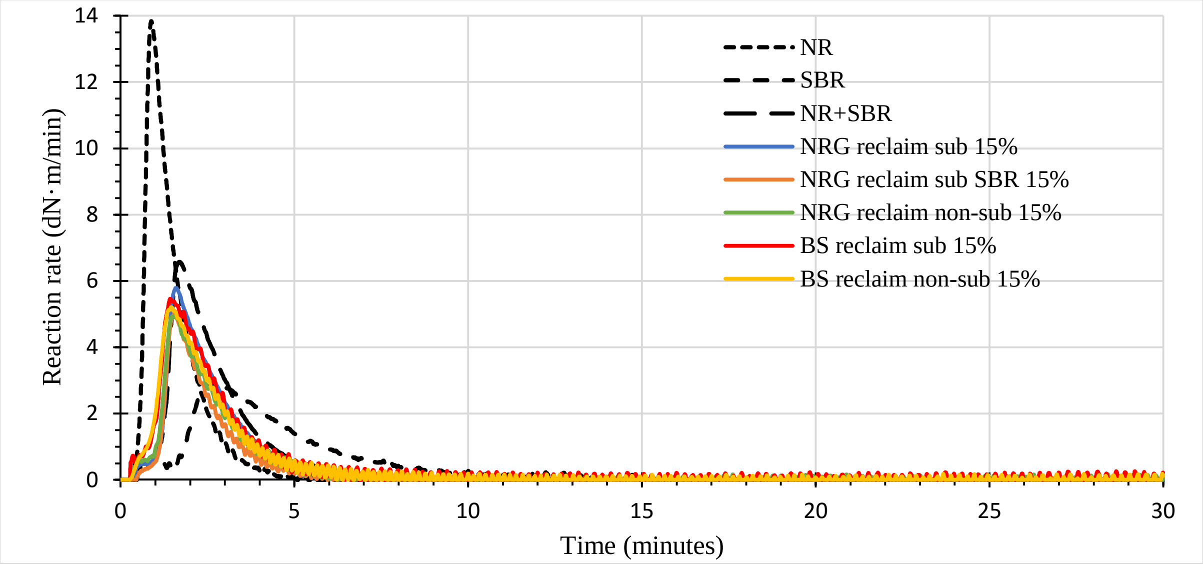

*Figure 5.9 Derivative of rheometry cure curves of the standard and reclaim formulations at 160$^o$C. BS = commercial tyre tread reclaim*

Like other reclamates (62), the addition of both NRG reclaim and the commercial tyre tread reclaim had the effect of reducing the scorch time. It is suggested that this is due to accelerators, activators and reactive curative intermediates present in the reclaim. $CaCO_3$, which was identified in the NRG-reclaim, has a very slight activating effect because of its basic pH which would contribute further to the reduction in scorch time (120).

The reduction in scorch time was greatest for the commercial tyre tread reclaim, suggesting this compound contained more intermediates. This is consistent with the fact that the NRG reclaim is diluted by processing oil (see Figure 4.9). Furthermore the high temperature process by which the NRG reclaim is produced may remove curative residues. The addition of reclaim also reduced the time to completion of cure ($\tau_{90}$). Interestingly when the NRG reclaim was used to replace the SBR fraction of the compound rather than both the NR &

SBR, the effect on $\tau_{90}$ is greater. It is suggested that this is because this formulation effectively has more NR and hence its curing behaviour is more like pure NR.

It is apparent that the addition of reclaim reduces the maximum cure rate as well as the maximum torque achieved. This would be because the addition of the processing oil in the NRG reclaim softens the rubber, reducing the torque required to deform the sample in the rheometer. The reduction in cure rate and maximum torque is also reduced with the commercial tyre tread reclaim. When the maximum torque is analysed there is a large deviation from all the virgin compounds and standard blend formation. This is expected as it is a common problem with reclaimed tyre rubber because of poor interfacial adhesion (27). Another possible reason could be that this reduction in properties is likely the result of reductions in crosslink density.

*Table 5.3 Curing characteristics of reference mixes and those containing reclaim*

| *Formulation* | $\tau_{10}$ *(min)** | $\tau_{90}$ *(min)* | $\tau_{90} - \tau_{10}$ *(min)* | *Max. cure rate dN·m/min* | $S_{max}$ *dN·m* |
|---|---|---|---|---|---|
| *Natural rubber* | 0.71 | 2.46 | 1.75 | 15.08 | 16.53 |
| *Styrene butadiene rubber* | 2.02 | 7.79 | 5.77 | 11.26 | 12.69 |
| *NR & SBR* | 1.41 | 4.46 | 3.05 | 12.76 | 14.51 |
| *NRG reclaim 15% sub* | 1.34 | 4.14 | 2.80 | 10.54 | 11.94 |
| *NRG reclaim 15% non-sub* | 1.22 | 4.12 | 2.90 | 9.50 | 10.83 |
| *NRG reclaim SBR 15% sub* | 1.30 | 3.81 | 2.51 | 7.98 | 8.90 |
| *Commercial tyre tread reclaim 15% sub* | 1.08 | 4.18 | 3.10 | 11.61 | 13.23 |

It was expected that the NRG reclaim non-substituted formulation would show improved properties when compared with the substituted formulation because the compound contained more total filler (both as carbon black and in NRG reclaim). From the rheometry curve it can be seen that the non-substituted formulation, in fact, performed worse than the substituted formulation. Inspection of Table 9.1 indicates that, as a mass percentage, the amount of curatives in this formulation is lower which may explain the phenomenon. Furthermore the carbon black in the NRG reclaim is likely similar to PyCB which has poorer reinforcing properties than N-220 CB (7).

To test the idea that the rheometry curves were showing a shift in the polymer composition

Hi-Res TGA$^{TM}$ was used to confirm the composition of these formulations. Figure 5.10 shows the comparison of the substituted and non–substituted formulations and their composition.

It is clear that the NRG reclaim formulations contain processing oil which would decrease the maximum torque achieved. When the reclaim formulations (Figure 5.10) are compared with the (NR&SBR) formulation (Figure 4.8), there is a noticeable decrease in the concentration of NR. The decrease for NR was from 32.8 % (as measured, 32.5% predicted; see Table 9.1) to 23.1% for the case where NRG reclaim was added. A small decrease in the concentration was noticed for SBR as well which dropped from 28.7% for (NR & SBR) to 26.2% for NRG reclaim. Note that the amount of SBR is lower than that in Table 9.1 for the (NR & SBR) reference material because the percentage SBR in Table 9.1 is of the oil-extended raw material. The SBR polymer content will be less.

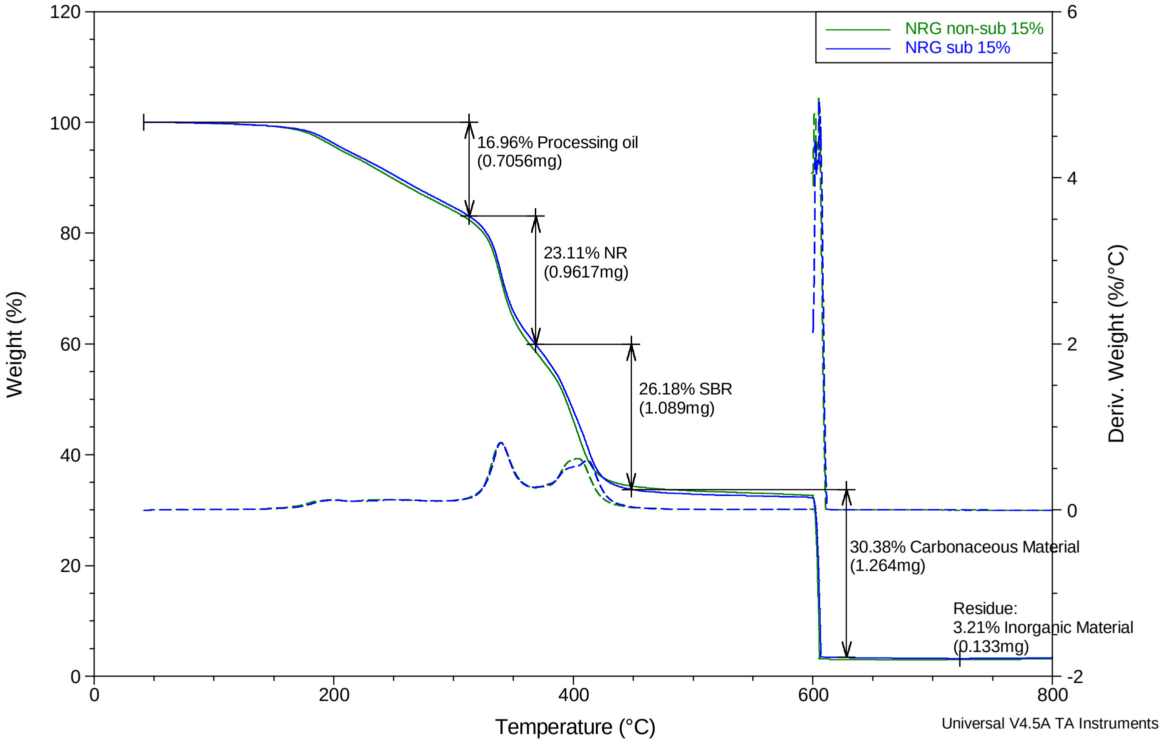

*Figure 5.10 Comparison and compositional analysis of the reclaim formulations*

The ratio of NR:SBR was calculated for the SBR+NR reference compound as 1.15:1 and for the NRG reclaim sample the ratio reversed to 1:1.13. Because of this the NRG reclaim compound was re-formulated. According to the compositional analysis of the NRG reclaim there was only a clearly defined decomposition peak in the derivative curve that would correspond to SBR. No lower temperature decomposition peak, associated with NR, could be observed. A compound was prepared in which only the SBR component was substituted and the amount of NR was left unchanged. Interestingly substituting the SBR produced a material with a much lower final torque but faster cure behaviour.

It is possible that the low temperature evaporating/decomposing component in the NRG reclaim is not just processing oil but also contains short chain polymers. These chains could be vulcanizable but because of their short nature would result in a network structure with numerous free ends. Many free ends are known to reduce the stiffness of a crosslinked network as these free ends remain mobile (125).

Figure 5.8 indicates that with the exception of the SBR formulation, all CV formulations display reversion – a decrease in torque after a maximum is achieved. This is especially noticeable in the NR formulation. Conventional vulcanization produces crosslinks with long sulfur bridges which break down/shorten/form cyclic sulfides at extended times (56). Reversion is typical of isoprene rubbers like NR, but not of others such as SBR (56). It appears that the addition of reclaim increases the extent of reversion with respect to the standard (NR & SBR) formulation.

### 5.2.1 Effect of TMTD and CTP on cure rheometry

The addition of the PVI, CTP, to a CV system is expected to increase the scorch time while the replacement of semi-ultra accelerators by an ultra accelerator, such as TMTD, is expected to increase the cure rate while reducing the scorch time (56). What is uncertain is what effect these will have on the extent of cure (maximum torque). Furthermore possible reactions between CTP and TMTD, and curative residues in the reclaim materials are possible.

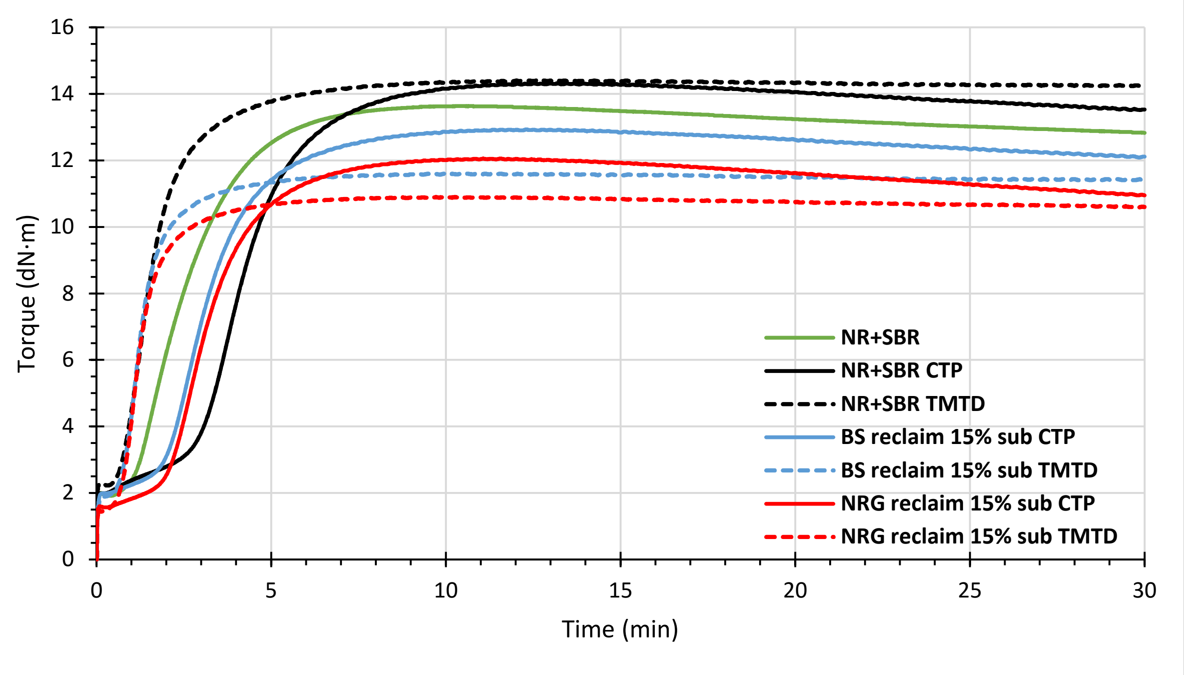

*Figure 5.11 Cure curves of some of the formulations containing CTP and TMTD at 160°C. BS = commercial tyre tread reclaim*

Figure 5.11 illustrates the effect of adding CTP and TMTD on curing behaviour. Table 5.4 provides descriptive statistics of the cure behaviour. Data for the reference CV system from Table 5.3 are provided for comparison. In Figure 5.11 the solid lines show the formulations with CTP and the dotted lines show the formulations containing TMTD. It can clearly be seen that the addition of TMTD reduced the scorch time as well as the $\tau_{90}$ time. This is expected of an ultra-accelerator (56). The changes to cure rate were small, and surprisingly showed a decrease in cure rate (maximum rate of torque increase), especially when reclaim was added. Inspection reveals that the maximum torque is reduced when TMTD was added; thus, although the ($\tau_{90}$-$\tau_{10}$) is reduced this is offset by the smaller torque increase. The smaller torque increase is likely a result of the nature of crosslinks formed in EV vs CV systems. The former form crosslinks of lower sulfur rank (56).

*Table 5.4 Curing characteristics of formulations containing CTP and TMTD*

| *Formulation* | $\tau_{10}$ *(min)* | $\tau_{90}$ *(min)* | $\tau_{90} - \tau_{10}$ *(min)* | *Max. cure rate dN.m/min* | $S_{max}$ *dN.m* |
|---|---|---|---|---|---|
| *NR & SBR (CV system)* | 1.41 | 4.46 | 3.05 | 12.76 | 14.51 |
| *NR & SBR TMTD* | 0.82 | 3.62 | 2.80 | 12.18 | 14.41 |
| *NRG reclaim 15% sub. TMTD* | 0.74 | 2.64 | 1.90 | 9.45 | 10.90 |
| *Commercial tyre tread reclaim 15% sub. TMTD* | 0.77 | 2.73 | 1.96 | 9.77 | 11.61 |
| *NR & SBR CTP* | 2.61 | 6.64 | 4.03 | 12.34 | 14.32 |
| *NRG reclaim 15% sub. CTP* | 2.02 | 5.44 | 3.42 | 10.49 | 12.06 |
| *Commercial tyre tread reclaim 15% sub. CTP* | 1.96 | 5.58 | 3.62 | 10.97 | 12.93 |

As expected CTP increased the scorch time and the time for cure completion. This indicates that although the addition of reclaim reduces scorch times (see Table 5.3), scorch safety can be regained by the addition of a pre-vulcanization inhibitor. There do not appear to be sufficient residues present that prevent the proper functioning of the PVI. The addition of CTP increased the maximum rate of cure when reclaim was added. The reasons for this are unclear but if might be the result of the formation of a delayed action but fast curing accelerator from the interaction of CTP and residues in the reclaim (53). Typically CTP only affects scorch time and does not change the rate of cure significantly, as can be seen to be the case with the base (NR & SBR) formulation (56). It can be seen that TMTD system did not revert while reversion was still experienced with CTP. TMTD-containing systems are efficient and as such form primarily monosulfidic crosslinks. Because of their greater intrinsic stability than polysulfidic crosslinks (C-S bonds are stronger than S-S bonds) they are more resistant to reversion (56).

## 5.3 Crosslink density

Swelling tests were performed to characterize the gel and sol fractions of each sample as well as the swelling ratio, from which apparent crosslink densities could be calculated. Jana *et al.* re-vulcanized rubber and discovered that the gel content of the vulcanizate was less than the original rubber vulcanizates. This was used as a reason for an observed decrease in the maximum rheometric torque for the re-vulcanized rubber (98). Table 5.5 presents solvent exposure measurements which were used to assess gel and sol content as well as apparent crosslink density. It can be seen that with the exception of the NR formulation, all formulations had a significant sol fraction. In the case of NR this would be extractable curatives and curative residues. Because the SBR that was used in the formulations was oil-extended, this oil would be extracted during sol-gel measurements. The Afsol 764 OE-SSBR, used, contained 37.5 phr (27.3%) RAE oil. This constitutes 17.7% of the overall formulation and would be extracted during a sol-gel experiment. This accounts for the high sol fraction seen for the cured SBR. Because the (NR & SBR) formulation contains a 50:50 ratio of NR:OE-SSBR, the sol fraction is reduced by about a half.

The high sol fraction observed with the addition of NRG reclaim is the result of both the extraction of oil from the OE-SSBR as well as from the NRG reclaim. Approximately 60% of the NRG reclaim (see Figure 4.9) is low molecular weight material (oil and/or polymer) which would comprise approximately 9% of the overall NRG reclaim 15% sub formulation. Since about 7.5% of the formulation is oil from the SBR, the high sol fraction (19.8%) suggests that very little of the low molecular weight material in the NRG reclaim was incorporated into the crosslinked gel. This might indicate that most of the low molecular weight material is processing oil, or degraded polymer that is no longer crosslinkable.

Note that the total sol fraction is greater than the sum of the oil in the SSBR and in the NRG reclaim because curatives will also be extracted in the sol fraction. A formulation was created that contained only a 5% substitution with NRG reclaim. As expected the sol fraction was reduced. The sol fraction with the commercial tyre tread reclaim was lower than with the NRG reclaim although larger than the (NR & SBR) base formulation. This is not surprising given that the low molecular weight of this reclaim comprised only 9% of the sample (see Figure 4.11)

*Table 5.5 Swelling behaviour and crosslink density measurements for CV systems*

| *Formulation* | *Gel fraction %* | *Soluble fraction %* | *$v_r$** | *Apparent crosslink density (mol/mℓ) – gel fraction* | *Apparent crosslink density (mol/mℓ) – whole rubber* |
|---|---|---|---|---|---|
| *Natural rubber* | 99.0 | 1.0 | 0.276 | $3.32 \times 10^{-4}$ | $3.29 \times 10^{-4}$ |
| *Styrene butadiene rubber* | 78.8 | 21.0 | 0.233 | $2.21 \times 10^{-4}$ | $1.74 \times 10^{-4}$ |
| *NR & SBR* | 89.6 | 10.4 | 0.272 | $3.19 \times 10^{-4}$ | $2.86 \times 10^{-4}$ |
| *NRG reclaim 15% sub* | 80.2 | 19.8 | 0.213 | $1.79 \times 10^{-4}$ | $1.44 \times 10^{-4}$ |
| *NRG reclaim 5% non-sub* | 86.6 | 13.4 | 0.218 | $1.88 \times 10^{-4}$ | $1.66 \times 10^{-4}$ |
| *NRG reclaim 15% non-sub* | 79.8 | 20.2 | 0.169 | $1.06 \times 10^{-4}$ | $0.85 \times 10^{-4}$ |
| *NRG reclaim SBR 15% sub* | 78.1 | 21.9 | 0.172 | $1.10 \times 10^{-4}$ | $0.86 \times 10^{-4}$ |
| *Commercial tyre tread reclaim 15% sub* | 86.2 | 13.8 | 0.232 | $2.19 \times 10^{-4}$ | $1.89 \times 10^{-4}$ |

* volume fraction of rubber in the swollen gel

Because the samples under investigation contain filler, the crosslink densities are only apparent crosslink densities rather than true crosslink densities which would require a Kraus plot correction (105). This would require detailed knowledge of the amount and type of filler in the swollen gel. Such detailed compositional analysis (especial type characterization) was deemed beyond the scope of this study. Because the filler content across all formulations is similar, the correction to the apparent crosslink density (derived from equations 3.5 and 3.6) would be similar (126), and thus the relative trends in Table 5.5 would remain. Note that as the volume fraction rubber in the swollen gel increases the crosslink density decrease. A less crosslinked gel displays less resistance to swelling (125). From the $v_R$ the crosslink density in the gel can be calculated (equation 3.5).

Because the gel is not the original sample but has had soluble components extracted, the crosslink density in the original sample can be calculated as (126)

$$XLD\ in\ sample\ =\ XLD\ in\ gel \times \frac{gel\ \ fraction(\%)}{100\%} \tag{5.1}$$

The data in Table 5.5 reveals that the NR formulation is the most crosslinked. A higher crosslink density than achieved with SBR is expected because only the butadiene repeating units (25%) of the SBR contain allylic carbon atoms at which crosslinking can occur. In NR, all isoprene repeating units have reactive allylic carbon atoms. Furthermore each isoprene unit has 3 reactive carbon atoms, a butadiene unit has only 2. The crosslink density of the (NR & SBR) formulation consequently lies between the NR and SBR formulations. The addition or reclaim has the effect of lower crosslink density. One reason for this, is that the reclaim contains material that is not crosslinkable, *e.g.* oils. The quantity of this material is lower in the commercial tyre tread reclaim and hence the crosslink density for this sample is higher.

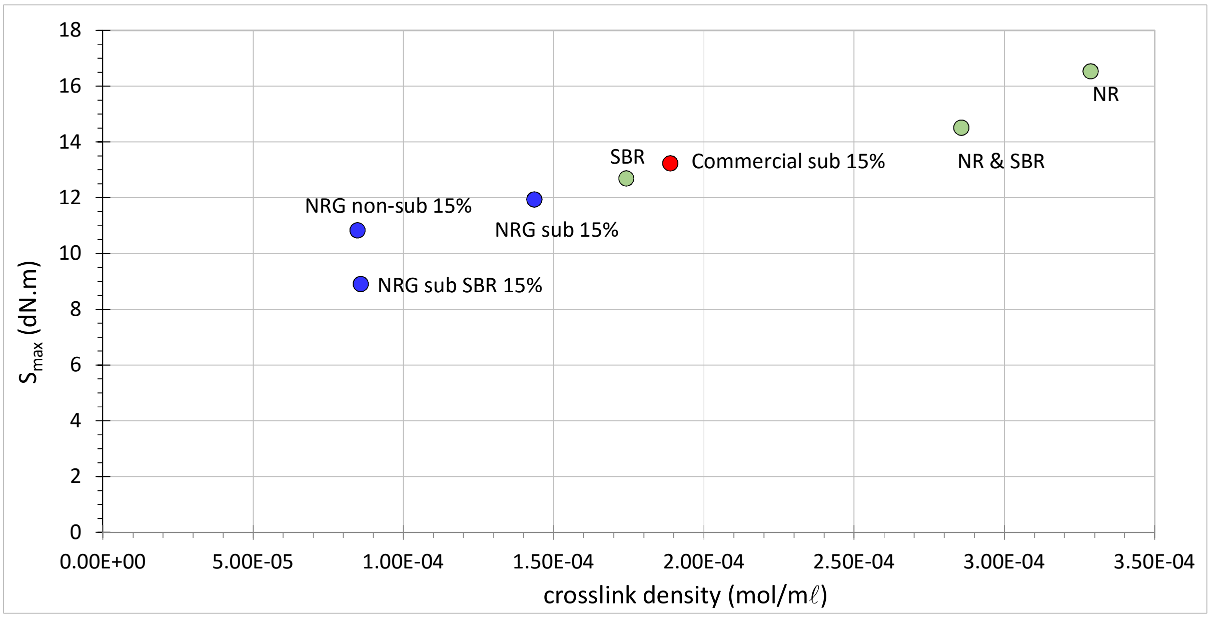

*Figure 5.12 Relationship between crosslink density and maximum torque achieved during rheometry. Reference samples (green), containing NRG reclaim (blue), containing commercial tyre tread reclaim (red)*

The reduction in crosslink density, however, is more than can be explained by just the presence of non-crosslinkable material and may also be a reflection of the types of crosslinks formed. A network structure with many loose chain ends will have fewer effective crosslinks which are those measured by swelling experiments (125).

Figure 5.12 explores the relationship between the maximum torque, as measured by rheometry, and the crosslink density of the cured formulations. It can be seen that the relationship is very close to linear. This indicates that the maximum torque, as measured by rheometer, is a very good measure of the extent of cure.

## 5.4 Mechanical properties

Tensometer testing allows the tensile strength at 100%, 200%, 300% strain (also called 100%, 200%, 300% secant modulus), ultimate tensile strength and elongation at break of the rubber materials to be evaluated. The conventional vulcanization formulations were prepared and their mechanical properties compared.

Figure 5.13 shows the results of the different tensometer tests. The curves are average curves obtained by combining individual tensile tests. Five samples of each rubber formulation were tested and the results were averaged (N = 3 to 5). Where the sample slipped in the grips, during testing, it was not included in the average.

Mandal *et al.* suggested that the gel fraction of a reclaimed rubber does not disperse throughout the rubber matrix and thus decreases the tensile strength. They proposed that the gel fraction created weak sites in the matrix and did not transfer the stress effectively to the matrix (103).

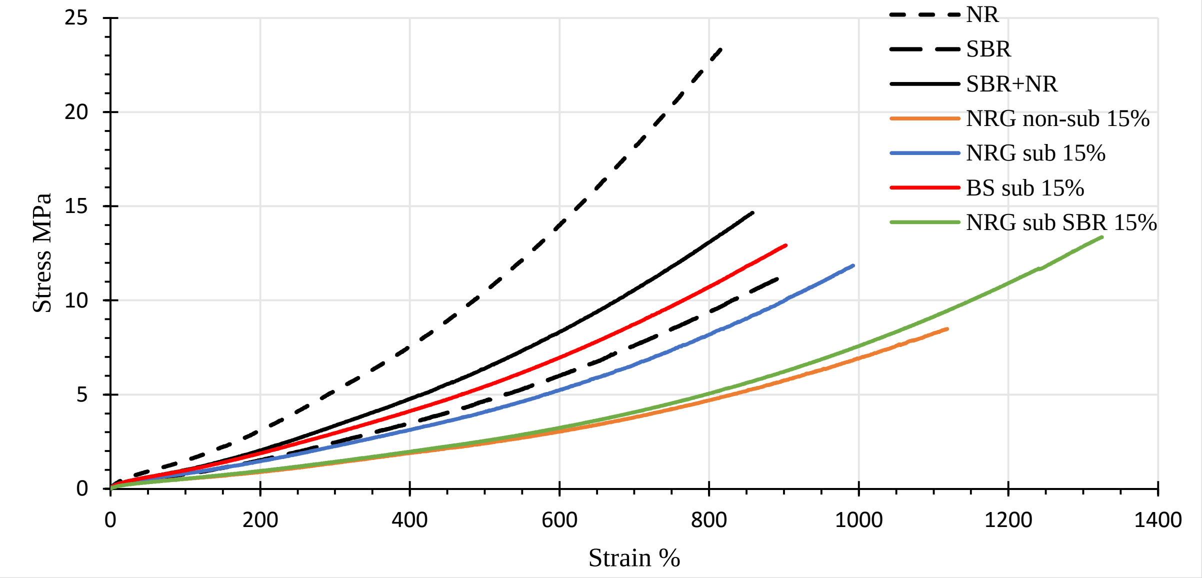

*Figure 5.13 Comparison of the average tensile tests of the different rubber formulations*

As with the rheometry curves the standards created formed upper and lower limits with NR & SBR falling somewhere between the two. The effect of adding reclaim, in particular the NRG reclaim, is to lower the modulus (slope) and UTS of the material while also increasing its extensibility ($\varepsilon_B$). No increase in extensibility was noted for the addition of the commercial tyre tread. Table 5.6 provides a summary of the key mechanical properties for the different

CV formulations (modulus, tensile strength and extension at break).

*Table 5.6 Tensile data for CV formulations*

| *Formulation* | *100% MPa* | *200% MPa* | *300% MPa* | *εB strain%* | *UTS MPa* | *Number of tests (n)* |
|---|---|---|---|---|---|---|
| *Natural Rubber* | 1.50 (0.12) | 3.10 (0.19) | 5.21 (0.29) | 901 (0.02) | 25.65 (1.00) | 5 |
| *Styrene Butadiene Rubber* | 0.77 (0.09) | 1.52 (0.11) | 2.46 (0.16) | 894 (0.01) | 11.20 (0.67) | 3 |
| *NR+SBR* | 1.00 (0.04) | 2.04 (0.12) | 3.35 (0.22) | 858 (0.01) | 14.66 (1.02) | 3 |
| *NRG Reclaim 5% non-sub.* | 0.85 (0.07) | 1.70 (0.04) | 2.72 (0.04) | 885 (0.01) | 11.98 (0.31) | 3 |
| *NRG Reclaim 15% sub.* | 0.81 (0.05) | 1.46 (0.06) | 2.26 (0.08) | 992 (0.07) | 11.85 (0.36) | 4 |
| *NRG Reclaim 15% non-sub.* | 0.52 (0.04) | 0.89 (0.06) | 1.37 (0.09) | 1118 (0.02) | 8.48 (0.42) | 3 |
| *NRG Reclaim SBR 15% sub.* | 0.54 (0.03) | 0.95 (0.05) | 1.44 (0.08) | 1325 (0.03) | 13.35 (0.64) | 4 |
| *Bridgestone Reclaim 15% sub.* | 0.98 (0.02) | 1.89 (0.04) | 2.97 (0.08) | 902 (0.02) | 12.92 (0.40) | 3 |

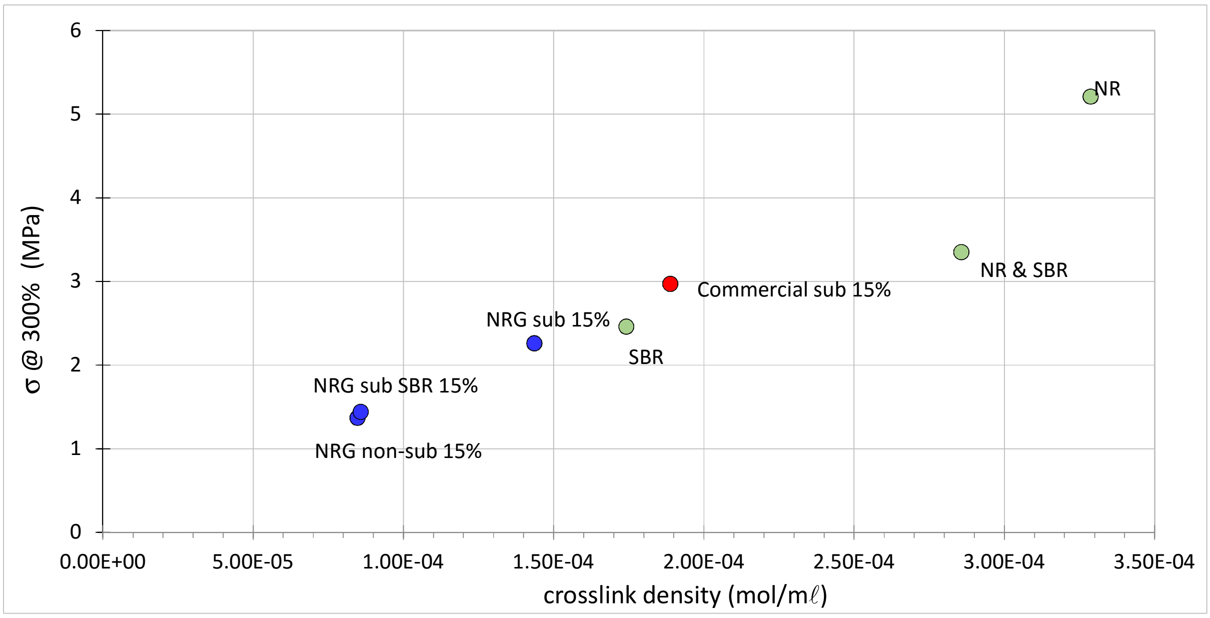

*Figure 5.14 Relationship between crosslink density and 300% modulus (stress at 300% strain). Reference samples (green), containing NRG reclaim (blue), containing commercial tyre tread reclaim (red)*

Figure 5.14 illustrates the relationship between the 300% modulus and the crosslink density. It can be seen that the relationship is near linear.

The reduction in modulus upon the addition of NRG reclaim can be explained as a reduction in the extent of curing, although a reduction in viscosity should not be ignored. Similar linear behaviour is seen for the 100% and 200% modulus.

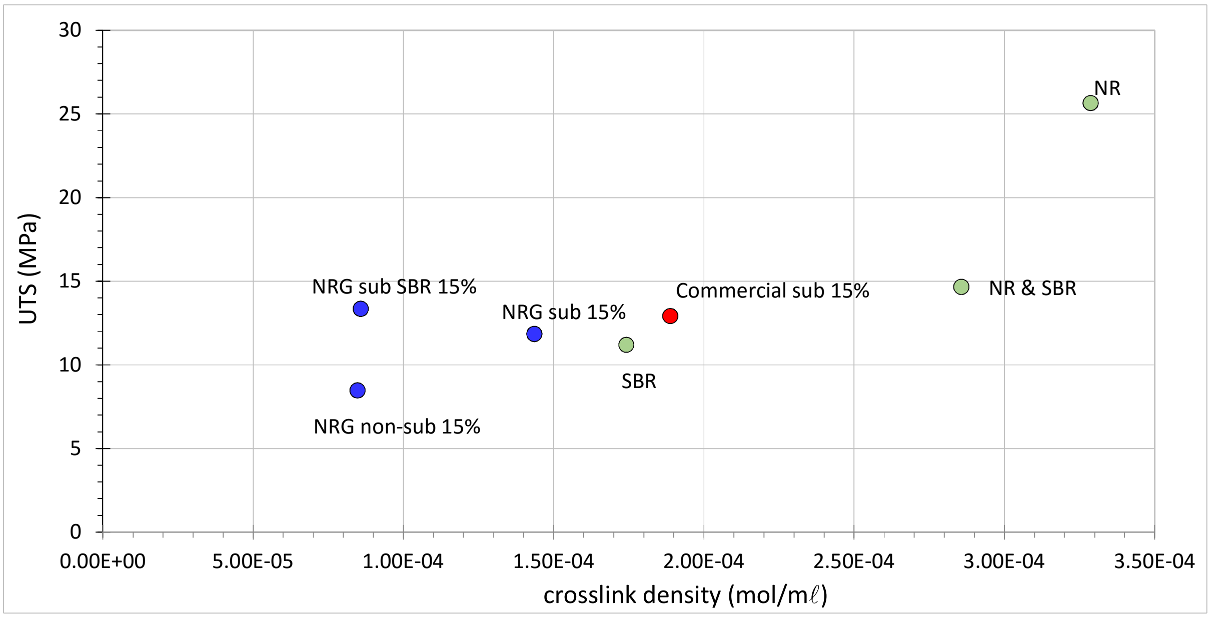

*Figure 5.15 Relationship between crosslink density and ultimate tensile strength. Reference samples (green), containing NRG reclaim (blue), containing commercial tyre tread reclaim (red)*

The effect on ultimate tensile strength is more complex. With the exception of the neat NR formulation, the UTS bear very little relationship to crosslink density.

This may be explained in terms of the processes occurring at failure. At low extension, the stress is determined by the resistance to extension and hence is strongly determined by crosslink density. At failure, however, other factors come into play. A material which can undergo stain crystallization, such as NR, will have a much greater UTS and modulus than would be expected based on crosslink density alone (42). This was, in fact, observed. It has been postulated that the increase in UTS in a strain crystallizing polymer, such as NR, is due to the formation of crystallites at the tips of crack flaws preventing further crack propagation until a much higher critical stress is reached (127).

Failure is the result of a crack being able to propagate through the sample. The likelihood of this occurring depends not only on the local stress of the material at the crack tip but also the ability of the material to lower this local stress. When the local stress exceeds a materials critical strength, the crack will propagate and the material will fail. A soft material which can deform is able to decrease the local stress and thus reduce the likelihood of failure. This has the consequence that although the addition of reclaim reduces UTS compared to the (NR & SBR) formulation, the effect on extension at break is more significant. A soft material may require significant extension before the material becomes stiff such that a crack will propagate. Being able to reach high extensions has the indirect effect of raising the UTS.

In a study of ethylene propylene diene monomer (EPDM) rubber, Dijkhuis showed that with a crosslink density of approximately $3x10^{-4}$ mol/mℓ and higher, there was almost no un-crosslinked rubber chains. Dijkhuis also found that there was an apparent lower limit of crosslink density where a good network structure formed, this was at a crosslink density of $1.5x10^{-4}$ mol/mℓ (1).

Thus, despite the addition of NRG reclaim decreasing the crosslink density, its function as a plasticiser/softening agent increases $\varepsilon_B$ and in turn UTS. This is especially noticeable where the reclaim was substituted for the SBR component. The high oil content imparts a plasticisation effect. The commercial tyre tread reclaim on the other hand is a much stiffer material which does not act as a plasticiser and is likely to be included into the vulcanizate network during crosslinking, unlike the oil. The material is thus unable to dissipate stress at the crack tip and failure is at lower $\varepsilon_B$. Nonetheless a decrease in crosslink density and a possible stress raising effect as noted by Mandal *et al.* (103) will lower UTS. In contrast to the material containing (NR & SBR) and that containing reclaim, the pure NR compound has only one rubber phase and no such stress raising phenomena. Unlike Saiwari *et al.*, no decrease in $\varepsilon_B$ was observed for the addition of either type or reclaim (62).

# CHAPTER 6

# 6 CONCLUSION

## 6.1 Characterization

It has been demonstrated that compositional analysis of rubber devulcanizates is possible when using Hi-Res TGA$^{TM}$. Good quantification was possible for low molecular weight components such as processing oils, natural rubber, carbon black and inorganic residues. Separation of components and thus compositional analysis is improved by increasing resolution and sensitivity. This, however, comes with an analysis time trade-off. Beyond a certain point, no improvement in compositional analysis is achieved while analysis time increases rapidly.

As the samples increase in complexity the ability to separate materials based on their decomposition temperature decreases. This is because of overlapping decomposition ranges. With rubber vulcanizates and devulcanizates this is further complicated by a number of factors:

- some vulcanizates (and hence devulcanizates) containing low volatility extender oils such as the RAE oil added to the SSBR used in this study. Such heavy oils decompose over the same temperature range as the rubber components. Ignoring them is likely to lead to an overestimation of rubber components such as SBR. More volatile processing oils, by contrast, are easily quantified.
- When the components in the devulcanizate are so broken down that they contain low molecular weight material, it becomes difficult to separate these fractions from the processing oils.
- The de-vulcanization process may cause further changes in the rubber constituents, for instance increasing their stability, such that their decomposition temperatures can no longer be directly associated with that of a reference virgin rubber standard.

A novel high viscous reclamate, supplied by NRG, was characterized and its performance compared with that of a more conventional reclamate, produced by mechanochemical devulcanization. The NRG reclaim is produced by a proprietary high temperature process. Characterization revealed that this reclaim was mainly processing oil and other low molecular weight material. Since no high molecular weight NR could be seen, it is suggested that this low molecular weight material contained low molecular weight polyisoprene. A glass transition, consistent with the presence of polyisoprene, was observed by DSC. Some high molecular weight polymer was present. This is likely SBR-derived, given its relatively high decomposition temperature. Analysis of a soluble extract from this reclaim indicated the presence of NR. A $T_g$ for SBR was also observed by DSC. It was observed that the inorganic residue contained a material, not typically seen in tyre tread reclamate. This was identified as CaO, derived from $CaCO_3$. The calcium carbonate may be derived from the proprietary NRG process.

Although methods, based on kinetic models, have been developed to quantify the rubber components in vulcanized samples, *e.g.* rubber crumb, they are not suitable for devulcanizates such as the NRG product (75,76). Where de-vulcanization causes significant molecular change, the decomposition profiles no longer match those of the virgin materials, and so a model for the decomposition of the devulcanizate cannot be built and quantification cannot be achieved (65).

Solvent extraction would suggest that future samples of a similar nature to the NRG reclaim could be analysed by prior separation with appropriate solvents. Acetone was shown to be useful for removing polar curative but not polymeric material. It was shown that using solvents with different characteristics made it possible to separate out processing oils and polymers. Using solvents in succession on a sample could result in the systematic removal of the various materials in the sample. Careful inspection of the mass loss curves in the Hi-Res™ TGA indicated that the carbon black fraction was still losing mass during carbonization process in $N_2$. This is in contrast to tyre CB. It is suggest that the carbon black in the NRG reclaim product may have properties similar to PyCB, making it less reinforcing (7).

One of the key characteristics of de-vulcanization and reclamation is the production of polymer chains that are not restricted by crosslinks. Therefore, when coupling solvent extraction with Soxhlet extraction, a simple technique was developed to estimate the polymer concentration that was un-bonded. Much of the NRG reclaim was soluble in toluene which suggests that most of the polymeric constituents is de-vulcanized. By contrast, a significant fraction of a commercial tyre tread devulcanizate could not be dissolved in toluene indicating that not all the material had been de-vulcanized. Hi-Res™ TGA revealed no carbonization occurring with the CB in this sample, indicating that the CB likely retained a similar structure to its original form.

## 6.2 Formulation development

Given the nature of the two reclaim samples it was expected that the oily NRG reclaim could act as a processing aid and the Bridgestone reclaim could act as a filler and/or extender. The NRG reclaim had important impacts on mixing behaviour. Maximum torque and hence process energies were reduced, opening up the possibility of cost savings, albeit that longer mixing cycles might be required. The lower maximum torque would also reduce the likelihood of breaking shear pins in the mixing equipment, increasing machine life. This could be solved by prior master-batching of the NRG reclaim with virgin rubber. Furthermore the NRG reclaim reduced mixing temperatures, introducing a degree of processing safety, making premature curing at this stage less likely. The commercial tyre tread reclaim was more of a reinforcing filler as the torque increased with the addition of the reclaim. This, though, may be indicative of difficulties of dispersion.

The NRG reclaim has a number of effects on cure rheometry. It was demonstrated that it reduced cure times. This is a common effect of reclamates (also seen with a commercial tyre tread reclaim in this study). It is suggested that this is the result of curative residues present in the NRG reclaim. This reduces scorch safety. It was, however, demonstrated that scorch safety can be restored by the use of the PVI, CTP. This study is the first study to investigate the effect of CTP in devulcanizates. CTP was also shown to be effective with a more conventional devulcanizate. This study is also one of the few to investigate a devulcanizate with an ultra accelerator, TMTD. As expected, TMTD reduced the scorch time but not below that of a reference compound containing TMTD. What was reduced was the total time for curing, as demonstrated by a reduction in $\tau_{90}$.

The addition of devulcanizate decreased the extent of cure as measured by the maximum torque generated in the rheometer. It was demonstrated that this is primarily an effect of crosslink density. Lower crosslink density samples are less stiff and thus a lower torque is required in the rheometer. This was corroborated by tensile testing where 100%, 200% and 300% moduli were all correlated with crosslink density. The reduction in crosslink density was shown to be the result of more than the reduction in crosslinkable rubber on reclaim addition. The exact mechanism of the crosslink reduction is unclear.

The tensile tests showed that there was a decrease in the tensile properties for the NRG reclaim formulations. At the same time a significant increase in the extension at break was observed. A linear, predictable relationship between crosslink density and UTS could not be established. The tensile behaviour suggested that in samples with NRG reclaim added, the reclaim acted as a plasticiser significantly increasing extension at break but decreasing UTS less so. With the commercial tyre tread reclaim a decrease in UTS with little or no change in $\varepsilon_B$ was observed. This could be attributed to decreased crosslink density or an incomplete transfer of stress between the polymer chains. This has been proposed by Jana *et al.* who suggested that the gel fraction of the devulcanizate was highly crosslinked and therefore when re-vulcanized this gel fraction would not transfer stress to the matrix efficiently (98).

The increase in elongation at break and a decrease in tensile strength is a result of the increased low $M_w$ material present in the formulation (both processing oil and low $M_w$ polymer). The low $M_w$ material could be increasing the mobility of the polymer chains making them more flexible. The lower crosslink densities would also allow greater flexibility and mobility of the polymer chains (1).

It was expected that the substituted NRG reclaim would have poorer qualities than the non-substituted formulation. The thought was that by not substituting the polymers and reinforcing filler (carbon black) there would be excess of these materials in the formulation. However, thermal analysis indicated that the two formulations had almost identical decomposition curves indicating they contained similar concentrations of material. What was revealed however is that in both cases the ratio of NR:SBR was opposite to that of the (NR & SBR) virgin formulation. This would suggest that the NR present in any formulation has a large impact on the physical properties of the final product.

Alternatively, to increase the tensile strength when NRG reclaim is added, more carbon black could be added or higher quantities of curatives (sulfur and accelerator) may be used.

Sol-gel experiments revealed that a significant amount of material in the blends containing reclamate was extractable. This was primarily oil and was higher for the NRG sample than the commercial tyre tread reclaim. Some of the extractables would also be polymer breakdown products and curative residues that breakdown during de-vulcanization.

# Chapter 7

# 7 RECOMMENDATIONS

## 7.1 Extended characterization techniques

From the results of the research done it became apparent that simply identifying low molecular weight material present in a reclamate is insufficient. With the NRG reclaim problems arose when curing and tensile test provided unexpected results. Understanding what the low molecular weight material contains would provide better direction for future compounding.

To better understand the NRG reclaim further testing on the sol fraction should be carried out. Once the sol fraction has been isolated, through the use of soxhlet extraction, GPC/SEC analysis should be carried out. This technique should allow for the identification of low $M_w$ polyisoprene and possibly poly (styrene-butadiene) co-polymer. This will help understand the severity of the reclaiming process used and identify possible alternate uses for the material.

A simpler technique for separating possible polymer from oil in the low $M_w$ fraction is to vulcanize the sol fraction by using high concentrations of sulfur and/or curatives. This can be done by reacting the components in an oil bath set a 160°C. As this technique should be used to only separate the polymeric material from the processing oil it can be carried out in an oxidizing environment (air). Using a suitable solvent after the vulcanization should separate out the vulcanized material from the processing oil.

A powerful technique for characterising the low $M_w$ material is NMR spectroscopy. By dissolving the low $M_w$ material in deuterated dichloromethane the low $M_w$ material can be analysed with the use of $^1$H-NMR and $^{13}$C-NMR for identify any aromatic, olefinic or aliphatic hydrogens and carbons present.

Just as important as knowing what a reclamate contains is knowing what makes up the virgin material. In the case of this study an oil extended SBR was used. The influence of the SBR-OE elastomer could be seen on the TGA thermograms and the effect it had on the physical properties could only be speculated. The method for separating polymeric material from processing oil explained above can be applied here. After vulcanizing the SBR and removing the oil component the SBR can be analysed using thermogravimetric analysis. The percentage SBR identified by TGA could be subtracted from SBR-OE resulting in the amount of RAE oil being quantified.

To obtain a better understanding of what happens to the curatives after the vulcanizing and reclaiming processes HPLC analysis could prove useful. By using HPLC and HPLC-MS the curatives that may be contained in the low $M_w$ material could be characterized. This technique should be used on both the commercial reclaim as well as the NRG reclaim as it may help explain the scorchiness of the devulcanizates.

Should the NMR or HPLC techniques be carried out it is important to stop any free carbon black from contaminating the sample. Therefore, after soxhlet extraction it is recommended that the sol fraction be centrifuged and the extract decanted. Alternatively the sol fraction can be passed through a syringe filter with a pore size of 25µm.

Because $CaCO_3$ was identified in the NRG reclaim it is also recommended that an analysis is done on the ash content. Elemental analysis is recommended as it could identify any calcium and/or silica present. Elemental analysis can be performed using XRF or the ash could be digested and AAS could be performed. $SiO_2$ could also be quantified by digesting it in HF acid and then analysed using ICP-MS/ICP-OES.

## 7.2 Further compounding and physical tests

Further investigation on the effect that EV and CV systems have on the physical properties of compounds containing de-vulcanized material should be carried out. In order to understand these phenomena, not only should conventional swelling be done, but swelling would also be performed in the presence of probes that selectively cleave polysulfidic linkages, disulfidic linkages and monosulfidic linkages (128,129,130). These would provide information about the number and distribution of C-C, C-S-C, C-S-S-C and C-Sx-C crosslinks in EV and CV systems.

A change in the strain crystallization could affect the modulus and UTS. The following mixes should be attempted to understand the influence that the NRG reclaim would have on strain crystallization; 15% NRG & 100 phr NR, 15% NRG & 100 phr SBR. The kinetics of NR systems are typically more sensitive to formulation changes than SBR systems (56). Such a study would allow the sensitivity of the pure virgin compounds to the reclaim to be assessed.

A Kraus analysis should be performed on the crosslink density calculations. This will reflect a more accurate value of sulfur crosslinks present. In order to increase the UTS of the NRG formulations carbon black should be added in higher quantities. The effects that this will have on how the polymer chains interact with each other can be better understood when comparing the corrected values with the uncorrected values. This way the role of carbon black can be better understood.

Carbon black is often added in black masterbatches before the addition of plasticiser (114). In the current study the NRG reclaim was added before the carbon black. Because the NRG reclaim is a highly viscous oil and thus behaves like a processing oil, the effect of switching the order of reclaim and CB addition could be explored. Alternatively mixing the carbon black into the NRG reclaim to form a paste before addition could help with possible dispersion problems. This may prevent the slipping that was observed in this study. Importantly the influence on maximum mixing torque, final torque and final temperature should be investigated.

RPA experiments can be used to identify branching that is as a result of de-vulcanization techniques. This would be done by using large angle oscillatory shear (LAOS) experiments. The effect that the addition of NRG will have on wet skid, rolling resistance and heat build-up can be investigated with the RPA. Tan δ at 20°C, 60°C and 80°C in accordance with the protocol of Nordsiek (133) after curing in the RPA could be measured. The tan δ data would then be used to make property measurements.

In this study tensile tests were performed at 200mm/min, this presented a problem as tensile behaviour (especially where you have plasticisation/softening) is strain rate dependent. Furthermore the dependence of UTS on crosslink density is more pronounced at higher strain rates (37). At 200 mm/min very little dependence on crosslink density was observed (Figure 5.14) but this may not be the case at high strain rates. Therefore future experiments should be carried out at a higher strain rate of 500 mm/min as specified in ASTM D412 (97).

## 7.3 Predictive modelling and improved kinetics

A model could be investigated that used various theoretical tools so that an overall curve can be predicted from a model decomposition. However, this would only be useful for conventional devulcanizates, as some de-vulcanization techniques may change the decomposition temperatures. This would pose a problem to the theoretical model. A model would need to be set up for NR, SBR, RAE oil, processing oil and carbon black.

Coran plots could be used to find rate constants for the initiation and crosslinking steps during vulcanization (54,128,129). Because this analysis provides rate constants, rather than rates, it allows concentration effects to be eliminated. It also allows more detailed comparison of CV and EV systems.

By using MDSC better $T_g$ data can be obtained. This would allow more detailed and sensitive experiments to be carried out. For instance, the dependence of glass transition temperatures on molecular weight could be investigated. This could be done by using polyisoprene standards of varying molecular weight. This has the benefit of confirming that a $T_g$ step is not mistaken for another thermal event.

# Chapter 8

## 8 REFERENCES

1. Dijkhuis DA. PhD thesis: Recycling of Vulcanized EPDM-Rubber: Mechanistic Studies into the Development of a Continuous Process using Amines as Devulcanization Aids. Enschede, Netherlands: Technical University of Twente; 2008.

2. REDISA. Recycling and Economic Development Initiative of South Africa. [Online]. [cited 2016 January. Available from: www.redisa.org.za.

3. Mavuso Z. Recycling process possible solution to waste tyres. Creamer Media's Engineering News. 2013; Feb 15.

4. Morin JE, Farris RJ. Recycling of 100% cross-linked rubber powder by high-temperature high-pressure sintering. In Proc. Annual Techn. Conf. Soc. Plast. Eng, ANTEC; 2000. p. 6-10.

5. Saiwari S. PhD thesis: Post-Consumer Tires Back into New Tires: De-vulcanization and Re-utilization of Passenger Car Tires. Enschede, Netherlands: Technical University of Twente; 2013.

6. Khait K. Chapter 4. Tire Rubber Recycling by Mechanochemical Processing. In De SK, Isayev AI, Khait K, editors. Rubber recycling. Boca Raton, FL: CRC Press; 2005. p. 155-187.

7. Raghavan D. Chapter 8. Strategies for Reuse of Rubber Tires. In De SK, Isayev AI, Khait K, editors. Rubber recycling. Boca Raton, FL: CRC Press; 2005. p. 299-325.

8. Barbin WW, Rodgers MB. Chapter 9. The Science of Rubber Compounding. In Mark JE, Erman B, Eirich FR, editors. Science and technology of rubber. 2nd ed. San Diego, CA: Academic Press; 1994. p. 419-469.

9. Schaefer R, Isringhaus RA. Chapter 18. Reclaimed Rubber. In Morton M, editor. Rubber technology. 3rd ed. London, UK: Chapman & Hall; 1995. p. 505-517.

10. Dierkes W. Chapter 3. Untreated and Treated Rubber Powder. In De SK, Isayev AI, Khait K, editors. Rubber recycling. Boca Raton, FL: CRC Press; 2005. p. 127-154.

11. Mangaraj D. Chapter 7. Rubber Recycling by Blending with Plastics. In De SK, Isayev AI, Khait K, editors. Rubber recycling. Boca Raton, Fl: CRC Press; 2005. p. 247-298.

12. Alexandre-Franco M, Fernandez-Gonzalez C, Alfaro-Dominguez M, Palacios Latasa JM, Gomez-Serrano V. Devulcanization and demineralization of used tire rubber by thermal chemical methods: a study by X-ray diffraction. Energy & Fuels. 2010; 4: p. 3401-3409.

13. Roy C, Chaala A, Darmstadt H, de Caumia B, Pakdel H, Yang J. Chapter 11. Conversion of Used Tires to Carbon Black and Oil by Pyrolysis. In De SK, Isayev AI, Khait K, editors. Rubber recycling. Boca Raton, FL: CRC Press; 2005. p. 429-467.

14. Padella F, Cavalieri F, d'Uva G, la Berbera A. Recycling of scrap tires rubber by mechanochemical devulanization. Polym. Recycl. 2001; 6: p. 11-16.

15. Myrhe M, Saiwari S, Dierkes W, Noordermeer JWM. Rubber recycling: chemistry, processing, and applications. Rubber Chem. Technol. 2012; 85: p. 408-449.

16. Bilgili E, Arastoopour H, Bernstein B. Pulverization of rubber granulates using the solid-state sheer extrusion (SSSE) process: Part I. Process concepts and characteristics. Powder Technol. 2001; 115: p. 265-276.

17. Bilgili E, Arastoopour H, Ivanov G. Analysis of rubber using modified solid state shear extrusion process (SSSE). Rubb. Chem. Technol. 2005; 73: p. 340-355.

18. Shahidi N, Arostoopour H, Ivanov G. Pulverization of rubber using modified solid state shear extrusion process (SSSE). J. Appl. Polym. Sci. 2006; 102: p. 119-127.

19. Adhikari B, De D, Maiti S. Reclamation and recycling of waste rubber. Progr. Polym. Sci. 2000; 25: p. 909-948.

20. Cavalieri F, Padella F, Cataldo F. Mechanochemical surface activation of ground tire rubber by solid-state devulcanization and grafting. J. Appl. Polym. Sci. 2003; 90: p. 1631-1638.

21. Si H, Chen T, Zhang Y. Effects of high shear stress on the devulcanization of ground tire rubber in a twin-screw extruder. J. Appl. Polym. Sci. 2013; 128: p. 2307-2318.

22. Vega B, Montero L, Lincoln S, Agullo N, Borros S. Controlling of vulcanizing/devulcanizing behavior of diphenyl disulfide with microwaves as the heating source. J. Appl. Polym. Sci. 2008; 108: p. 1969-1975.

23. Fukumori K, Matsushita M. Material recycling technology of crosslinked rubber waste. R&D Rev. Toyota. 2003; 38: p. 39-47.

24. Myrhe M. Chapter 10. Devulcanization by chemical and thermomechanical means. In De SK, Isayev AI, Khait K, editors. Rubber recycling. Boca Raton, FL: CRC Press; 2005. p. 401-427.

25. Rajan VV. PhD thesis: Devulcanisation of NR Based Latex Products for Tyre Applications Enschede, Netherlands: Technical University of Twente; 2005.

26. De D, Maiti S, Adhikari B. Reclaiming of rubber by a renewable resource material (RRM). II. Comparative evaluation of recaliming process of NR vulcanizate by RRM and diallyl disulfide. J. Appl. Polym. Sci. 1999; 73: p. 2951-2958.

27. Saiwari S, Noordermeer JWM, Dierkes WK. Pathway for high-quality reclaim from sulphur-vulcanized SBR. In Deutsche Kautschuk-Tagung; 2012.

28. De SK, Isayev A, Khait K, editors. Rubber Recycling. Boca Raton, FL: CRC Press; 2005.

29. van den Heever PJ, inventor; Process for reprocessing a polymeric product. South Africa patent ZA1998/10600. 1998.

30. Taylor B. The art of reinvention. Recycling Today. 2012; July.

31. Sunthonpagasit N, Duffey MR. Scrap tires to crumb rubber: feasibility analysis for processing facilities. Res. Cons. & Recyc. 2004; 40: p. 281-299.

32. Ohm RF, editor. The Vanderbilt Rubber Handbook. 13th ed. Norwalk, CT: R.T. Vanderbilt Company; 1990.

33. Rouse MW. Chapter 2. Quality Performance-Factors for Tire-Derived Materials. In De SK, Isayev AI, Khait K, editors. Rubber recycling. Boca Raton, FL: CRC Press; 2005. p. 101-125.

34. Morton M, editor. Rubber Technology. 3rd ed. London, UK: Chapman & Hall; 1995.

35. Subramaniam A. Chapter 6. Natural Rubber. In Morton M, editor. Rubber technology. 3rd ed. London, UK: Chapman & Hall; 1995. p. 179-208.

36. Subramaniam A. Natural rubber. In Ohm RF, editor. The Vanderbilt Handbook. 13th ed. Norwalk, CT: R.T. Vanderbilt Company; 1990.

37. Gent AN. Chapter 10. Strength of Elastomers. In Mark JE, Erman B, Eirich FR, editors. Science and technology of rubber. 2nd ed. San Diego, CA: Academic Press; 1994. p. 471-512.

38. Karbochem. Afsol - Solution Styrene Butadiene Rubber (SSBR). [Online]. [cited 2016 January. Available from: http://www.karbochem.co.za/index.php/product-catalogue/afsol-ssbr.

39. Hibbs J. Styrene-butadiene rubbers. In Ohm RF, editor. The Vanderbilt Handbook. 13th ed. Norwalk, CT: R.T. Vanderbilt Company; 1990. p. 54-91.

40. Saiwari S, Dierkes WK, Noordermeer JWM. Paper #36. Comparative investigation of the de-vulcanization parameters of tire rubbers. In 182nd Technical Meeting of the Rubber Division, American Chemical Society; 2012; Cincinnati, OH.

41. de Candia F, Romano G. Melting behavior of cis-polybutadiene crystallized under stress. J. Appl. Polym Sci. 1989; 38: p. 249-256.

42. Flory PJ. Thermodynamics of crystallization in high polymers. I. Crystallization induced by stretching. J. Phys. Chem. 1947; 15: p. 397-408.

43. Mekkriengkrai D, Sakdapipanich JT, Tanaka Y. Structural characterization of terminal groups in natural rubber: origin of nitrogenous groups. Rubber Chem. Technol. 2006; 79: p. 366-379.

44. Duck W. Plastics and Rubber. New York, NY: Philosophical Library; 1971.

45. Layer RW. Introduction to rubber compounding. In Ohm RF, editor. The Vanderbilt Handbook. Norwalk, CT: R.T. Vanderbilt Company; 1990. p. 11-21.

46. Stephens HL. The Compounding and Vulcanization of Rubber. In Morton M, editor. Rubber technology. 3rd ed. London, UK: Chapman & Hall; 1995. p. 20-58.

47. Campbell RH, Wise RW. Vulcanization. Part I. Fate of Curing system during the sulfur vulcanization of natural rubber accelerated by benzothiazole derivatives. Rubber. Chem. Technol. 1964; 37: p. 635-649.

48. Scheele W, Lorenz O, Dummer W. Studies of the vulcanization of high elastic polymers. I. The vulcanization of natural rubber with thiuram disulfides. Part 1. Rubber Chem. Technol. 1956; 29: p. 1-14.

49. Porter M. In Tobolsky V, editor. The Chemistry of Sulfides. New York, NY: Interscience Publishers. 1968, p. 165.

50. Boretti LG, Woolard CD. An appropriate model compound for the accelerated sulfur vulcanization of polyisoprene: I. The mechanism of bisbenzothiazole-2,2'-disulfide accelerated vulcanization of squalene in the absence of ZnO. Rubber Chem. Technol. 2006; 79: p. 135-151.

51. Nieuwenhuizen PJ, Reedijk J, van Duin M, McGill WJ. Thiuram-and dithiocarbamate-accelerated sulfur vulcanization from the chemist's perspective; methods, materials and mechanisms reviewed. Rubber Chem. Technol. 1997; 70: p. 368-429.

52. Kresja MR, Koenig JL. The nature of sulfur vulcanisation. In Cheremisinoff N, editor. Elastomer Technology Handbook. Boca Raton, FL: CRC Press. 1993.

53. Boretti LG. PhD thesis: N-(cyclohexylthio)phthalimide Inhibition of Benzothiazole Accelerated Vulcanization of Squalene. Port Elizabeth, South Africa: University of Port Elizabeth; 2002.

54. Coran AY. Vulcanization. Part VI. A model and treatment for scorch delay kinetics. Rubber Chem. Technol. 1964; 37: p. 689-697.

55. Ahmed K, Nizami SS, Raza NZ, Shirin K. Cure characteristics, mechanical and swelling properties of marble sludge filled EPDM modified chloroprene rubber blends. Adv. Mat. Chem. Phys. 2012; 2: p. 90-97.

56. Coran AY. Chapter 7. Vulcanization. In Mark JE, Erman B, Eirich FR, editors. Science and Technology of Rubber. 2nd ed. San Diego, CA: Academic Press; 1994. p. 339-385.

57. Greensmith HW, Mullins L, Thomas AG. The Chemistry and Physics of Rubber-Like Substances London, UK: Maclaren; 1963.

58. Lal J. Effect of crosslink structure on properties of natural rubber. Rubber Chem. Technol. 1970; 43: p. 664-686.

59. Grobler JHA, McGill WJ. Effect of network heterogeneity on tensile and tear strengths of radiation, peroxide, efficient and conventional cured polyisoprene. J. Polym. Sci. Part B: Polym. Phys. 1994; 32: p. 287-295.

60. Hamed GR. Effect of crosslink density on the critical flaw size of a simple elastomer. Rubber Chem. Technol. 1983; 56: p. 244-251.

61. Rouse MW. Chapter 1. Manufacturing Practices for the Development of Crumb Rubber Materials from Whole Tires. In De SK, Isayev AI, Khait K, editors. Rubber Recycling. Boca Raton, FL: CRC Press; 2005. p. 1-100.

62. Saiwari S, Waisateh K, Lopattananon N, Thititammawong A, Kaesaman A. Study on reuse of diphenyl disulfide-devulcanized natural rubber from truck tyres. Macromol. Symp. 2015; 354: p. 155–162.

63. Rajan VV, Dierkes WK, Joseph R, Noordermeer JWM. Comparative investigation on the reclamation of NR based latex products with amines and disulfides. Rubber Chem. Technol. 2005; 78: p. 855-867.

64. Myrhe M, MacKillop DA. Rubber recycling. Rubber Chem. Technol. 2002; 75: p. 429-474.

65. Fernandez-Berridi MJ, Gonzalez N, Mugica A, Bernicot C. Pyrolysis-FTIR and TGA techniques as tools in the characterization of blends of natural rubber and SBR. Thermochim. Acta. 2006; 444: p. 65-70.

66. Lee YS, Lee WK, Cho SG, Kim I, Ha CS. Quantitative analysis of unknown compositions in ternary polymer blends: A model study on NR/SBR/BR system. J. Anal. Appl. Pyrol. 2007; 78: p. 85–94.

67. Sircar AK, Galaska ML, Rodrigues S, Chartoff RP. Glass transition of elastomers using thermal analysis techniques. Rubber Chem. Technol. 1999; 72: p. 513-552.

68. Bilgili E, Arastoopour H, Bernstein B. Pulverization of rubber granulates using the solid state shear extrusion process. Part II. Powder characterization. Powder Technol. 2001; 115: p. 277-289.

69. Chiu J. Applications of thermogravimetry to the study of high polymers. Appl. Polym. Symp. 1966; 2: p. 25-43.

70. Maurer J. Advances in thermogravimetric analyses of elastomer systems. J. Macromolec. Sci.- Chem. 1974; 8: p. 73-82.

71. Sircar AK, Lamond TG. Identification of elastomers in tire sections by total thermal analysis. I. Tread and black sidewall. Rubber Chem. Technol. 1975; 48: p. 301-309.

72. TA Instruments - Waters LLC. Discovery TGA Getting Started Guide. New Castle, DE. 2013.

73. TA Instruments - Waters LLC. TGA Hi-Res Option Operator's Guide. New Castle, DE. 2011.

74. Yang J, Kaliaguine S, Roy C. Improved quantitative determination of elastomers in tire rubber by kinetic simulation of DTG curves. Rubber Chem. Technol. 1993; 66: p. 213-229.

75. Danon B, Mkhize NM, van der Gryp P, Gorgens JF. Combined model-free and model-based devolatilisation kinetics of tyre rubbers. Thermochim. Acta. 2015; 601: p. 45–53.

76. Danon B, Gorgens J. Determining rubber composition of waste tyres using devolatilisation kinetics. Thermochim. Acta. 2015; 621: p. 56–60.

77. Williams PT, Besler S. Pyrolysis-thermogravimetric analysis of tyres and tyre components. Fuel. 1995; 74: p. 1277-1283.

78. Varkey JT, Augustine S, Thomas T. Thermal degradation of natural rubber/styrene butadiene rubber latex blends by thermogravimetric method. Polym. Plast. Technol. Eng. 2000; 39: p. 415-435.

79. Cui H, Yang J, Liu Z. Thermogravimetric analysis of two Chinese used tires. Thermochim. Acta. 1999; 333: p. 173-175.

80. Sircar AK. Analysis of elastomer vulcanizate composition by TG-DTG techniques. In 139th meeting of the Rubber Division, American Chemical Society; 1991; Toronto, Canada.

81. Shield SR, Ghebremeskel GN, Hendrix C. Pyrolysis-GC/MS and TGA as tools for characterizing blends of SBR and NBR. Rubber Chem. Technol. 2001; 74: p. 803-813.

82. Shields SR, Ghebremeskel GN. FEATURES-Tech Service: Determining styrene content of SBR-TGA is used to estimate the styrene content of SBR. Rubber World. 2000; 223: p. 24-34.

83. Gill PS, Sauerbrunn BS, Crowe J. High resolution thermogravimetry. J. Therm. Anal. Calor. 1992; 38: p. 255-266.

84. Groves IF, Whitehouse RS. Characterisation of polymer masterbatches by modern thermal methods of analysis. J. Therm. Anal. 1993; 40: p. 587-596.

85. Xu J, Shen M, Wang X, Chen C, Xin Z. The effect of reclaim softner on properties of reclaimed rubber. J. Macromol. Sci. Part B. Phys. 2013; 53: p. 37-41.

86. Tawfic ML, Younan AF. Feasible and economic process for using organic disulfide and organic mercaptane as a reclaiming agent for ground tire powder (GTP). J. Elastom. Plast. 2014; 46: p. 19-32.

87. Rajan VV, Dierkes WK, Joseph R, Noordermeer JWM. Effect of diphenyldisulfides with different substituents on the reclamation of NR based latex products. J. Appl. Polym. Sci. 2007; 104: p. 3562-3580.

88. Rajan VV, Dierkes WK, Joseph R, Noordermeer JWM. Recycling of NR based cured latex material with 2,2'dibenzamidodiphenyldisulfphide in a truck tyre compound. J. Appl. Polym. Sci. 2006; 102: p. 4194-4206.

89. Shi J, Jiang K, Ren D, Zou H, Wang Y, Lv X, et al. Structure and performance of reclaimed rubber obtained by different methods. J. Appl. Polym. Sci. 2013; 129: p. 999-1007.

90. Coran AY. Chemistry of the vulcanization and protection of elastomers: A review of the achievements. J. Appl. Polym. Sci. 2003; 79: p. 24-30.

91. Gibb K. Plant manager, Bridgestone, Port Elizabeth, South Africa - personal communication. 2015.

92. Meyer B, editor. Elemental Sulfur. New York, NY: Interscience publishers; 1965.

93. Mphahlehle M. MSc dissertation. N,N’-dipentamethylenethiuram Disulfide Accelerated Sulfur Vulcanization of Squalene. Port Elizabeth: Nelson Mandela Metropolitan University; 2006.

94. Waddell WH, Bhakuni RS, Barbin WW, Sandstrom PH. Pneumatic tire compounding. In Ohm RF, editor. The Vanderbilt Handbook. Norwalk, CT: R.T. Vanderbilt Company; 1990. p. 596-612.

95. Selesnick IW, Burrus CS. Generalized digital Butterworth filter design. Signal Processing, IEEE Transactions. 1998; 46: p. 1688-1694.

96. Gradwell MHS, Morgan B, McGill WJ. Rate of formation of polysulfides of 2-bisbenzothiazole-2-2′-disulfide in the presence of sulfur and 2-mercaptobenzothiazole. J. Appl. Polym. Sci. 1995; 56: p. 1581–1588.

97. ASTM D412 - 06a(2013) Standard test methods for vulcanized rubber and thermoplastic elastomers - tension West Conshohocken, PA: ASTM International; 2013.

98. Jana GK, Mahaling RN, Das CK. A novel devulcanization technology for vulcanized natural rubber. J. Appl. Polym. Sci. 2006; 99: p. 2831-2840.

99. Flory PJ, Rehner J. Statistical mechanics of crosslinked polymer networks II. Rubberlike elasticity. J. Chem. Phys. 1943; 11: p. 512-520.

100. Flory PJ. Statistical mechanics of swelling of network structures. J. Phys. Chem. 1950; 18: p. 108-111.

101. Wall FT, Flory PJ. Statistical thermodynamics of rubber elasticity. J. Chem. Phys. 1951; 19: p. 1435-1439.

102. Haynes WM, editor. Handbook of Chemistry and Physics. 91st ed. Boca Raton, FL: CRC Press; 2010.

103. Mandal SK, Alam N, Debnath SC. Reclaiming of ground rubber tire by safe mulfifunctional rubber additives. I. Tetra benzyl thiuram disulfide. Rubber. Chem. Technol. 2012; 85: p. 629-644.

104. De D, Das D, De D, Denath SC, Roy BC. Reclaiming of ground rubber tire (GRT) by a novel reclaiming agent. Eur. Polym. J. 2006; 42: p. 917-927.

105. Kraus G. Swelling of filler-reinforced vulcanizates. Rubber Chem. Technol. 1964; 37: p. 6-13.

106. Burfield DR, Lim KL. Differential scanning calorimetry analysis of natural rubber and related polyisoprenes. Measurement of the glass transition temperature. Macromolec. 1983; 16: p. 1170-1175.

107. Ohm RF. Introduction to the structure and properties of rubber. In Ohm RF, editor. The Vanderbilt Rubber Handbook. 13th ed. Norwalk, CT: R.T. Vanderbilt Company; 1990. p. 1-20.

108. Henderson JM. Chapter 7. Styrene-Butadiene Rubber. In Morton M, editor. Rubber Technology. 3rd ed. London, UK: Chapman & Hall; 1995. p. 209-234.

109. Kow C, Morton M, Fetters LJ, Hadjichristidis N. Glass transition behavior of polyisoprene: The influence of molecular weight, terminal hydroxy groups, microstructure, and chain branching. Rubber Chem. Technol. 1982; 55: p. 245-252.

110. Jia ZX, Du ML, Guo BC, Fang L, Luo YF, Jia DM. Structure characterization of liquid polyisoprene. Syn. Mater. Aging Appl. 2005; 4: p. 006.

111. Subramaniam A. Gel permeation chromatography of natural rubber. Rubber Chem. Technol. 1972; 45: p. 346-358.

112. Schlesinger W, Leeper HM. Chicle-cis-and trans-polyisoprenes from a single plant species.

Ind. Eng. Chem. 1951; 43: p. 398-403.

113. Medalia AI, Kraus G. Chapter 8. Reinforcement of elastomers by particulate fillers. In Mark JE, Erman B, Eirich FR, editors. Science and technology of rubber. 2nd ed. San Diego, CA: Academic Press; 1994. p. 387-418.

114. Norman DT. Rubber grade carbon blacks. In Ohm RF, editor. The Vanderbilt Handbook. 13th ed. Norwalk, CT: R.T. Vanderbilt Company; 1990. p. 397-422.

115. Kaldcak J, Kuritka I, Konecny P, Cermak R. The effect of ZnO modification on rubber compound properties. In 4th WSEAS International Conference on Energy and Development-Environment-Biomedicine; 2011; Corfu, Greece.

116. Dannenberg EM. Bound rubber and carbon black reinforcement. Rubber Chem. Technol. 1986; 59: p. 512-524.

117. Cataldo F. Preparation of pyrolytic carbon black from scrap tire rubber crumb and evaluation in new rubber compounds. Macromolec. Mater. Eng. 2005; 290: p. 463–467.

118. Guinier A. X-Ray Diffraction in Crystals, Imperfect Crystals, and Amorphous Bodies. Chicago, IL: Courier Corporation; 1994.

119. Slough CG. TA Instruments. [Online]. New Castle, DE [cited 2016 January. Available from: https://www.google.co.za/url?sa=t&rct=j&q=&esrc=s&source=web&cd=1&cad=rja&uact=8&ved=0ahUKEwij1qqU2KTKAhXBWRQKHZfTAdoQFggaMAA&url=http%3A%2F%2Fwww.tainstruments.co.jp%2Fapplication%2Fpdf%2FThermal_Library%2FApplications_Briefs%2FTA306.PDF&usg=AFQjCNGDPx06.

120. Wagner MP. Chapter 4. part II. Nonblack fillers. In Morton M, editor. Rubber technology. 3rd ed. London, UK: Chapman & Hall; 1995. p. 86-104.

121. White JR, De SK, editors. Rubber Technologist's Handbook. Shrewsbury, UK: RAPRA; 2001.

122. Bosch RM. MSc dissertation. The Effect of Silica Inclusion on Blends of Natural Rubber

(NR) and poly(Styrene-co-Butadiene) (SBR). Port Elizabeth, South Africa: University of Port Elizabeth; 2003.

123. Gradwell MHS, Stephenson NR. Pre-vulcanization inhibition of a N-t-butyl-2-benzothiazole sulfenamide cure by N-(cyclohexylthio) phthalimide. Rubber Chem. Technol. 2004; 77: p. 931-946.

124. van der Horst M, Hendrikse KG, Woolard CD. The role of thiol intermediates in 2-mercaptobenzothiazole accelerated sulfur vulcanization of rubber model compounds. J. Appl. Polym. Sci. 2003; 89: p. 47-54.

125. Flory PJ. Principles of Polymer Chemistry. Ithaca, NY: Cornell University Press; 1953.

126. Saiwari S, Dierkes WK, Noordermeer JWM. Devulcanization of whole passenger car tire material. Kautschuk Gummi. Kuns. 2013; 7-8: p. 20-25.

127. Thomas AG, Whittle JM. Tensile rupture of rubber. Rubber Chem. Technol. 1970; 43: p. 222-228.

128. Ding R, Leonov AI, Coran AY. A study of the vulcanization kinetics of an accelerated-sulfur SBR compound. Rubber Chem. Technol. 1996; 69: p. 81-91.

129. Ding R, Leonov AI. A kinetic model for sulfur accelerated vulcanization of a natural rubber compound. J. Appl. Polym. Sci. 1996; 61: p. 455-463.

130. Naylor RF. Syntheses in the thiapyran series. Part II. Dihydro-derivatives. J. Chem. Soc. (resumed). 1949; p. 2749-2755.

131. Cunneen JI, Russell RM. Occurrence and prevention of changes in the chemical structure of natural rubber tire tread vulcanizates during service. Rubber Chem. Technol. 1970; 43: p. 1215-1224.

132. Saville B, Watson AA. Structural characterization of sulfur-vulcanized rubber networks. Rubber Chem. Technol. 1967; 40: p. 100-148.

133. Nordsiek KH. Paper no 48. Integral elastomer. In 125th Meeting of the Rubber Division, American Chemical Society; 1984; Indianapolis.

# Chapter 9

# 9 APPENDICES

## 9.1 Appendix A - Formulations

*Table 9.1 Conventional cure formulations used for testing mixing behaviour, cure rheometry and mechanical properties*

| *Component* | *NR* | *SBR* | *NR & SBR* | *NRG sub. 15%* | *NRG sub. SBR 15%* | *NRG non-sub. 5%* | *NRG non-sub. 15%* | *Commercial tyre tread sub. 15%* | *Commercial tyre tread non-sub. 15%* |
|---|---|---|---|---|---|---|---|---|---|
| *NR* | 100 (65.0%) | - | 50 (32.5%) | 41.8 (27.2%) | 50 (32.3%) | 50 (30.7%) | 50 (27.7%) | 35.4 (23.0%) | 50 (27.7%) |
| *SBR-OE* | - | 100 (65.0%) | 50 (32.5%) | 41.8 (27.2%) | 39.9 (25.8%) | 50 (30.7%) | 50 (27.7%) | 50 (32.5%) | 50(27.7%) |
| *NRG reclaim* | - | - | - | 23 (15.0%) | 25.7 (16.6%) | 9 (5.5%) | 27 (14.9%) | - | - |
| *Commercial tyre tread reclaim* | - | - | - | - | - | - | - | 23.4 (15.2%) | 27 (14.9%) |
| *Carbon black* | 45 (29.3%) | 45 (29.3%) | 45 (29.3%) | 38.4 (25.0%) | 30.2 (19.5%) | 45 (27.6%) | 45 (24.9%) | 36.4 (23.6%) | 45 (24.9%) |
| *Sulfur* | 1.6 (1.0%) | 1.6 (1.0%) | 1.6 (1.0%) | 1.6 (1.0%) | 1.6 (1.0%) | 1.6 (1.0%) | 1.6 (0.9%) | 1.6 (1.0%) | 1.6 (0.9%) |
| *CBS** | 0.8 (0.5%) | 0.8 (0.5%) | 0.8 (0.5%) | 0.8 (0.5%) | 0.8 (0.5%) | 0.8 (0.5%) | 0.8 (0.4%) | 0.8 (0.5%) | 0.8 (0.4%) |
| *DPG†* | 0.4 (0.3%) | 0.4 (0.3%) | 0.4 (0.3%) | 0.4 (0.3%) | 0.4 (0.3%) | 0.4 (0.2%) | 0.4 (0.2%) | 0.4 (0.3%) | 0.4 (0.2%) |
| *Stearic acid* | 3 (2.0%) | 3 (2.0%) | 3 (2.0%) | 3 (2.0%) | 3 (1.9%) | 3 (1.8%) | 3 (1.7%) | 3 (1.9%) | 3 (1.7%) |
| *ZnO* | 3 (2.0%) | 3 (2.0%) | 3 (2.0%) | 3 (2.0%) | 3 (1.9%) | 3 (1.8%) | 3 (1.7%) | 3 (1.9%) | 3 (1.7%) |
| *Total* | 153.8 (100%) | 153.8 (100%) | 153.8 (100%) | 153.8 (100%) | 154.6 (100%) | 162.8 (100%) | 180.8 (100%) | 154.0 (100%) | 180.8 (100%) |

* N-cyclohexyl-2-benzothiazole sulfenamide
† diphenyl guanidine

Values are reported as phr. Those in brackets are as a percentage by mass. Sub. indicates formulations in which part of the rubber (100 phr) has been replaced by reclaim. In the case of non-sub. the NR&SBR combinations is a 100 phr reference and the reclaim is added in addition.

*Table 9.2 Efficient cure formulations used for testing mixing behaviour, cure rheometry and mechanical properties*

| *Component* | *NR & SBR TMTD* | *NRG sub. 15% TMTD* | *Commercial tyre tread sub. 15% TMTD* | *NR & SBR CTP* | *NRG sub. 15% CTP* | *Commercial tyre tread sub. 15% CTP* |
|---|---|---|---|---|---|---|
| *NR* | 50 (32.7%) | 41.8 (27.3%) | 35.4 (23.1%) | 50 (32.4%) | 41.8 (27.1%) | 35.4 (22.9%) |
| *SBR-OE* | 50 (32.7%) | 41.8 (27.3%) | 50 (32.6%) | 50 (32.4%) | 41.8 (27.1%) | 50 (32.4%) |
| *NRG reclaim* | - | 23 (15.0%) | - | - | 23 (14.9%) | - |
| *Commercial tyre tread reclaim* | - | - | 23.4 (15.3%) | - | - | 23.4 (15.2%) |
| *Carbon black* | 45 (29.4%) | 38.4 (25.1%) | 36.4 (23.8%) | 45 (29.2%) | 38.4 (24.9%) | 36.4 (23.6%) |
| *Sulfur* | 0.4 (0.3%) | 0.4 (0.3%) | 0.4 (0.3%) | 1.6 (1.0%) | 1.6 (1.0%) | 1.6 (1.0%) |
| *CBS* | - | - | - | 0.8 (0.5%) | 0.8 (0.5%) | 0.8 (0.5%) |
| *DPG* | - | - | - | 0.4 (0.3%) | 0.4 (0.3%) | 0.4 (0.3%) |
| *TMTD** | 1.6 (1.0%) | 1.6 (1.0%) | 1.6 (1.0%) | - | - | - |
| *CTP†* | - | - | - | 0.4 (0.3%) | 0.4 (0.3%) | 0.4 (0.3%) |
| *Stearic acid* | 3 (2.0%) | 3 (2.0%) | 3 (2.0%) | 3 (1.9%) | 3 (1.9%) | 3 (1.9%) |
| *ZnO* | 3 (2.0%) | 3 (2.0%) | 3(2.0%) | 3 (1.9%) | 3 (1.9%) | 3 (1.9%) |
| *Total* | 153.0 (100%) | 152.9 (100%) | 153.2 (100%) | 154.2 (100%) | 154.1 (100%) | 154.4 (100%) |

* tetramethyl thiuram disulfide
† N-cyclohexylthiophthalimide

## 9.2 Appendix B - Comparison of SDT and Hi-Res$^{TM}$ instruments

Thermal analysis on the highly viscous NRG reclaim material was initially investigated using an SDT instruments. The aim of this experiment was not only to decompose the reclaim to identify the various components present but to also investigate the best heating profile for a TGA instrument that does not have Hi-Res$^{TM}$ capabilities. Figure 9.1 shows the impact of changing the flow rate of nitrogen to the SDT furnace. The flow rates used were 1, 10, 20, 30, 40, 50 and 60 mℓ/min.

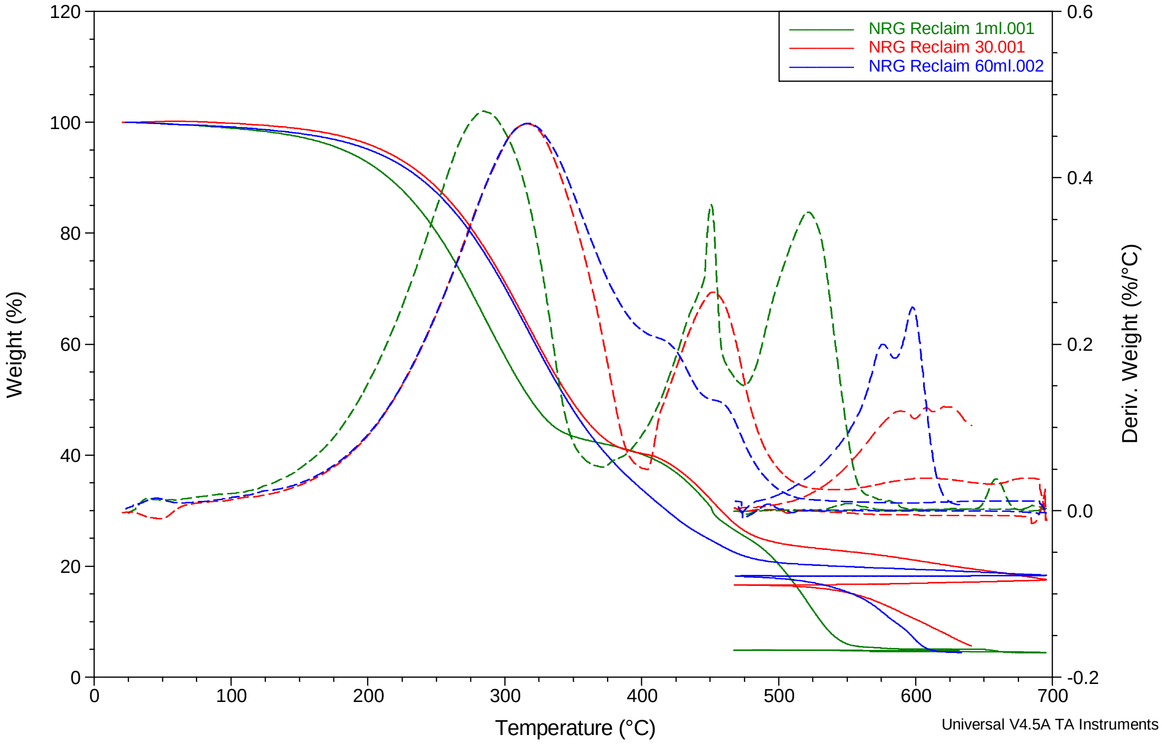

*Figure 9.1 Comparison between different flow rates and the impact on resolution. The dashed lines show the derivative curves of the weight loss curves (solid lines). Flow rate = 1 mℓ/min (green); 30 mℓ/min (red) and 60 mℓ/min (blue)*

Figure 9.1 shows the trend that occurs as the flow rate moves from a low to high flow rate. The intermediate flow rates are not illustrated from greater clarity. When analysing the decomposition in nitrogen atmosphere it can be seen that the resolution decreases as the flow rate is increased. This is evidenced by the weight % loss moving from a step curve (flow rate of 1 mℓ/min) to a smooth sloping curve (flow rate 60 mℓ/min).

From the derivative curves, it can be seen that a low flow rate (solid line) gives the best resolution. The derivative of the low flow rate is sharper and a shoulder can be seen around

450°C. This shoulder is not evident when higher flow rates are used. As the flow rate increases the trend in the derivative curve is that the peaks begin to broaden which may overlap and obscure other peaks.

The second step of the thermal program is carried out in oxygen/air. This allows combustion of the sample. For the SDT procedure, the furnace is cooled before heating in oxygen/air. The thermogram should therefore show a level mass where there is no weight loss since carbon black in the sample should only decompose in the presence of oxygen/air. From Figure 9.1 it is evident that at low flow rates the oxygen present in the furnace is sufficient to cause the decomposition of carbon black before the change to oxygen/air. Note that the SDT furnace has a large volume, so a large flow rate is required to remove air entrapped when the furnace is closed.

As the flow rate increases this problem decreases which is shown not only from the weight loss curve but also the derivative curve. The thermogram at a flow rate of 60 mℓ/min still shows the effect of oxygen on the sample. The double peak at the end of the 60 mℓ/min curve indicates that the carbon black starts to decompose before the switch to oxygen where after the rate of decomposition increase. This would indicate that previous assumptions of oxygen being a contaminant during the nitrogen section of the experiment is confirmed. Note, however, that these experiments were performed on the NRG reclaim. The carbon black present in this sample is more likely to have structure similar to a PyCB, rather than a commercial CB. Like PyCBs it may undergo, carbonization with associated mass loss, as oxygen-containing groups and asphaltene molecules are lost (13).

The role of nitrogen quality was also tested to show what impact it might have on the experiment. The thermogram in Figure 9.2 shows a comparison between technical grade, high purity (HP) and ultra-high purity (UHP, Baseline 5.0) nitrogen. This comparison has important consequences for the cost of analysis. Technical grade nitrogen is significantly cheaper than UHP.

From Figure 9.2, it can be seen that the change in the quality of gas does not play as large a role as the flow rate. There are minimal changes to the weight percentage loss and the major changes can be seen in the derivative curves. However, the trend in the thermogram is not a case of an increase in resolution as the gas is changed to a higher quality, nor does the effects of oxygen contamination decrease with an increase in gas purity. This can be seen when analysing the high purity nitrogen curve. It shows an increase in resolution for the weight percent loss but it also shows a decreased ability to remove or decrease the effects of oxygen present in the furnace. This suggests that air is still entrapped in the large SDT furnace. The Discovery Series Hi-Res$^{TM}$ TGA used later has a much smaller furnace which is easier to purge properly. As an additional improvement, an oxygen and moisture trap was added to the UHP $N_2$ line for experiments using the Hi-Res$^{TM}$ TGA.

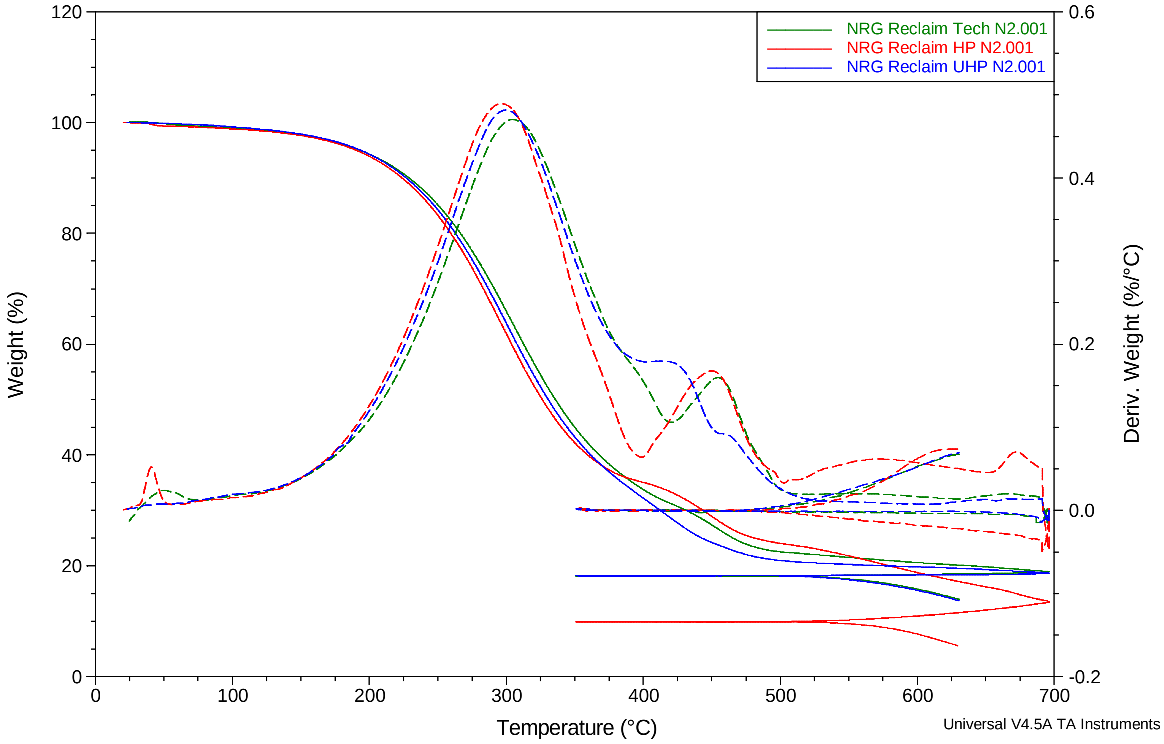

*Figure 9.2 Thermogram showing a comparison between different quality nitrogen. The quality is technical grade (solid line), high purity (dashed line) and ultra high purity nitrogen (dash dot line)*

Thermal analysis was performed in a Hi-Res$^{TM}$ TGA using the same sample to compare the two machines. Figure 9.3 shows an overlay of the two thermograms.

It can be seen that the Hi-Res$^{TM}$ TGA does not have a problem with oxygen contamination. This provides a more reliable weight percentage loss as premature decomposition of the sample due to oxygen can be ruled out. Quantification of carbon black is thus much more accurate. The Hi-Res TGA$^{TM}$ also provides a more complete decomposition of the sample which reduces the possibility of overlapping peaks.

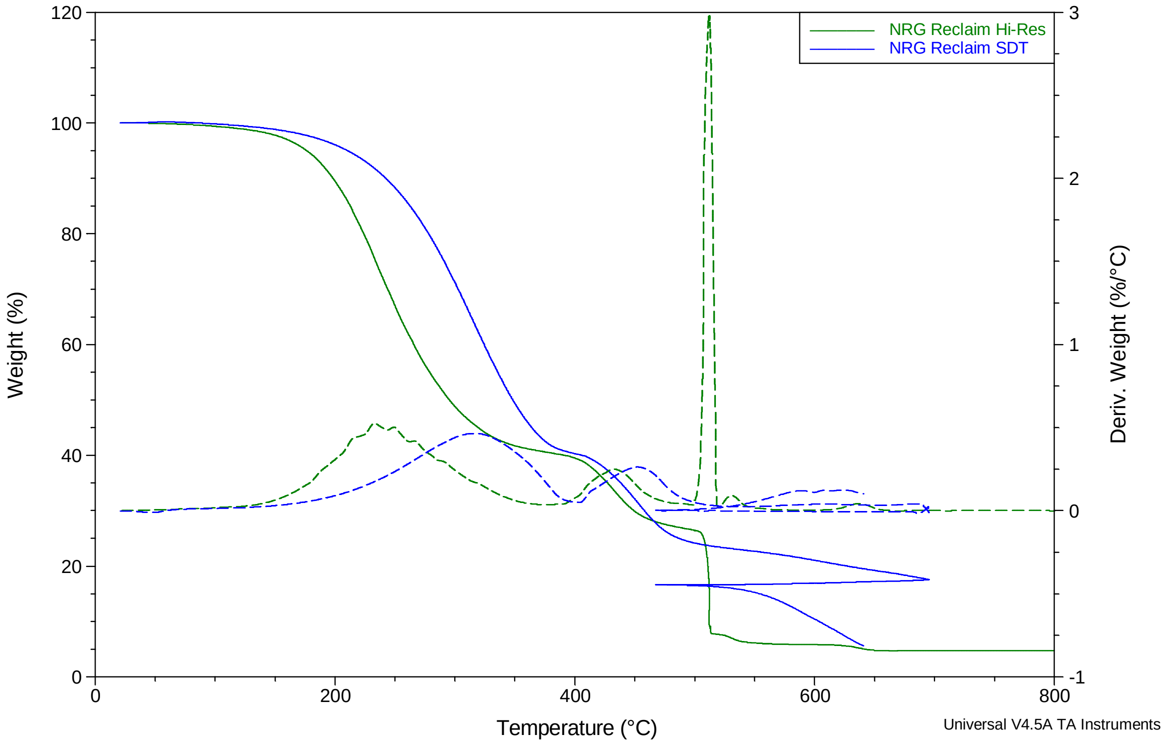

*Figure 9.3 Comparison between Hi-Res*$^{TM}$ *TGA and SDT analysis*

It is important to point out that the heating program for the Hi-Res$^{TM}$ TGA was different from that of the SDT. This is due to the nature of the two machines. While the Hi-Res$^{TM}$ TGA is automatically programmed to decrease heating rates when weight loss is detected and increase again once decomposition is complete the SDT has to be programmed manually. The SDT requires the increase or decrease of the heating rate to be programmed before the start of the analysis which would only be possible if the sample had already been analysed.

Because of difficulties with furnace purging, large volume furnaces such as the SDT are not recommended for the analysis of samples that are sensitive to small quantities of oxygen.

## 9.3 Appendix C - Sulfur thermogram

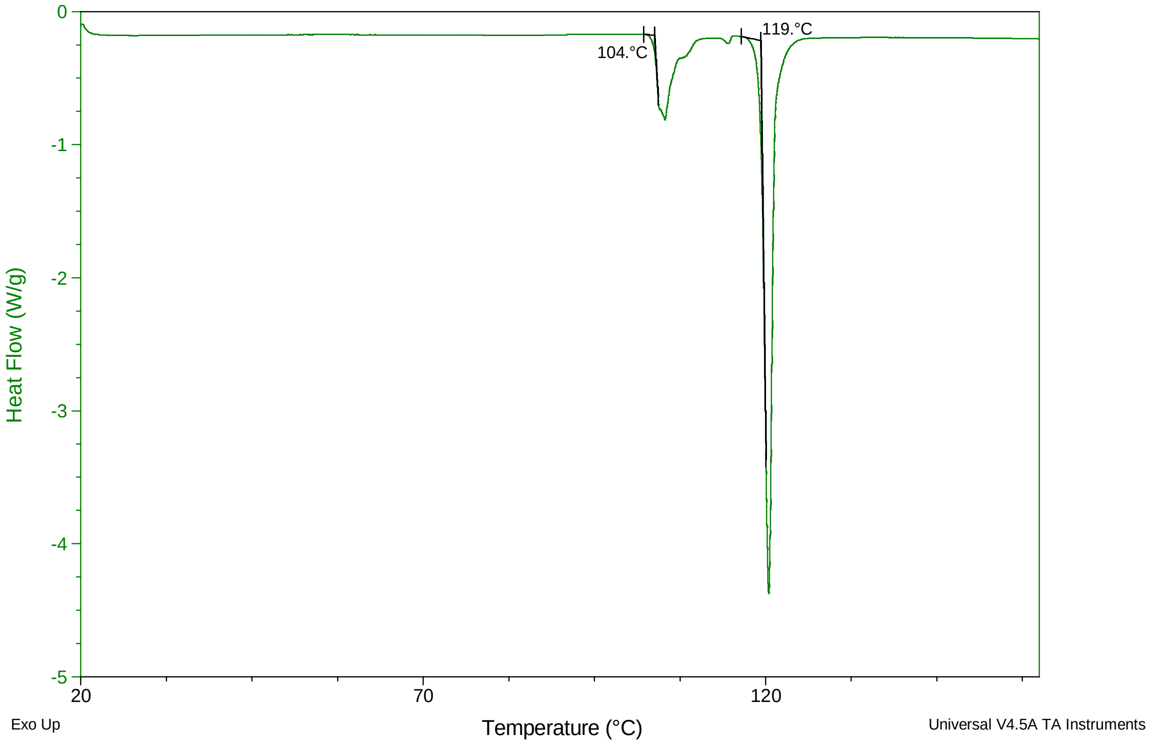

*Figure 9.4 Thermogram of sulfur showing the onset of the α-β transition (104°C) and melting transition (119°C) values. The DSC was heated from 20°C to 160°C at a heating rate of 10C/min*

The analysis of the sulfur indicated that the sulfur was rhombic. Rhombic sulfur can be identified by its transition temperature from rhombic to monoclinic sulfur (α-β transition) in the range of 102°C-112°C. The melting transition in the range of 117°C-127°C also confirms that the sulfur used in this study was rhombic sulfur.

## 9.4 Appendix D – DTG curves

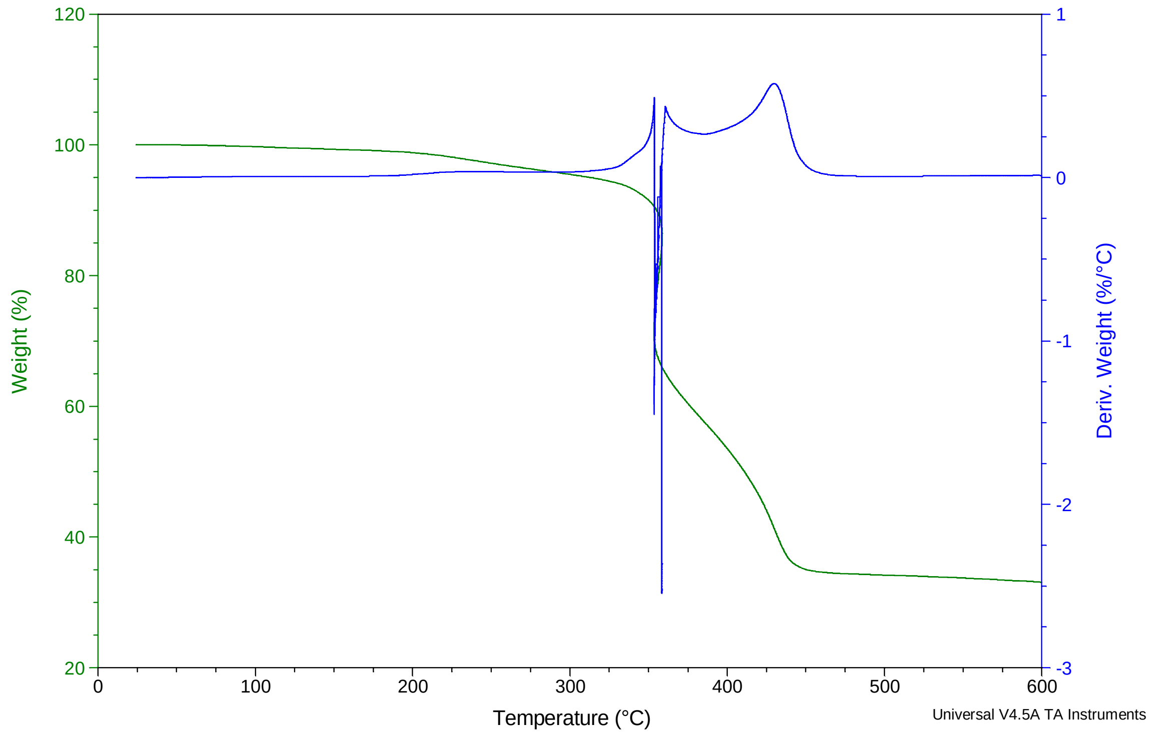

*Figure 9.5 Hi-Res™ constant reaction rate with a base heating rate of 20°C/min, resolution -2 and sensitivity 1*

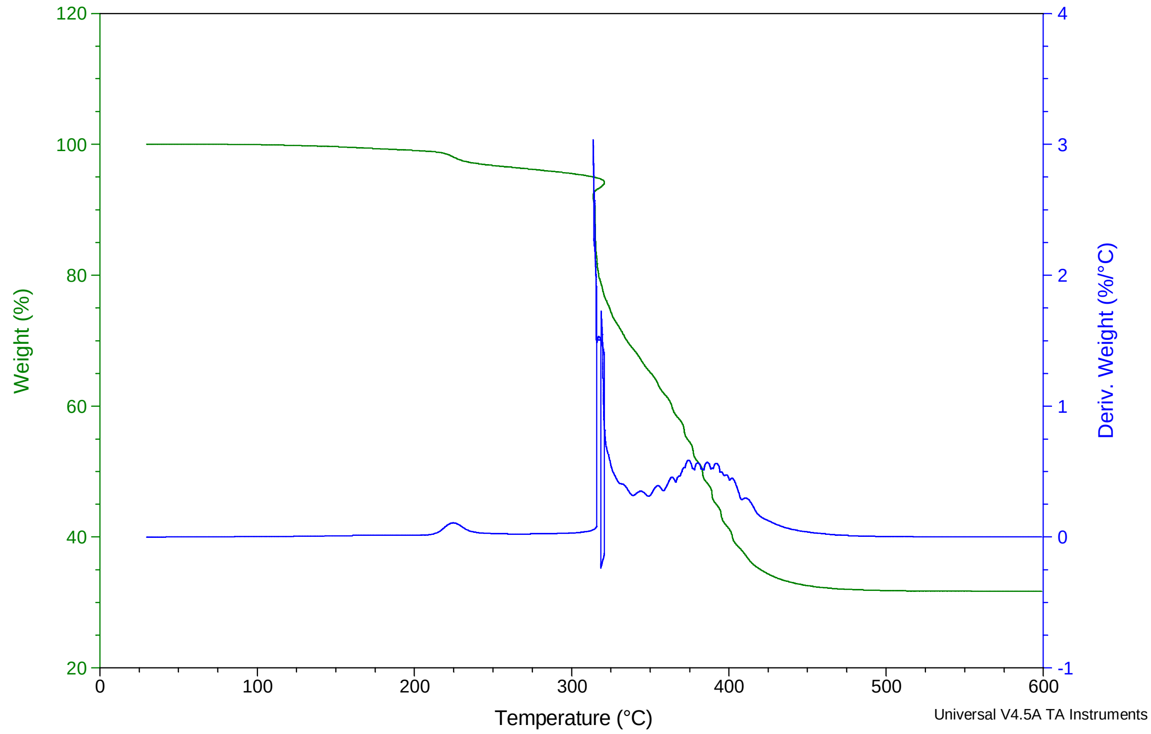

*Figure 9.6 Hi-Res™ constant reaction rate with a base heating rate of 50°C/min, resolution*
*-4 and sensitivity 1*

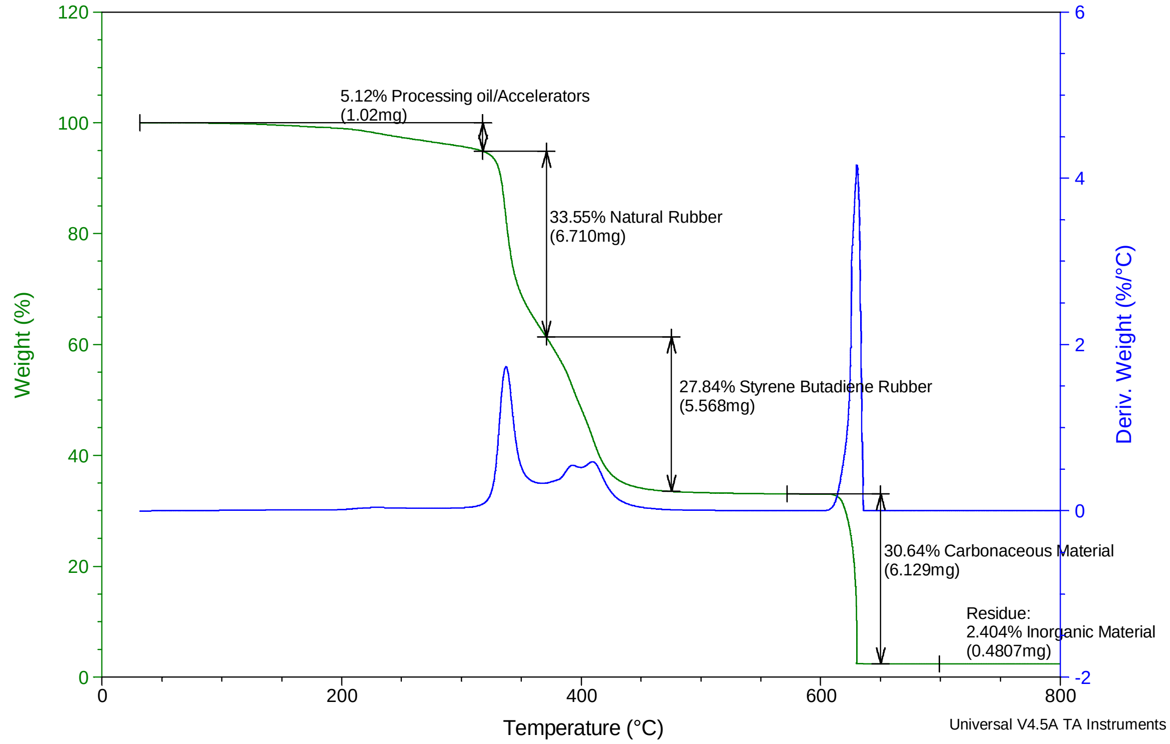

*Figure 9.7 Quantification of the standard rubber formulation. Hi-Res™ dynamic rate with a base heating rate of 20°C/min, resolution 5 and sensitivity 1*

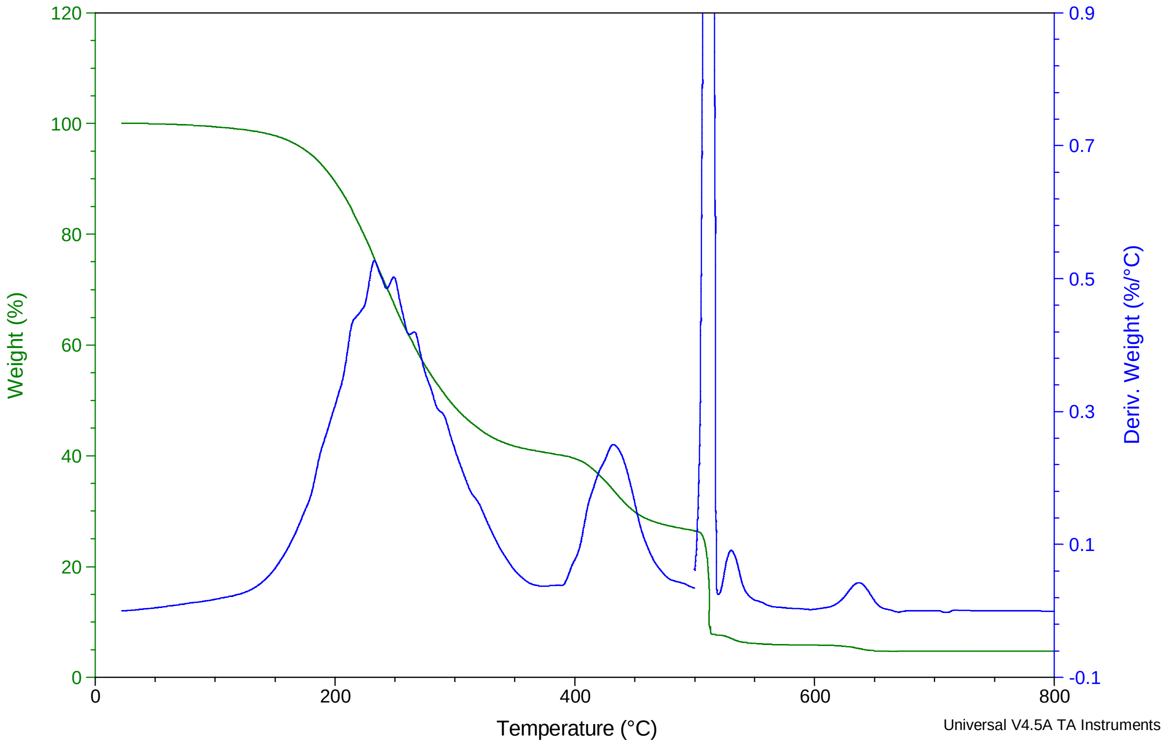

*Figure 9.8* *NRG reclaim thermogram with the DTG curve. Hi-Res™ dynamic with a base heating rate of 20°C/min, resolution 5 and sensitivity 1*

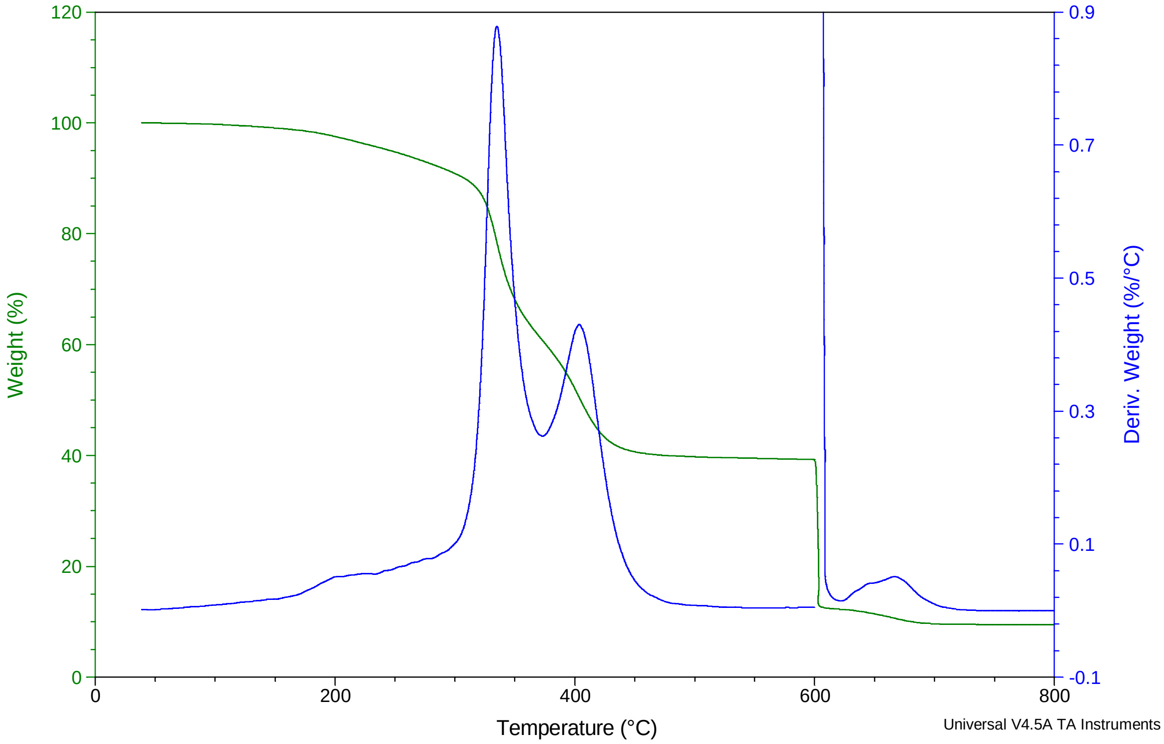

*Figure 9.9* *Commercial tyre tread reclaim with the DTG curve. Hi-Res™ dynamic mode with a heating rate of 20°C/min, resolution 5 and sensitivity 1*

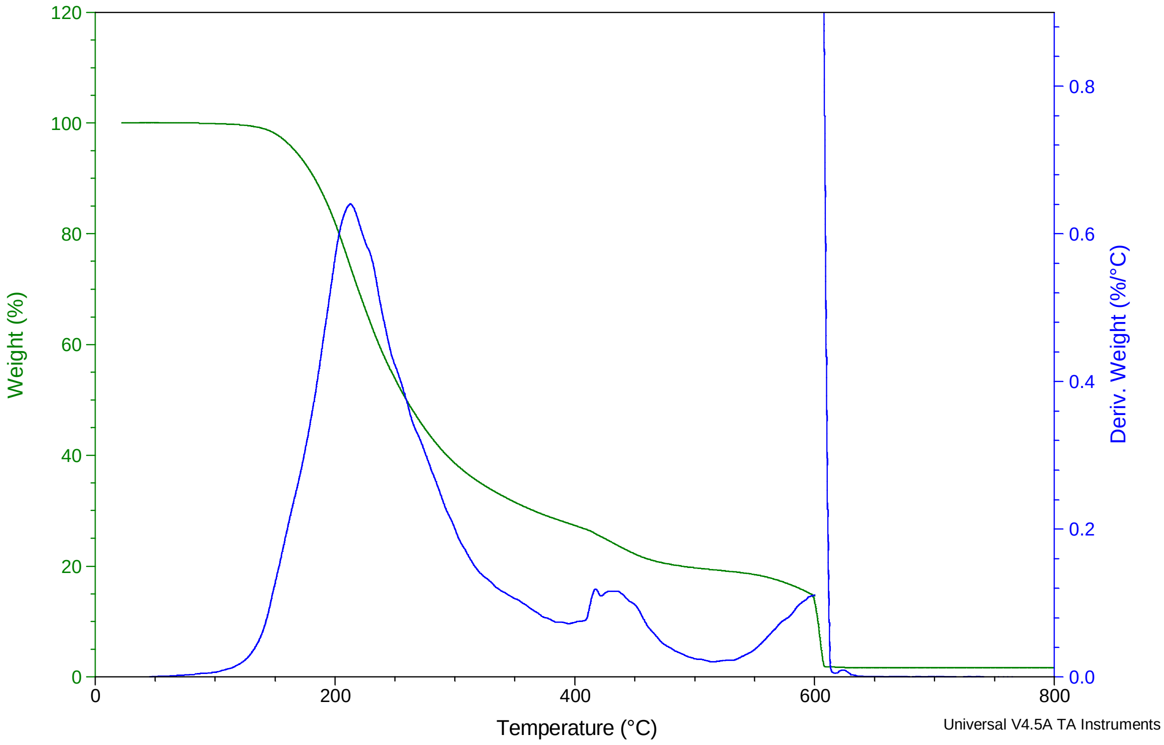

*Figure 9.10 Toluene solvent extract with the DTG curve. Hi-res™ dynamic mode with base heating rate of 20°C/min, resolution 5 and sensitivity 1*

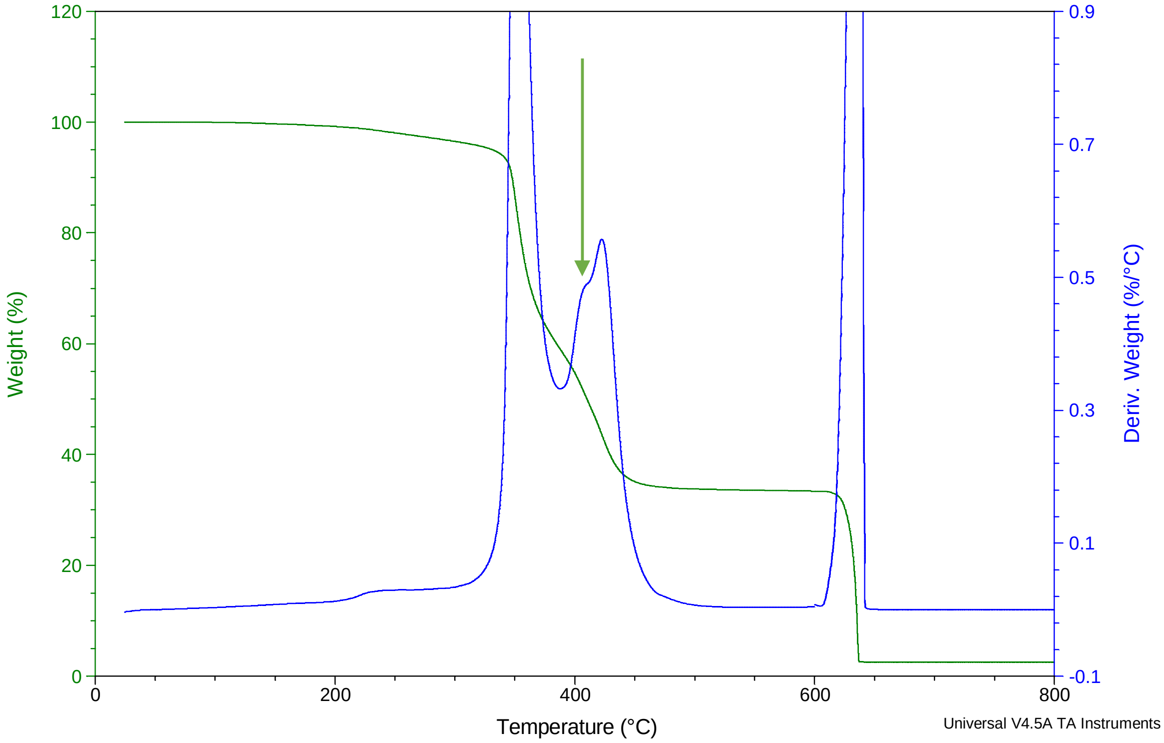

*Figure 9.11 Standard tread formulation showing the typical shoulder of SBR on the DTG curve. Hi-Res™ dynamic mode with base heating rate of 20°C/min, resolution 4, sensitivity 1*

## 9.5 Appendix E – Constant ramp

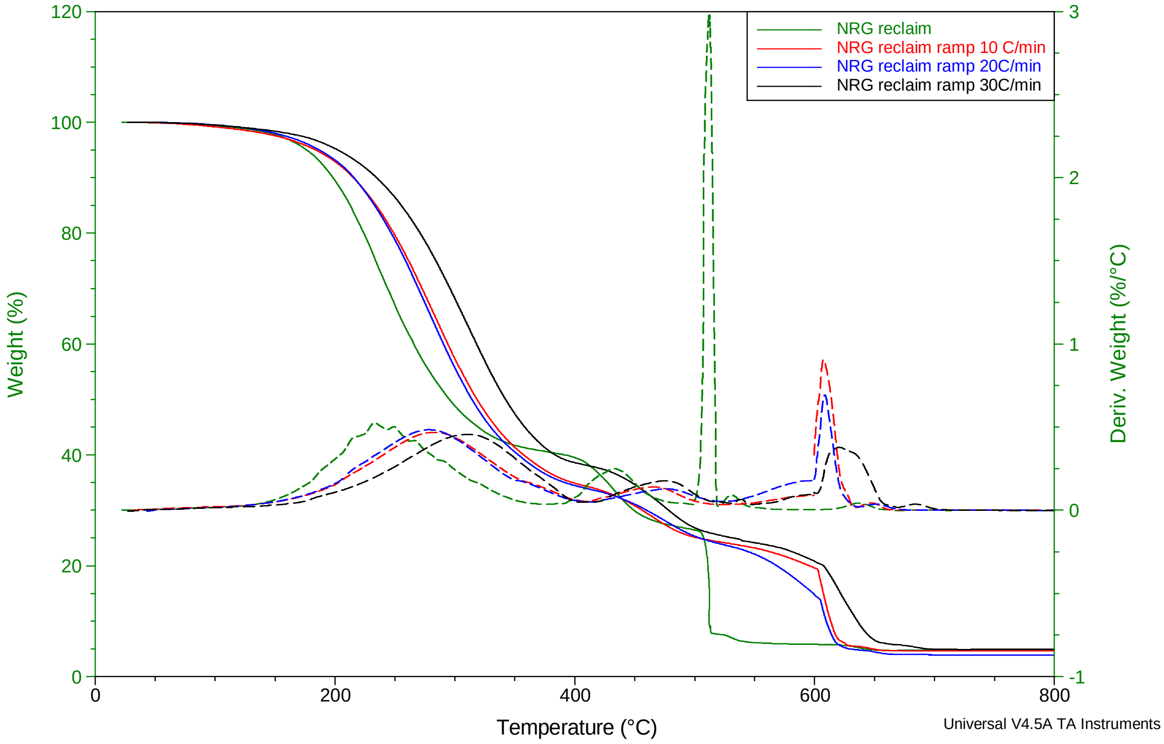

*Figure 9.12 Comparison of Hi-Res™ dynamic mode with resolution 5, sensitivity 1 and base heating rate of 20°C/min (Green) and constant heating rate of 10°C/min (red), 20°C/min (blue) and 30°C/min (black)*

## 9.6 Appendix F - Multiple runs to show reproducibility

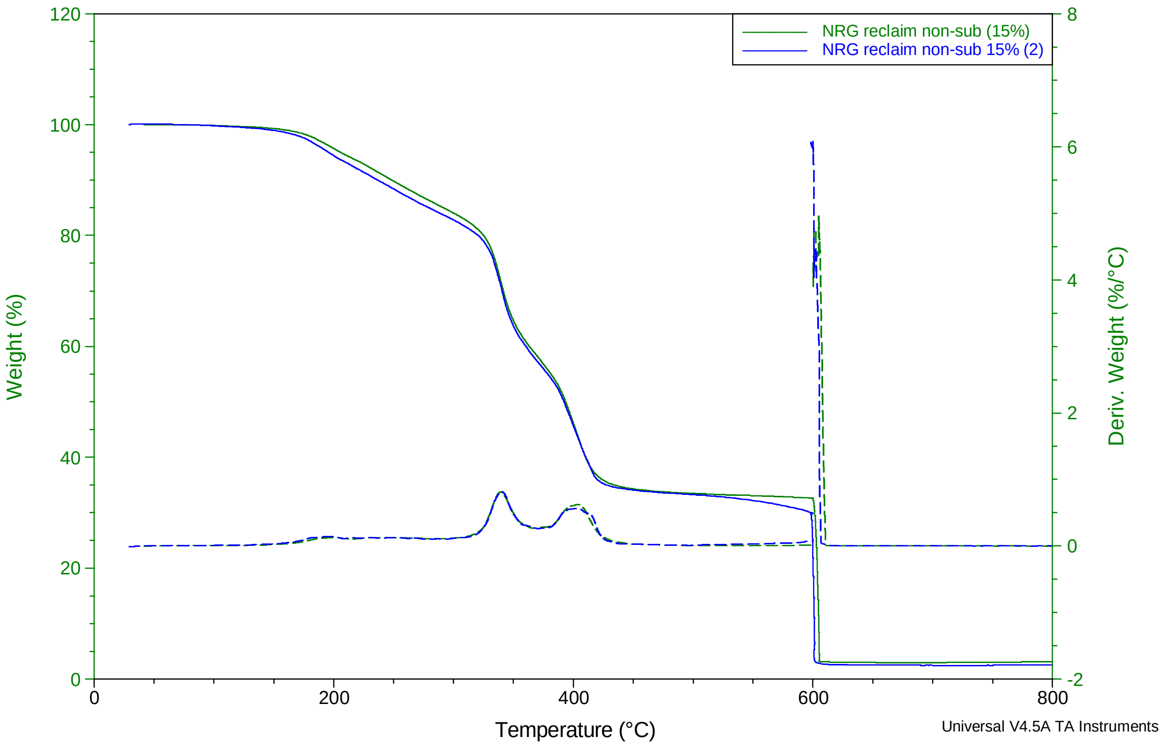

*Figure 9.13 Duplicate run of NRG reclaim. Hi-Res™ dynamic mode with heating rate of 20°C/min, resolution 5 and sensitivity 1*

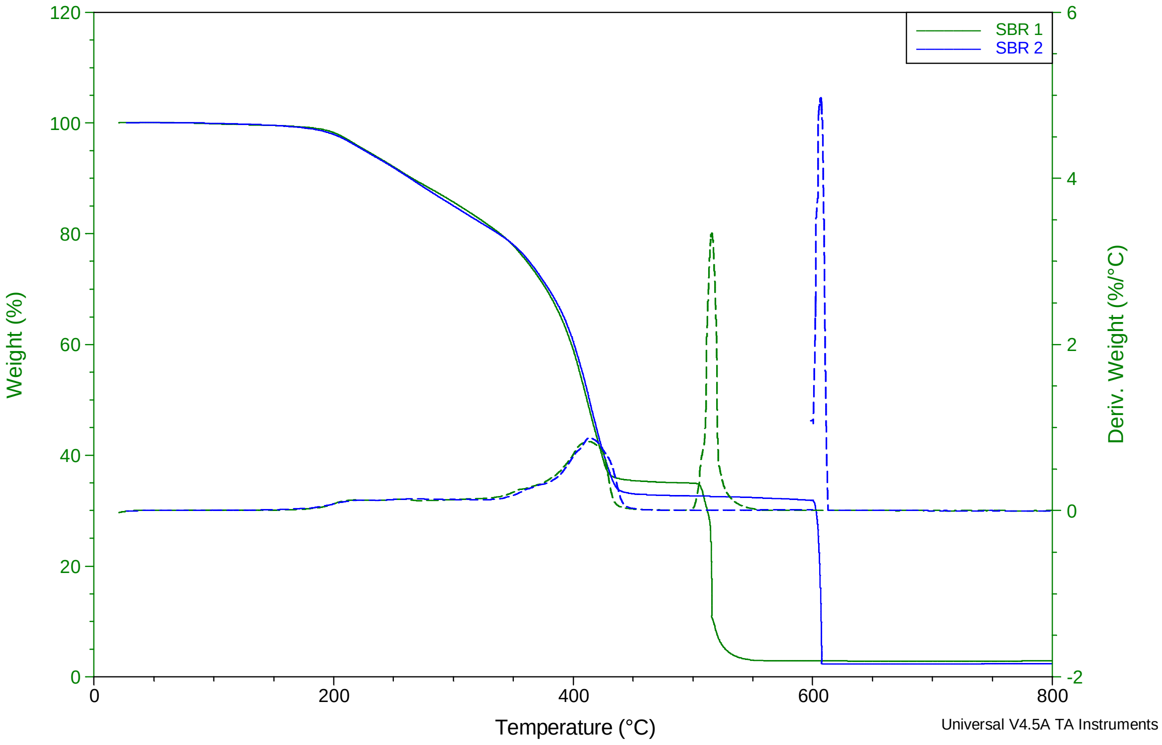

*Figure 9.14 Duplicate run of vulcanized SBR sample performed in Hi-Res™ dynamic mode with base heating rate of 20°C/min, resolution 5 and sensitivity 1*

## 9.7 Appendix G – Mixing kinetics for TMTD and CTP

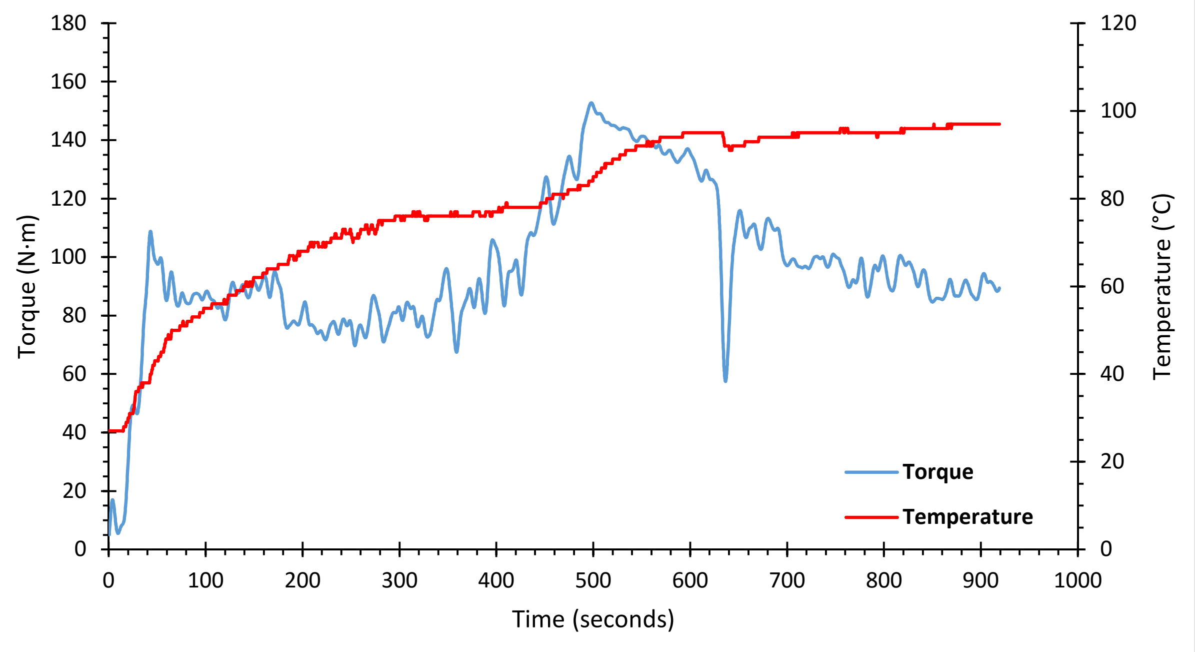

*Figure 9.15 Mixing kinetics for NR&SBR with TMTD*

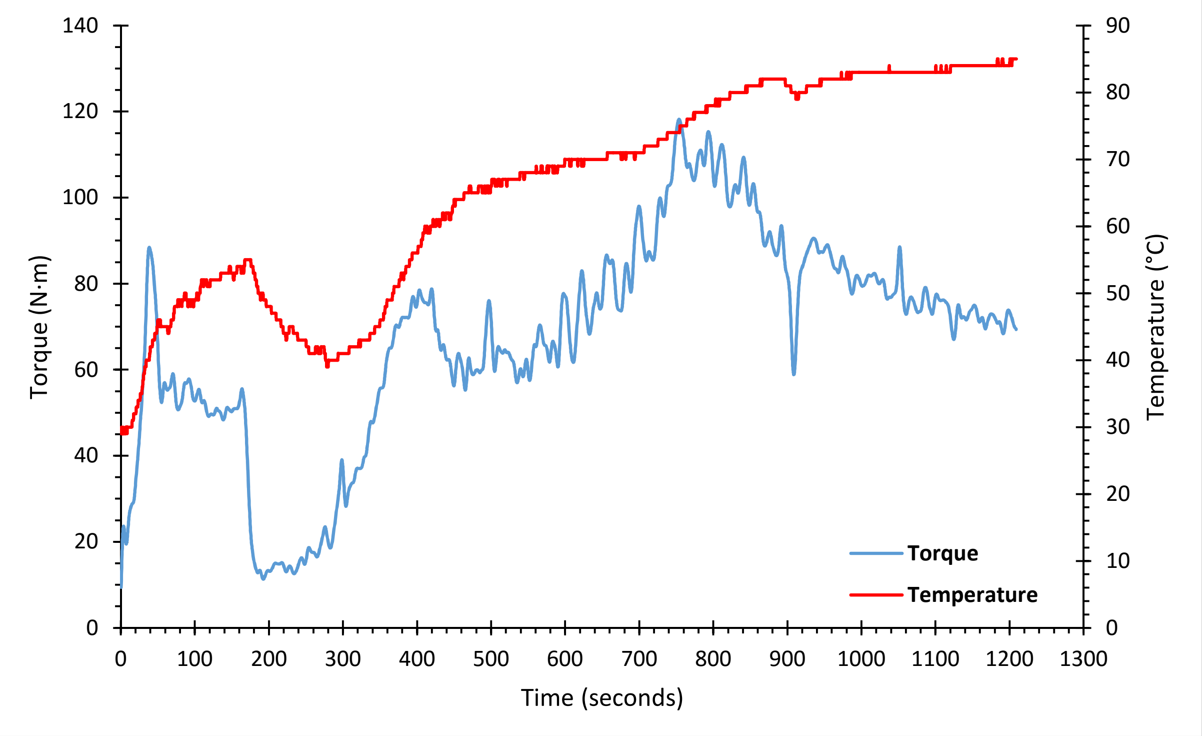

*Figure 9.16 Mixing kinetics for NRG reclaim 15% substituted with TMTD*

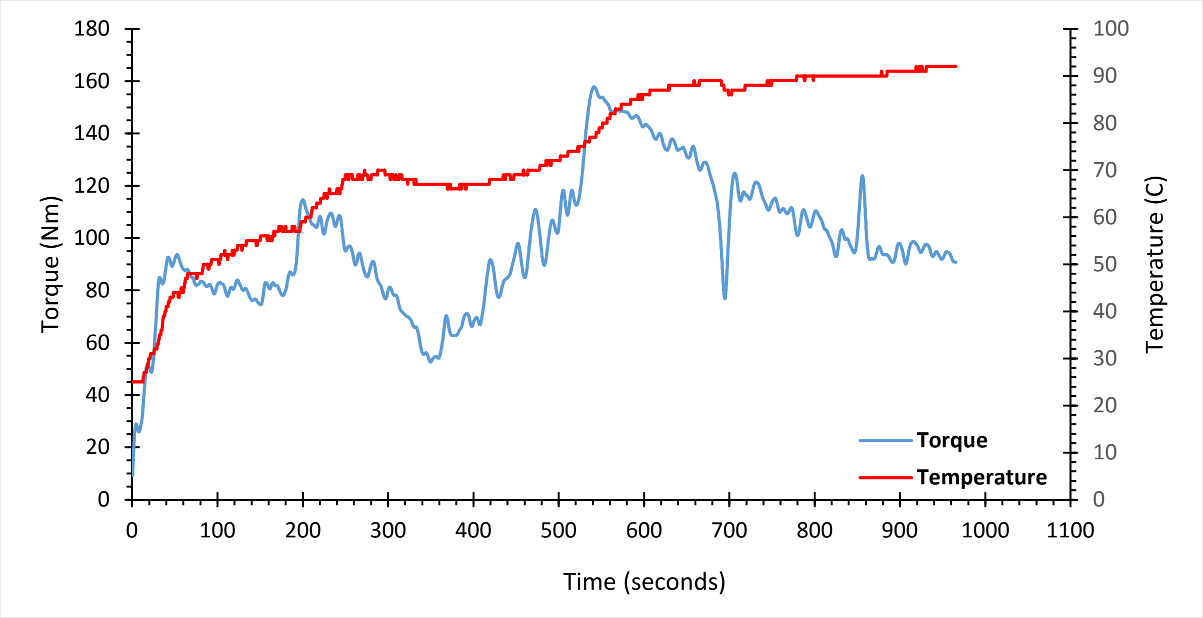

*Figure 9.17 Mixing kinetics of commercial tyre tread reclaim 15% substituted with TMTD*

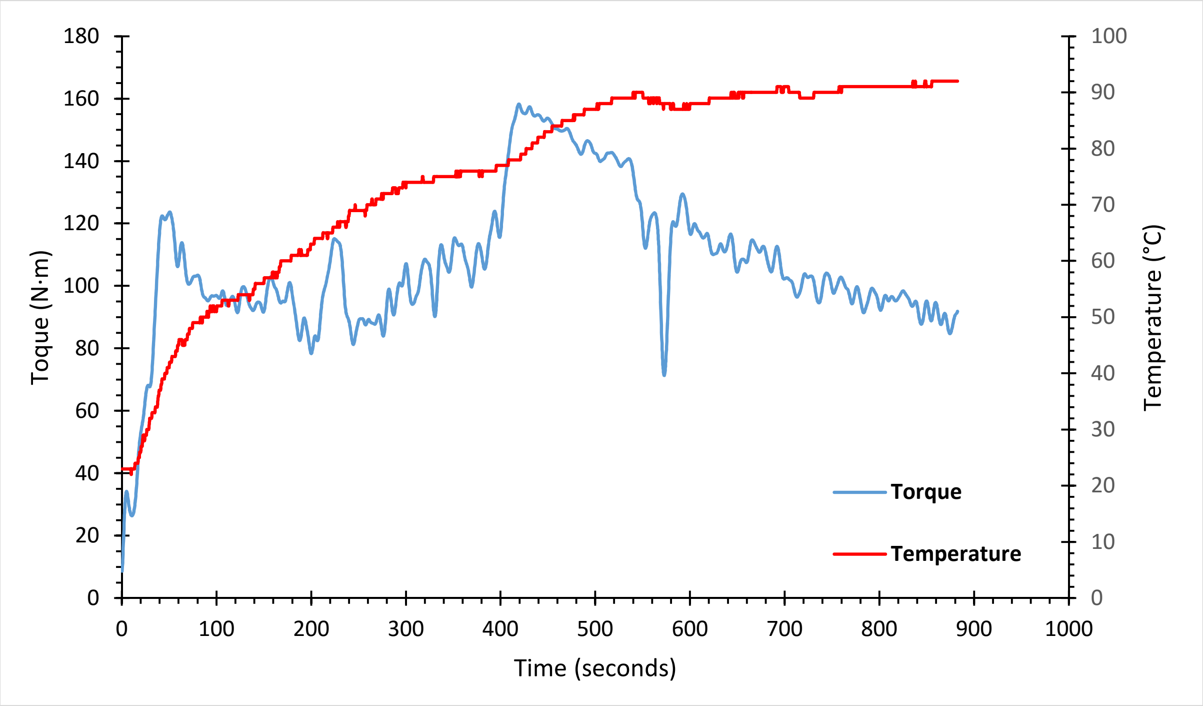

*Figure 9.18 Mixing kinetics of NR&SBR with CTP*

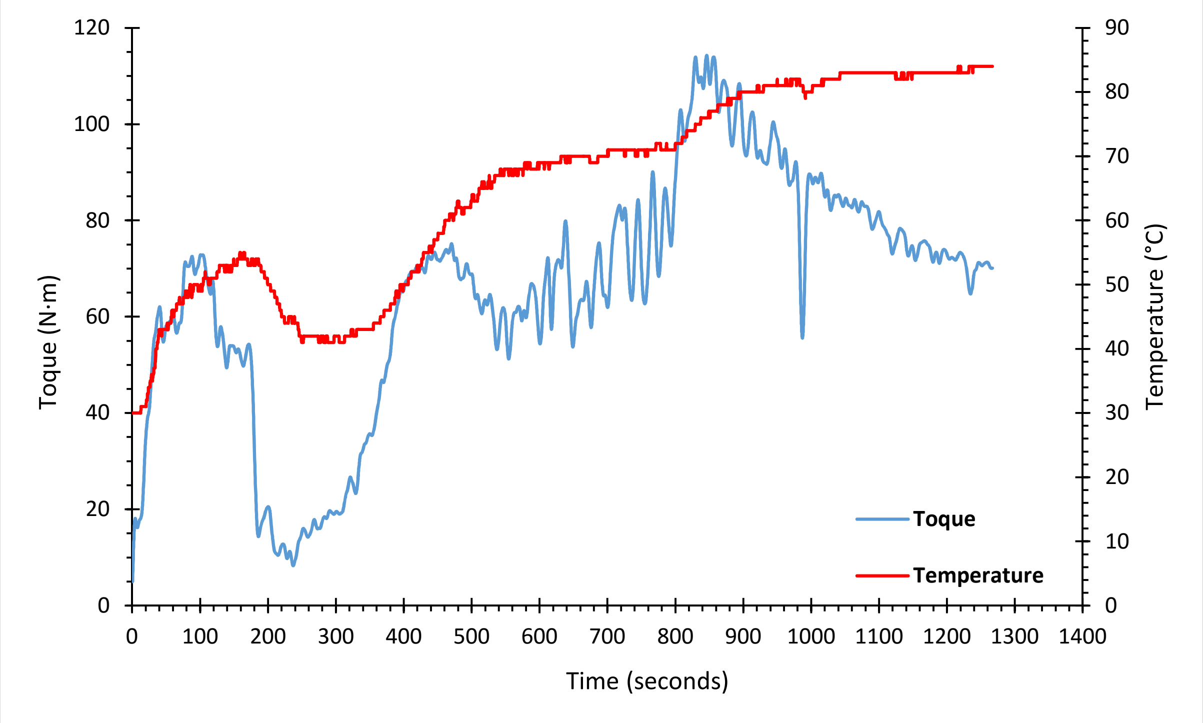

*Figure 9.19 Mixing kinetics of NRG reclaim 15% substituted with CTP*

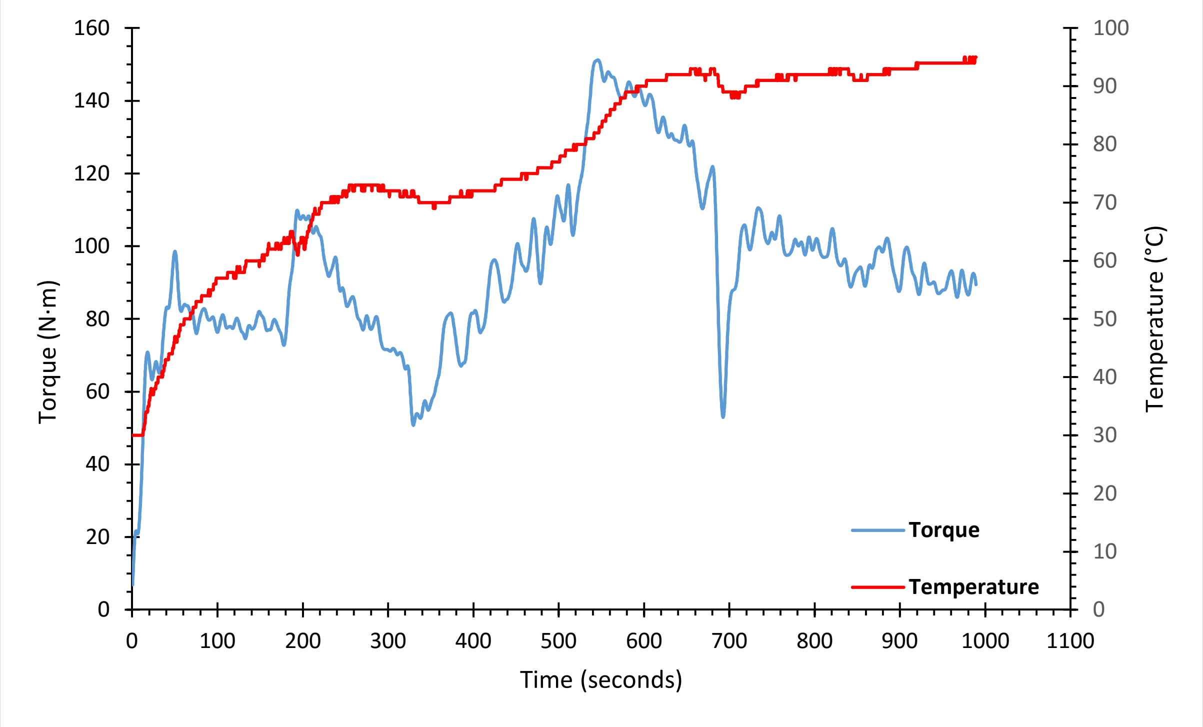

*Figure 9.20 Commercial tyre tread reclaim 15% substituted with CTP*

# Plagiarism declaration

I know that plagiarism is wrong. Plagiarism is to use another's work and pretend that it is one's own.

Each significant contribution to, and quotation in, this project from the work, or works of other people has been attributed and referenced.

I have not allowed, and will not allow, anyone to copy my work with the intention of passing it off as his or her own work.

I acknowledge that copying someone else's assignment or project, or part of it, is wrong, and declare that this report is my own work.

I declare that this project is my own work.

SIGNATURE: S vonBerg

Stuart von Berg

DATE: 15 March 2016